**UNIVERSITA' POLITECNICA DELLE MARCHE**

FACULTY OF ENGINEERING

MASTER'S DEGREE IN **BIOMEDICAL ENGINEERING**

---

# Correlation in time-frequency domain among EMG signals from muscles recruited by the same synergy during walking

Advisor:

Prof. **Fioretti Sandro**

Co-Advisor:

Dott. **Di Nardo Francesco**

Dott. **Borzelli Daniele**

Candidate:

**Falconi Barbara**

A.Y. **2023 / 2024**

*Alla mia famiglia, che non ha mai smesso di credere in me.*

# Summary

**Abstract……..……...4**

**1 Introduction…….…….5**

**2 The Central Nervous System….....7**

**2.1 Structure of the Central Nervous System ..... 7**

**2.2 Physiology of the Central Nervous System……..9**

**2.3 CNS Control of Movement…….……10**

**2.4 Motor Synergy and CNS Coordination…….…….12**

**3 Gait analysis…….…….…….....…….13**

**3.1 Gait Cycle……...……...…...…….13**

**3.2 Fundamental Functions of Gait……..…...……..…18**

**3.3 Analysis of Normal Gait……...……...20**

**3.4 Muscle Synergy During gait cycle……...……...23**

**4 EMG Signal Processing Techniques……...……..25**

**4.1 Surface EMG……...……25**

**4.2 EMG signal processing……27**

**4.3 Continuous Wavelet Transform (CWT) ……....28**

**4.3.1 Scalogram and Pooled Scalogram…….....29**

**4.4 Non-Negative Matrix Factorization (NMF)…….....31**

**4.4.1 NMF-based synergy extraction from sEMG signal……...32**

**5 Materials and Methods…….....34**

**5.1 Dataset.....34**

**5.1.1 Participants.....34**

**5.1.2 Experimental setup and experimental protocol.....35**

**5.2 EMG Signal Processing.....37**

**5.2.1 EMG Signal Filtering and Noise Reduction.....37**

**5.2.2 NMF.....40**

**5.2.3 CWT-based scalogram and pooled scalogram.....42**

**6 Results.....43**

**6.1 Results of 31 Subjects……..……...44**

**7 Discussion.....109**

**7.1 Conclusions.....112**

**Bibliography.....113**

# Abstract

This study proposes and validates an advanced method, the pooled scalogram, for quantifying muscle synergies in the time-frequency domain. The pooled scalogram, originally developed by Borzelli et al. at the Polytechnic University of Marche, enables a more detailed analysis of muscle co-activation compared to traditional methods. In this research, the pooled scalogram was applied to surface electromyography (sEMG) signals collected from five lower limb muscles, Tibialis Anterior, Lateral Gastrocnemius, Rectus Femoris, Vastus Lateralis, and Hamstrings, during a motor task. The signals were pre-processed using a 50 Hz notch filter, rectified, and normalized to ensure proper analysis. Subsequently, Non-Negative Matrix Factorization (NMF), a method commonly used to decompose sEMG signals into simpler components, namely muscle synergies, was applied, selecting the optimal number of modules to explain at least 90% of the variance in the sEMG signals. This process yields two fundamental matrices, W and C. The W matrix suggests the muscle composition of a synergy, by representing how much each specific muscle contributes to each synergy. On the other hand, the C matrix reflects such temporal organization; it provides an outline of when each synergy is recruited (or not) on motor task accomplishment. The W and C matrices, taken together, offer a full account of the muscle content of the synergies as well their associated activation timing with respect to movement. The results revealed that the Rectus Femoris (RF) and Vastus Lateralis (VL) were the most frequently co-active muscles during the motor task. To identify the synergy where these muscles were most active, the sum of squares of the weights for these muscles was calculated, and the pooled scalogram was generated, including all muscles and excluding contributions below 0.2. The results indicate that the pooled scalogram is highly effective in characterizing and quantifying muscle synergies, with potential clinical applications for assessing neuromuscular conditions and monitoring motor rehabilitation. By identifying key muscles involved in co-activation, this approach opens new perspectives for designing personalized rehabilitation strategies.

# 1 Introduction

Human movement is a complex process that regulates the coordinated action of muscles, bones, and ligaments through the control of the central nervous system (CNS). Whether during walking, maintaining balance, or engaging in demanding activities such as athletic performance or rehabilitation, the CNS is considered a key element [1]. The CNS manages multiple muscles, each of which contributes dynamically to movement, and given the complexity of the musculoskeletal system, it requires a strategy to efficiently manage this complexity [2]. One way the CNS achieves this result is through muscle synergies, a concept that refers to groups of muscles being activated together as a unit to perform a task. This means that the CNS does not control each muscle in isolation but simplifies the control of movement by activating these synergies [3]. By using synergies, the CNS reduces the complexity of motor control, making it more efficient. Many studies have shown that a small number of synergies can explain a wide range of movements, from walking and running to more specialized motor activities [4]. This strategy helps the CNS manage motor redundancy, meaning the human body has more muscles than are strictly necessary for most movements. While this redundancy allows for flexibility, it also complicates coordination. Synergies offer a solution by reducing the number of variables that the CNS must handle [5] and non-negative matrix factorisation (NMF), which breaks down complex electromyographic (EMG) signals into simpler components, can be used to analyse them. Using the NMF, researchers can identify groups of muscles that activate together, shedding light on the synergies underlying movement control. The NMF has proven particularly useful for analysing repetitive tasks such as walking, where stable patterns of muscle activation emerge over time [6]. However, while NMF has provided valuable insights into the temporal dynamics of muscle synergies, it often overlooks another important aspect: the frequency domain. Muscle force production is influenced not only by the timing of muscle activation but also by the frequency at which muscles fire. For example, during tasks requiring precise motor control or high levels of effort, different frequency bands can reflect different levels of muscle force. Ignoring the frequency domain can thus limit our understanding of how muscles work during complex tasks [7]. To capture both the timing and frequency aspects of muscle activity, newer techniques such as the Continuous Wavelet Transform (CWT) have been introduced. CWT provides a more comprehensive picture of muscle activation, allowing

researchers to study how muscles coordinate not just over time but across different frequency ranges as well [8]. This approach is particularly useful for understanding complex movements such as walking or running, in which both precise timing and muscle force control are required. Based on these advances, Borzelli et al. [2] developed the pooled scalogram, which is constructed by analyzing the co-scalograms of multiple muscles, so as to represent not the single activation but the synergy between the muscles under examination, in the time and frequency domain. Initially tested in gait analysis, the pooled scalogram has proven to be a powerful tool for understanding how muscle synergy's function. In this study, the work of Borzelli et al. [2] was extended by applying the pooled scalogram technique to surface electromyography (sEMG) signals recorded from five specific muscles of the lower limb, namely Tibialis Anterior, Lateral Gastrocnemius, Rectus Femoris, Vastus Lateralis and Hamstrings, during walking.

Specifically, the aim of the present study is to evaluate the applicability of the pooled scalogram [2], for analyzing walking by using CWT cross-energy localization to quantify muscle synergies in the time-frequency domain. The validation during walking was carried out by directly comparing the results of the pooled scalogram approach with those obtained using NMF, which is one of the most widely employed methods for muscle synergy analysis [6]. By analysing the data through the pooled scalogram, there is an opportunity to provide new insights that can improve clinical approaches to rehabilitation for individuals with motor disabilities.

# 2 The Central Nervous System

The central nervous system plays a critical role in motor function, integrating and coordinating all human movement from voluntary functions (e.g. walking) to involuntary functioning such as balance and reflex response [9]. Given the need for fine-tuning muscle coordination and proper information processing to modify movements according to both external environments and internal conditions of the body, it is easy to see that this layered structure obeys an intricate CNS network [1].

## 2.1 Structure of the Central Nervous System

The core nervous system is composed of bilaterians central nervous systems (CNS), that consist in the brain and spinal cord. Such a system is composed of countless neurons, responsible for decoding sensory inputs and producing motor outputs with the result that human movement (voluntary actions) as well as reflexes and balance (involuntary functions), are controlled very accurately [1]. The brain, the largest and most complex part of the CNS, is surrounded by the skull, so it also has a series of structural defences. It is separated into two halves with a white matter seizure at the center called corpus callosum for communication between these two sides. These are then divided into 4 lobes: frontal, parietal, temporal and occipital. Each lobe performs specialized functions essential for movement, perception, and cognition. For instance, the frontal lobe controls in voluntary motor control and executive functions, while the parietal lobe integrates sensory information, and the occipital lobe is primarily involved in processing visual stimuli (Figure 1) [9].

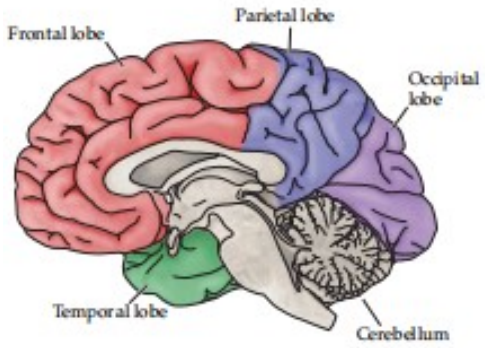



***Figure 1. Major Lobes of the Brain.***

Beyond the cerebral cortex, subcortical systems play an essential feature withinside the law of movement. Among these, the basal ganglia are vital for modulating voluntary movement. The cerebellum, frequently known as the "coordination center" of the mind, is prime for motor coordination, balance, and motor learning. It guarantees that motor instructions are finished easily and appropriately via way of means of integrating sensory inputs and adjusting actions in actual time [10]. These subcortical areas paintings in live performance with the cerebral cortex to alter movement, underscoring the complexity and interdependence of the CNS in motor control [1]. The brainstem, located at the bottom of the mind, serves as a critical connection among the mind and the spinal twine. It includes the midbrain, pons, and medulla oblongata, which collectively alter vital autonomic features together with breathing, blood pressure, and coronary heart rate. The spinal twine, a protracted and slim column of nerve tissue extending from the brainstem to the decrease back, is split into cervical, thoracic, lumbar, and sacral segments. Each of those segments controls particular areas of the frame and serves because the number one conduit for motor instructions from the mind to the muscles, in addition to sensory facts relayed from the frame to the mind [10]. The CNS is likewise covered via way of means of numerous protection mechanisms. These consist of the meninges, which include 3 layers: the dura mater, arachnoid mater, and pia mater. Together, they offer mechanical safety and structural guide for the mind and spinal twine [9]. Another shielding degree is the cerebrospinal fluid (CSF), which cushions the mind and spinal twine at the same time as imparting vital vitamins and retaining intracranial pressure. Additionally, the blood-mind barrier safeguards the CNS via way of means of selectively filtering dangerous materials from the bloodstream and permitting handiest essential vitamins to biskop through [1].

## 2.2 Physiology of the Central Nervous System

The frame shape of the CNS is basically rooted in its capability to regulate sensory and motor abilities via a complex network of neurons. Neurons communicate thru synapses, wherein neurotransmitters like glutamate and gamma-aminobutyric acid (GABA) performs an essential function. Glutamate, because the precept excitatory neurotransmitter, lets in signal transmission amongst neurons, at the same time as GABA acts due to the fact the primary inhibitory neurotransmitter, preventing excessive neuronal firing and preserving the critical balance for coordinated movement [1]. Key structures concerned in motor manage embody the cerebellum and the basal ganglia. The cerebellum constantly video show devices and fine-tunes movements to make sure they'll be smooth and accurate, at the same time as the basal ganglia facilitate the selection of appropriate motor movements and inhibit unwanted movements. These strategies are essential for duties like walking, wherein regular adjustment is critical to keep balance and adapt to uneven terrain or specific environmental challenges [9]. The spinal cord, every distinctive critical a part of the CNS, performs a extraordinary function in transmitting motor alerts from the mind to muscle corporations and conveying sensory records from the frame once more to the mind. It furthermore mediates reflex actions, which embody the stretch reflex, which permits rapid, involuntary responses to stimuli like muscle stretch, keeping muscle tone and stopping injury [10]. Another critical detail of the CNS`s capability is motor learning, the tool through which moves are touchy through practice. This is essentially ruled with the beneficial aid of using synaptic plasticity mechanisms which embody long-time period potentiation (LTP), which strengthens neural connections. This tool complements motor standard overall performance and accuracy over time, allowing humans to recognize each recurring duties like taking walks and additional complicated motor skills [1]. The integration of sensory and motor records is vital for specific motion control. Proprioceptive receptors, which constantly supply records approximately frame and limb position, permit the CNS to regulate moves in actual time. The cerebellum perfects those moves, making sure they stay coordinated and fluid. In situations which includes Parkinson`s disorder, the position of the basal ganglia in modulating motor interest turns into especially evident. Symptoms such as tremors, muscle rigidity, and problems in motion manage spotlight the significance of those structures in handling voluntary motor manage. Parkinson's disease is characterized by degeneration of dopamine-generating cells within the basal ganglia, particularly in the substantia nigra,

impairing the brain's ability to easily manage movements. This emphasizes the essential position of the basal ganglia in motor regulation [9].

### 2.3 CNS Control of Movement

The central nervous system (CNS) controls both voluntary and involuntary movements by coordinating actions through various structures, such as the cerebral cortex, cerebellum, basal ganglia, brainstem, and spinal cord. The primary motor cortex (M1) regulates voluntary movements, such as grasping an object or walking, by sending signals to the muscles through the corticospinal tract. This pathway is essential for controlling fine motor movements, particularly in distal muscles, such as those in the hands and fingers [1]. The premotor cortex and the supplementary motor area (known as SMA) play a role in organizing and coordinating complex movements. Information is combined in these areas to facilitate activities that require precision and timing, such as reaching for objects or performing a series of coordinated movements [10]. There is also cerebellum which resides in the back of our brain, and this regulates and refines all those motor commands based upon perception that we have -- again to help us move smoothly, quickly, accurately. This is especially important when it comes to balance and coordination, which are needed for walking. By modulating movement imitative and inhibitory control through both direct and indirect pathways, the basal ganglia provide coordination of motor acts. Motor deficits in disorders involving basal ganglia, including Parkinson's disease (PD), which attests the extraordinary importance of these structures for motor control [1]. The brainstem and spinal cord also contribute to motor control. In particular, the brainstem regulates postural adjustments and reflex integration, supporting dynamic activities such as walking through pathways like the reticulospinal and vestibulospinal tracts, while the spinal cord manages reflexive movements and rapid responses to external stimuli, which are crucial for maintaining balance and preventing injuries [10]. These descending systems send signals to local circuit neurons and motor

neuron pools in the spinal cord, which in turn activate the skeletal muscles for movement coordination (Figure 2).

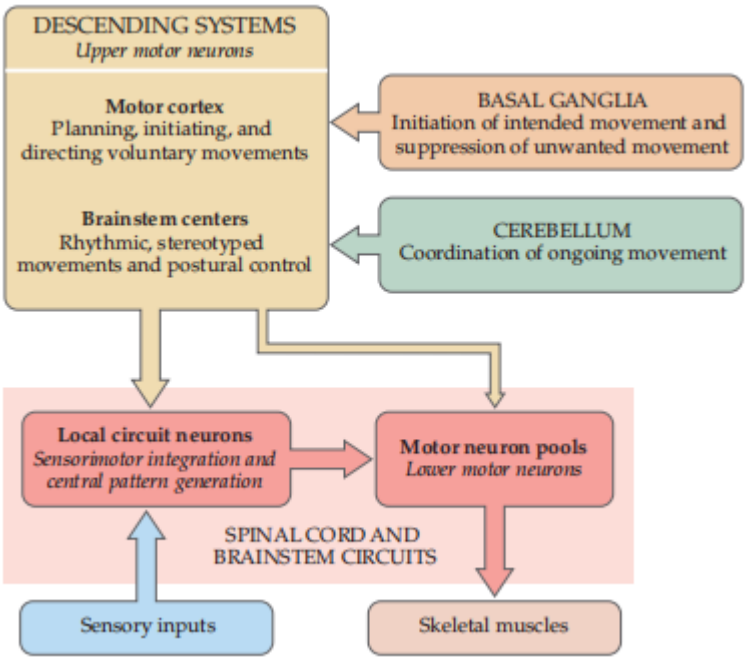



***Figure 2. Organization of neural structures.***

Through proprioception, the CNS is always kept abreast of what movements the body are making and therefore what adjustments need to be made in real time. In fact, this feedback, in conjunction with visual and vestibular information are essential for maintaining balance and orientation. With repetition, the brain performs movement more efficiently and effectively as well, due to neural plasticity, whereby the brain changes and adapts with experience. The movement when repeated begins to forge the connections strength (neurons) resulting in that movement. This process is known as long-term potentiation and serves to refine movements to improve accuracy and speed over time [11].

## 2.4 Motor Synergy and CNS Coordination

Motor synergies refer to the CNS's strategy for managing the complexity of movement. Instead of controlling each muscle individually, the CNS activates groups of muscles in coordinated patterns known as synergies. This modular approach significantly reduces the number of variables the CNS must control, making movement more efficient and adaptable [2]. During walking, a limited number of muscle synergies can explain most of the muscle activity required to maintain balance and propel the body forward. Research has demonstrated that a small set of basic synergies underlies the control of human locomotion. For example, Ivanenko et al. [11] identified five fundamental synergies that account for most of the muscle activity during walking. This suggests that the CNS optimizes motor control by selecting and modulating these synergies in response to different walking conditions [12]. As mentioned in section 2.3, the cerebellum and basal ganglia adjust motor output based on sensory feedback, and these structures allow the CNS to modify synergies in real time to adapt to various situations, ensuring that movements remain smooth and stable. For instance, the stretch reflex enables rapid adjustments in muscle activation in response to external stimuli without requiring input from higher brain centers [10]. This is particularly relevant in rehabilitation settings, where restoring functional synergies is essential for improving motor control in individuals with neuromuscular impairments [11].

# 3 Gait analysis

Gait analysis represents the detailed study of walking patterns and provides information on posture, stride, joint functionality, and coordination between the nervous system and the musculoskeletal system. It is, therefore, a tool for understanding the biomechanics of human movement. It distinguishes between normal walking patterns, found in healthy individuals, and abnormal patterns, present in individuals with medical conditions. This helps in diagnosing disorders, optimizing athletic performance, and designing orthopedic devices and prostheses [13]. The analysis is compared with a healthy subject to detect abnormal behaviors and thus pathological conditions [14].

## 3.1 Gait cycle

The gait cycle (GC) is the fundamental unit of walking, comprising the movements of one leg from the moment its heel contacts the ground until the same heel strikes again. This cycle is divided into two main phases: the stance phase, during which the foot is in contact with the ground (60 % of GC), and the swing phase, during which the foot is airborne as it moves forward for the next step (40% of GC) (Figure 3) [12].




***Figure 3. Divisions of the gait cycle.***

Within the stance phase, there are several sub-phases that describe the body's progression during walking:

- Initial contact: The heel strikes the ground, beginning the weight-bearing process (Figure 4).

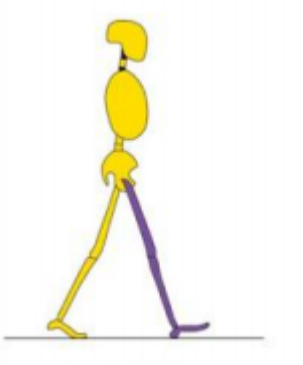


***Figure 4. Phase of Initial Contact.***

- Loading response: The body absorbs shock as the foot fully contacts the ground, with the knee and hip providing stabilization (Figure 5).

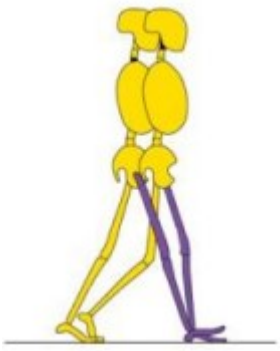


***Figure 5. Phase of Loading Response.***

- Mid-stance: The body's weight moves over the foot, supported by the hip abductors and quadriceps [12] (Figure 6).

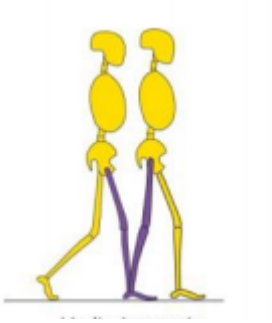


***Figure 6. Phase of Mid-stance.***

- Terminal stance: The heel rises, and the body pushes forward using the gastrocnemius and soleus muscles [12] (Figure 7).

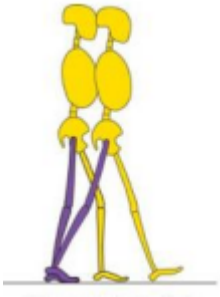


***Figure 7. Phase of Heel Off.***

- Pre-swing: The foot leaves the ground, and the weight shifts to the opposite limb [12] (Figure 8).

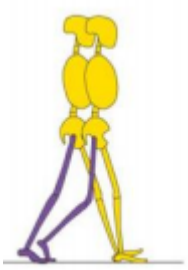


***Figure 8. Phase of Toe Off.***

The swing phase also consists of key movements:

- Initial swing: The foot lifts off the ground, with the knee flexing to help clear the ground [12] (Figure 9).

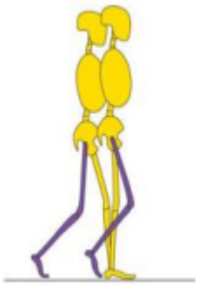


***Figure 9 . Phase of Initial Swing.***

- Mid-swing: The leg advances as the hip flexes, positioning the foot forward [12] (Figure 10).

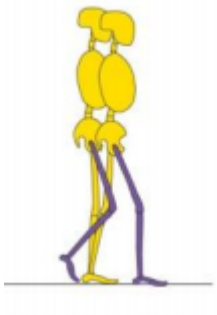


***Figure 10. Phase off Mid Swing.***

- Terminal swing: The knee extends, preparing the foot for the next heel strike [12] (Figure 11).

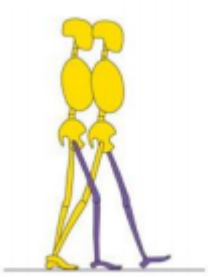


***Figure 11. Phase of Terminal Swing.***

Balance, propulsion, and transitions between steps are ensured by a coordinated sequence of muscle activities in each phase (Figure 12). If there are no abnormalities, such as changes in muscle activity coordination or strength, this could indicate the presence of pathologies [14].

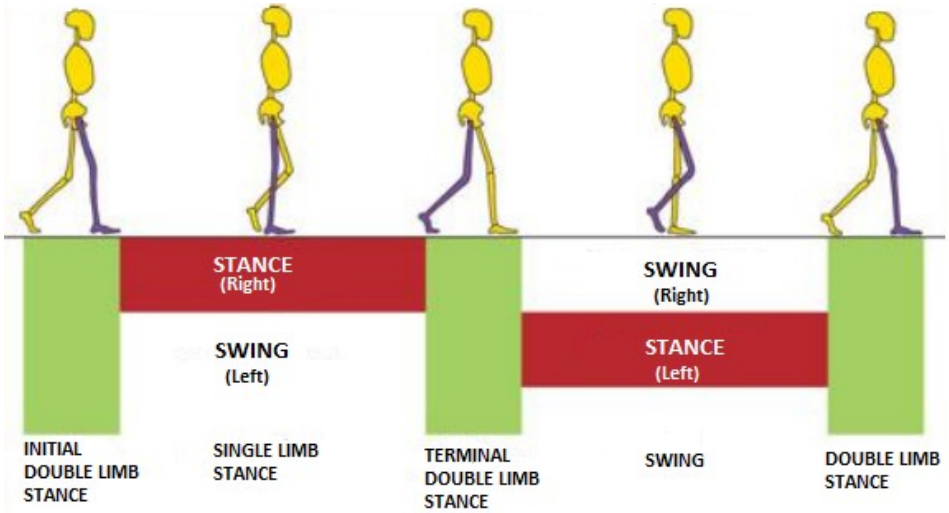



***Figure 12. Subdivisions of the gait cycle.***

## 3.2 Fundamental Functions of Gait

The fundamental functions of gait are critical to achieving efficient and safe locomotion. These include propulsion, shock absorption, stabilization, and adaptation, all of which are coordinated by the central nervous system (CNS). The CNS manages two main components during walking: the locomotor system, responsible for generating movement, and the passenger unit, which involves the stabilization of the upper body (Figure 13) [12].

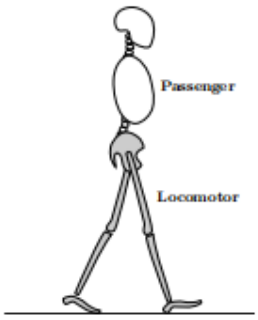



***Figure 13. Functional division of the body.***

These key functions of gait include:

- Propulsion: Propelling the body forward requires the coordinated action of lower limb muscles, particularly the gastrocnemius and soleus, which are present during the push-off phase. These muscles contract to generate the force needed to lift the body off the ground and move it forward [12].
- Shock Absorption: As the foot contacts the ground, the body must absorb the resulting impact forces. This is where muscles such as the quadriceps come into play. By contracting eccentrically, they cushion the knee and reduce the stress on the joints. Simultaneously, the tibialis anterior helps control the foot's descent to prevent a "foot slap" upon landing [12].
- Stabilization: Maintaining balance during walking requires continuous stabilization of the body, particularly during the stance phase. This involves the hip abductors and trunk muscles, which work together to control the center of mass and keep the body steady, preventing excessive sway or imbalance [12].

- Adaptation: Walking is not a repetitive activity; the body constantly adapts to changes in the environment, such as uneven terrain or varying walking speeds. This adaptability is governed by the CNS, which utilizes sensory inputs, especially from the proprioceptive system, to make quick adjustments in muscle coordination [14].

Gait analysis can be used not only as a diagnostic tool but also as a useful instrument for analyzing a patient's progress during therapy. It allows doctors to adjust treatment plans according to the patient's needs, thus ensuring optimal results [14].

## 3.3 Analysis of Normal Gait

During each phase of the gait cycle, specific joints contribute to different functions:

- Knee Joint: During the stance phase, the knee extends to support the body's weight, while during the swing phase, it flexes to ensure the foot clears the ground.
- Hip Joint: The hip moves through both flexion and extension throughout the gait cycle, contributing to forward propulsion and providing stabilization of the pelvis during the stance phase [15].
- Ankle Joint: The ankle plays a pivotal role by controlling foot placement during initial contact and providing the strong push-off needed for propulsion during the terminal stance phase [12].

Throughout the gait cycle, the central nervous system (CNS) coordinates muscle activation to maintain posture, conserve energy, and respond to environmental demands.

For instance, when we lift the front part of the foot, so that it does not touch the ground, the Tibialis Anterior is activated. Its activity peaks at the beginning of the swing phase and decreases as the foot prepares to strike the ground again (Figure 14) [12].

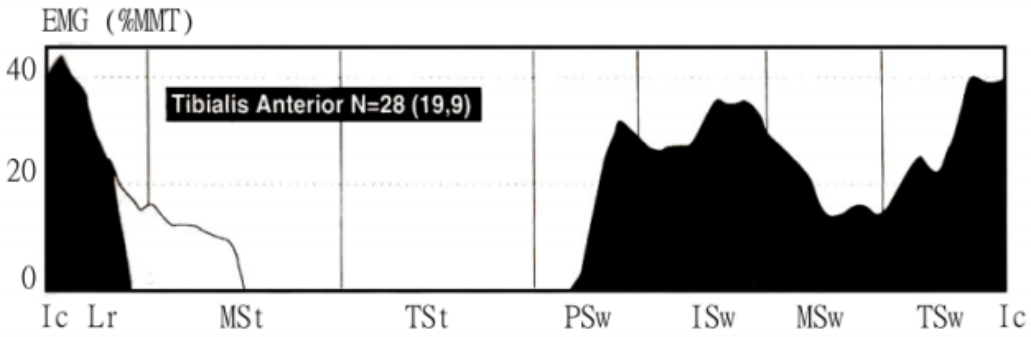



***Figure 14. EMG Activation of Tibialis Anterior.***

Similarly, the Gastrocnemius activates during the late stance phase, providing essential force to push the body forward during walking. This muscle is particularly active during the terminal stance, propelling the body into the next step (Figure 15) [12] [16].

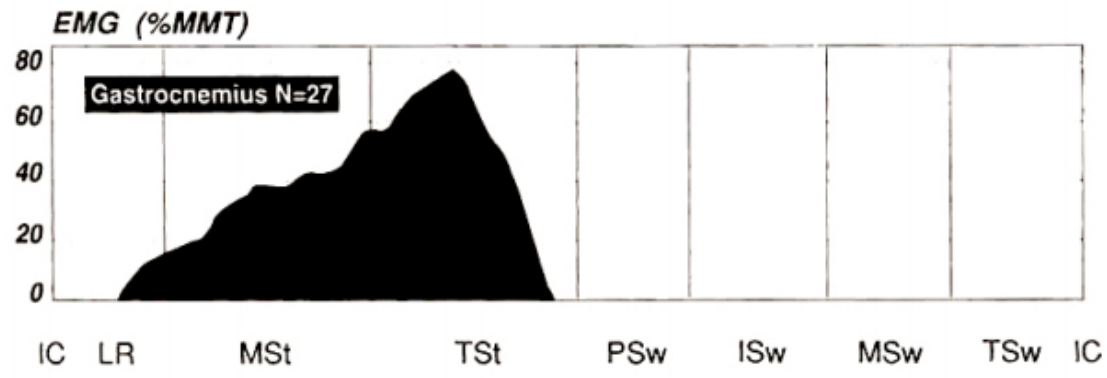



***Figure 15. EMG Activation of Gastrocnemius.***

The Rectus Femoris and Hamstrings exhibit complementary activation patterns. The Rectus Femoris is engaged during the swing phase, contributing to hip flexion and knee extension, especially during the pre-swing and initial swing phases (Figure 16) [12] [15].

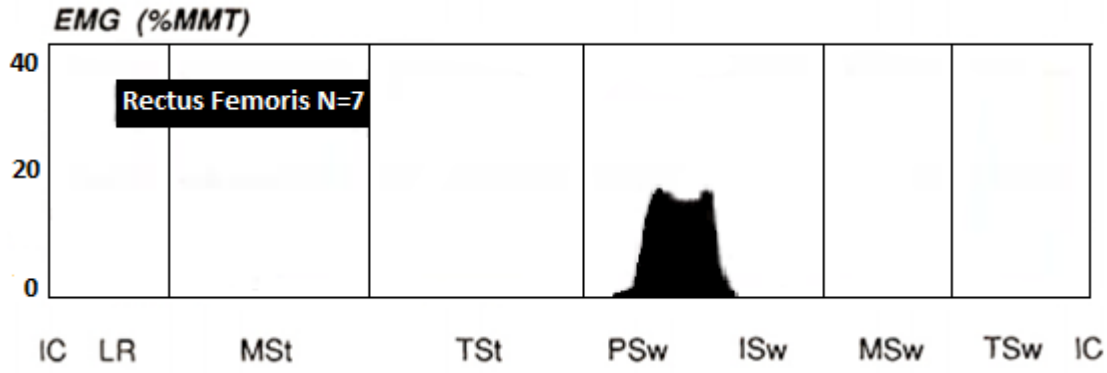



***Figure 16. EMG Activation of Rectus Femoris.***

In contrast, the Hamstrings are primarily active during the terminal swing, slowing the forward motion of the leg and stabilizing the knee joint as the foot prepares for heel strike (Figure 17) [12].

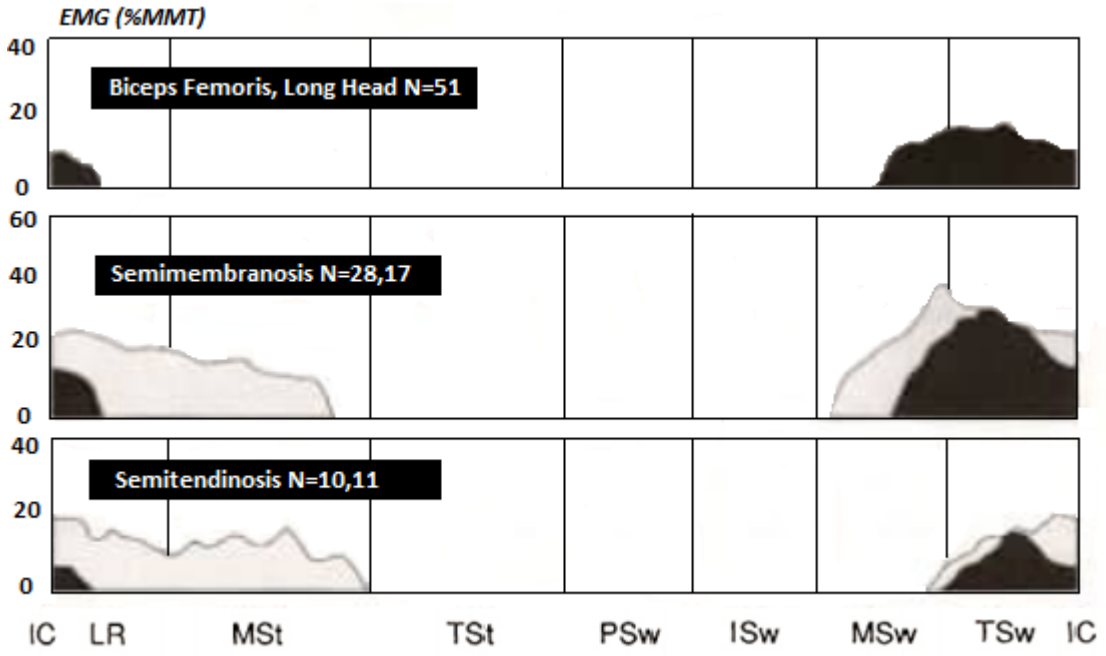



***Figure 17. EMG Activation of Hamstrings.***

Lastly, the Vastus Lateralis, part of the quadriceps group, provides knee stability during the stance phase, peaking in activity during the terminal swing and early stance phases (Figure 18) [12] [15].

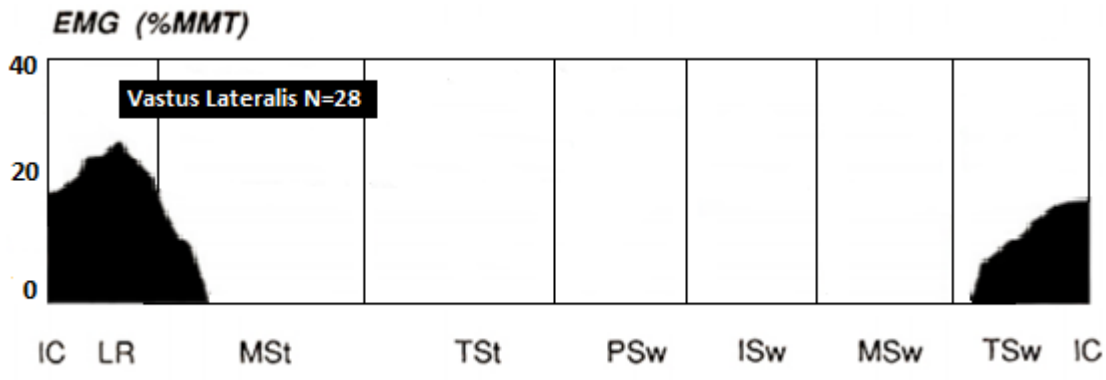



***Figure 18. EMG Activation of Vastus Lateralis.***

Abnormal gait patterns often arise from neurological impairments, muscle weakness, or joint pathology [16].

## 3.4 Muscle Synergy During Gait Cycle

Without muscle synergies, there would not be an organization that allows for efficient and adaptable movements, enabling individuals to walk smoothly and adjust their gait [17]. Several studies have identified fundamental muscle synergies consistently activated during walking, demonstrating how the CNS reduces the complexity of motor control. For example, Ivanenko et al. [11] identified five core synergies responsible for most muscle activity during locomotion. These synergies involve groups of muscles that coordinate their actions to perform different phases of the gait cycle:

1. **First Synergy (Early Stance Phase)**: Muscles such as the gluteus maximus, quadriceps, and gastrocnemius stabilize the body as the heel strikes the ground and prepares for weight acceptance.
2. **Second Synergy (Mid-Stance Phase)**: As the body's center of mass moves forward, weight support and balance maintenance rely on the coordinated action of the soleus, gastrocnemius, and hamstrings. This coordination ensures stability when the body is supported by a single limb.
3. **Third Synergy (Late Stance Phase)**: The triceps surae (gastrocnemius and soleus) generate the propulsion needed to push the body forward during the push-off phase.
4. **Fourth Synergy (Swing Phase)**: The rectus femoris and tibialis anterior lift the foot off the ground, allowing it to swing forward without dragging, preparing for the next step.
5. **Fifth Synergy (Pre-Heel Strike)**: As the leg moves forward, the hamstrings and gastrocnemius decelerate the motion to ensure a controlled landing during heel strike [18].

A key feature of these muscle synergies is their flexibility. While the core synergies are present in all individuals, their activation can adapt to meet different task demands, such as varying terrain, walking speed, or fatigue. Previous research has shown that the central

nervous system (CNS) exerts exquisite control over when and to what extent muscles are functionally grouped into synergies, optimizing movement speed, efficiency and versatility. It is suggested that this homeostasis mechanism is especially important when individual muscle synergies are restricted in the normal population due to damage to higher centres, e.g. stroke or cerebral palsy, so that the motor system loses its capacity for optimal synergy recruitment. As a result, they have less efficient gait patterns and use compensations which require more energy. An insight into normal muscle synergies is a stepping stone to design rehabilitation strategies that aim at regaining efficient movements. In fact, different approaches such as strength training with a targeted muscle or robot-assisted therapies could be utilized to re-train the CNS and improve co-ordination of muscles balance thus flexibility [19] [20]. Research on muscle synergies remains as an important source of information about the strategies used by the CNS to solve the motor control problem. This has now moved classical clinical practice one step further, as rehabilitation professionals are provided with the ability to design individualized interventions that target specific motor deficits. Targeting interventions to correct the disturbances of muscle synergies might further enhance recovery and movement competency in patients with gait disorders [21].

# 4 EMG Signal Processing Techniques

This chapter gives a comprehensive review on the basic methods and main conceptual approaches employed in the analysis of electromyographic (EMG) signals, especially surface EMG (sEMG). This study investigates this new approach, termed the pooled scalogram and then compares it with some current methods to help determine whether this provides greater information on muscle coordination and synergy.

This chapter starts with the brief introduction of sEMG, and its features and uses before proceeding to several treatment methods that can help improve processing quality as well as outcomes of EMG. Lastly, more sophisticated methods such as the Continuous Wavelet Transform (CWT) and Non-Negative Matrix Factorization (NMF), which are particularly important for our work on examining muscle activation patterns during dynamic activities like walking.

## 4.1 Surface EMG

Surface electromyography (sEMG) is a widely adopted, non-invasive technique for recording muscle activity through the detection of electrical signals generated by muscle fibers during contraction. Unlike needle EMG, which involves inserting electrodes directly into the muscle tissue, sEMG uses electrodes placed on the skin surface. This makes it ideal for applications where long-term monitoring or dynamic tasks, such as walking, need to be studied [22].

One of the primary advantages of sEMG is its ability to provide real-time data on the timing, intensity, and duration of muscle activation during movement. The quality of the sEMG signal largely depends on the type and placement of electrodes. For example, gel electrodes are commonly used in clinical and research settings for their ability to reduce impedance and improve signal quality (Figure 19).



***Figure 19. Example of Gel electrodes.***

Several electrode configurations are utilized in sEMG to optimize signal detection while minimizing interference from surrounding muscles. Bipolar electrodes are widely used due to their effectiveness in capturing muscle activity while filtering out external noise. In more complex movements, tripolar configurations can further reduce interference by adding a third electrode to improve signal isolation [23].

For accurate signal collection, electrode placement is critical, and guidelines such as those established by the SENIAM (Surface EMG for Non-Invasive Assessment of Muscles) project provide a standardized framework. These guidelines ensure consistency in electrode positioning and skin preparation, which is essential for both clinical and research applications [24].

In biomechanics, sEMG plays a pivotal role in analyzing muscle function during dynamic activities, improving the development of rehabilitation protocols, and even preventing injuries by understanding how muscles work together during movement [25]. However, the method is limited to surface muscles, and cross-talk from nearby muscles can complicate the interpretation of data. Careful electrode placement and data filtering are essential to mitigate these challenges [26].

## 4.2 EMG signal processing

The electromyographic (EMG) signal captured by surface electrodes represents the electrical activity of muscles, reflecting the action potentials generated by muscle fibers during contraction. However, the raw signal is often influenced by various forms of noise and artifacts, which must be removed for accurate clinical or biomechanical analysis. The goal of EMG signal processing is to isolate the key information about muscle activity, enabling a clear interpretation of how muscles work together during movement. One of the first steps in processing EMG data is to filter out noise. A common source of interference is the electrical grid, which operates at 50 or 60 Hz depending on the country. To address this, notch filters are employed to remove this specific frequency. Then, high-pass filters help eliminate low-frequency signals associated with motion artifacts, while low-pass filters target irrelevant high-frequency components. Advanced techniques, such as adaptive filtering, have proven particularly useful in dynamic scenarios like walking or athletic performance. These methods not only suppress noise more effectively but also improve signal stability during sudden or rapid changes in muscle activity. Some studies suggest that hardware-based denoising, such as spatial filtering, can further enhance the signal-to-noise ratio, improving data quality from the start of the acquisition process [26]. Once the noise has been minimized, the next step is rectification, where negative values in the bipolar EMG signal are converted to positive values. This allows for the total muscle activity to be calculated over time, providing a more complete picture of muscular effort without losing key details. Smoothing techniques like moving averages or the Root Mean Square (RMS) method further clarify the signal by creating a more continuous representation of muscle activity. Advanced smoothing methods, such as the Savitzky-Golay filter, are used to preserve the essential features of the muscle activity while still enhancing the signal's visual clarity [27]. To compare EMG data across subjects or even experimental sessions, normalisation was necessary. It typically calls for normalization of the signal to a Maximum Voluntary Contraction (MVC) in every individual. Normalization minimizes variability and enables better comparisons of data between sets so that muscle function can be more readily interpreted across individuals or conditions. Normalization should include biomechanical considerations - like limb position or joint angle during muscle contraction to achieve more accurate measures as other studies have shown [28]. A crucial part of EMG analysis is determining when muscles begin and end

their activity, known as onset and offset detection. This is typically done by applying thresholds to the rectified and smoothed signal, identifying points where muscle activity exceeds a baseline level of noise. More refined methods, like frequency analysis, provide even more precision in identifying these events. The frequency content of the signal can be used to offer better understanding on muscle control mechanisms, when high-intensity or complex movements are performed [29]. Many algorithms can also convert the EMG signal into a spectrum, such as Fourier Transform (FFT), Continuous Wavelet Transform (CWT) etc. These methods facilitate analysis of how energy is distributed across different frequency bands and thus provide a nuanced representation of muscle activation over different phases of movement. CWT offers a more sophisticated analysis, as it captures transient events and provides insights on both time and frequency distributions [30].

## 4.3 Continuous Wavelet Transform (CWT)

The Continuous Wavelet Transform (CWT) is a useful mathematical method often used for signal analysis, e.g., needs in electromyographic (EMG) signals processing since it allows representing the signal in its time and frequency domains simultaneously. But instead of using sine and cosine waves of infinite duration as in the Fourier case, it employs wavelets, which are oscillatory functions localized in space. These wavelets enable detection of transient events making the CWT especially relevant to muscle activation which is characterized by rapid changes in the signal. The CWT reduces a signal to wavelets, which are dilated and shifted versions of a “mother wavelet”. With the CWT, it comes with a mother wavelet is its core function which stretches and compresses to match different frequencies within the signal.

Mathematically, this process is expressed as follows:

$$CWT_x(t, a, b) = \int x(t) \cdot \psi^*_{a,b}(t)dt \quad (a \neq 0) \tag{1}$$

where the basis function $\psi_{a,b}(t)$ represents the mother wavelet, which acts as a bandpass filter oscillating in the time domain. The wavelet is characterized by scale *a* and shift *b* parameters, defined as follows:

$$\psi_{a,b}(t) = \frac{1}{\sqrt{a}} \cdot \psi\left(\frac{t-b}{a}\right) \tag{2}$$

In equation (2), *a* represents the scale parameter, controlling the dilation or compression of the wavelet. The mother wavelet $\psi_{a,b}(t)$ is designed to act as a bandpass signal, quickly decaying in time to ensure good time resolution. One of the main advantages of the CWT is its invertibility, meaning that the original signal can be reconstructed from its wavelet coefficients without losing any information. This is essential because it ensures that during the transformation process, no critical signal information is lost everything is simply rearranged in the time-frequency domain. However, a limitation of the CWT is that, in many studies, it often provides qualitative rather than quantitative results. This is due to the complexity of converting a one-dimensional time series into a two-dimensional time-frequency image, making it harder to extract precise numerical data from the wavelet coefficients [8].

### 4.3.1 Scalogram and Pooled Scalogram

A scalogram is a graphical representation commonly used in signal processing and wavelet analysis. It displays how the energy of a signal is distributed over time and across different frequency bands. In this plot, the x-axis represents time, the y-axis represents frequency (or scale), and the color intensity indicates the magnitude (or energy) of the signal at a specific time and frequency (Figure 20). This type of visualization is extremely useful for understanding the dynamic behavior of a system over time. The scalogram helps in visualizing how the frequency characteristics of a signal change over time, making it a powerful tool in both research and clinical settings for analyzing time-frequency energy density [2].

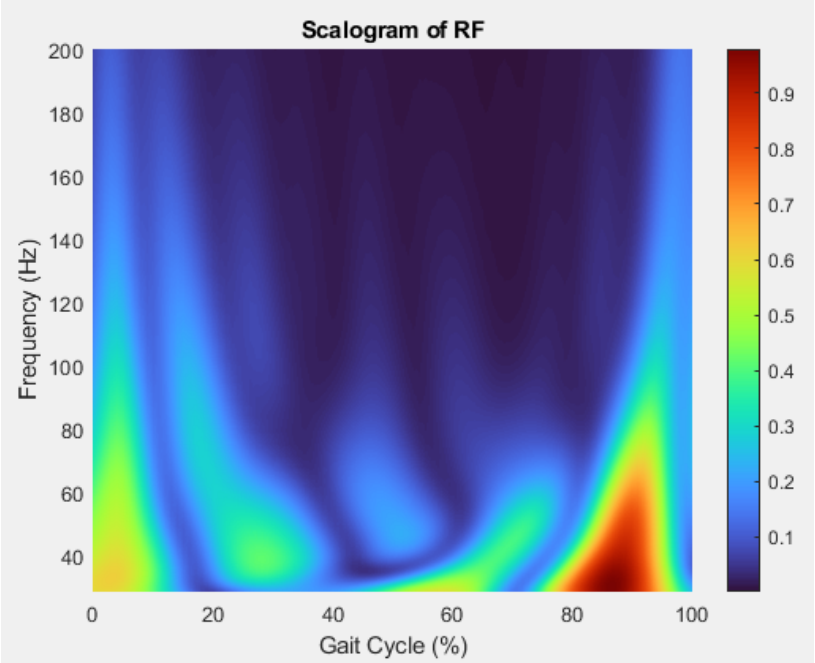



***Figure 20. Example of scalogram of Subject 1.***

The mathematical representation of the scalogram function, $P_x(a,b)$ is:

$$P_x(a,b) = W_x|(a,b)| \tag{3}$$

where, $W_x(a,b)$ represents the matrix of wavelet coefficients at time $b$ and scale $a$, which are derived from the CWT. Each point on the scalogram corresponds to a specific time-frequency combination, and the color intensity at that point indicates the energy level of the wavelet coefficient at that time and frequency.

The pooled scalogram, developed by Borzelli et al. [2], is an advanced method that builds on the coscalogram by analyzing the co-activation of more than two muscles simultaneously. This technique is especially useful in contexts such as walking, where coordination between multiple muscles is crucial. The pooled scalogram provides a comprehensive view of muscle coordination by extending the coscalogram's methodology to analyze multiple signals together.

The pooled scalogram function $PSC_x(a,b)$ is computed as follows:

$$PSC_x(a,b) = [W_{x1}(a,b) \cdot W_{x2}^*(a,b)] \cdot W_{x3}^*(a,b) \quad (4)$$

In this equation, $W_{x1}(a,b)$, $W_{x2}(a,b)$ and $W_{x3}(a,b)$ represent the matrices of CWT coefficients for the three signals at scale *a* and time *b*. This method quantifies the cross-correlation of muscle activation patterns and is a powerful tool for studying the coordination between multiple muscles in the time-frequency domain. It holds significant promise for applications in personalized rehabilitation strategies, especially for improving movement quality in patients with motor impairments [2].

## 4.4 Non-Negative Matrix Factorization (NMF)

Non-negative Matrix Factorization (NMF) is a mathematical technique used in data analysis and machine learning, useful to extract meaningful patterns or components from complex datasets. The approach is deeply scientific and engineering-oriented, namely that there is a hidden order, a simple structure underneath the chaos, beneath an apparent complexity. Multivariate data analysis, especially with the aid of new technological progress, necessitates good dimensionality reduction techniques. Now, in this context, it becomes very important to lessen down the feature set of its original data and finding Principal components (or features) in that data. NMF dimensionality reduction works by taking an original matrix and factorize it into two factor matrices. NMF enforces non-negativity to the factorization and yields a parts-based representation, making it more interpretable than other methods such as PCA or LDA that enable use of negative components [31].

Mathematically, the decomposition of a non-negative matrix *V* can be expressed as:

$$V \approx WH \quad (5)$$

where *V* is the data matrix (e.g., sEMG signals), *W* is the matrix of muscle synergies, and *H* is the matrix of the synergies' temporal activations. The matrix *W* contains synergy vectors representing the relative contribution of each muscle to a synergy, while *H*

describes the temporal activation pattern of each synergy. The value of *r* is usually chosen so that it is smaller than both *n* and *m*, thus reducing the dimensionality of the data.

The non-negative approach allows for a representation of synergies that reflects real data, where negative values do not make sense (for example, in sEMG signals, muscle activations cannot be negative). This non-negativity constraint improves the interpretability of the results, enabling a clearer and more understandable representation [32]. NMF has gained popularity due to its interpretability and ability to handle non-negative data, and it has been applied in various fields such as pattern recognition, image processing, and electromyographic signal analysis.

### 4.4.1 NMF-based synergy extraction from sEMG signal

In the field of biomechanics and electromyographic signal analysis, NMF is widely used to extract muscle synergies from sEMG signals. The sEMG signal, sampled from electrodes placed on multiple muscles, is represented as a matrix *M* with dimensions $N_M \times N_S$, where $N_M$ is the number of recorded muscles, and $N_S$ is the number of time samples. NMF is applied to decompose *M* into two non-negative matrices: the synergy matrix *W*, with dimensions $N_M \times k$, and the activation matrix *H*, with dimensions $k \times N_S$. Each column of *W* represents a synergy vector indicating the relative contribution of each muscle to the synergy, while each column of *H* represents the temporal activation coefficients for each synergy [33].

The quality of the approximation is assessed through metrics such as the Variance Accounted For (VAF) or the coefficient of determination $R^2$, which indicate how well the model explains the total variance in the data. Synergies are extracted by varying the number from 1 up to the total number of recorded muscles, and the minimum number of synergies that exceed a predefined threshold (e.g., a VAF higher than 90%) is selected [34]. NMF is a robust methodology for extracting and quantifying muscle synergies from sEMG signals, providing valuable insights into how muscle groups coordinate over time during complex motor tasks. This approach has great clinical potential, especially for neuromuscular rehabilitation, where muscle synergy analysis provides essential

information on the reorganization of motor control in individuals with neuromotor dysfunctions [33].

# 5 Materials and Methods

The starting point of this work is the pooled scalogram proposed by Borzelli et al. [2]. In brief, the procedure followed to achieve our goal is as follows:

1. Identification of synergies by applying the NMF algorithm to sEMG signals recorded from 5 muscles of the right lower limb.

2. Identification of the synergy of the muscles most frequently co-active.

3. Extraction of contributions greater than or equal to 0.2 from all 5 muscles analyzed.

4. Application of the scalogram pool to the muscles included in the synergy, to quantify their time-frequency content.

## 5.1 Dataset

The original experimental data are part of the PhysioNet online database [35]; they consist in long-lasting (approximately 5 minutes) surface electromyographic (sEMG) signals collected since 2011 and up to 2018 on a population recruited at the Movement Analysis Laboratory, Università Politecnica delle Marche, Ancona, Italy.

### 5.1.1 Participants

Amid the group, 31 like individual young and healthy subjects (normal-bodied), of both sexes aged between 20-30 years. This dataset does not include subjects who are underweight (body mass index, BMI < 18.5 kg/m 2) or overweight and obese (BMI > 25 kg/m 2), have any pathological conditions (including joint pain or orthopedic surgery) (Table 1) [2] [35].

*Table 1. Anthropometric characteristics of recruited subjects.*

| Subject | Gender | Age | Height (m) | Mass (kg) |
|---|---|---|---|---|
| 1 | F | 25 | 1.52 | 45 |
| 2 | M | 24 | 1.82 | 70 |
| 3 | F | 24 | 1.58 | 49 |
| 4 | M | 24 | 1.75 | 76 |
| 5 | F | 22 | 1.64 | 50 |
| 6 | F | 23 | 1.63 | 53 |
| 7 | M | 27 | 1.81 | 66 |
| 8 | F | 23 | 1.64 | 50 |
| 9 | M | 25 | 1.81 | 63 |
| 10 | F | 24 | 1.65 | 60 |
| 11 | F | 23 | 1.65 | 52 |
| 12 | F | 22 | 1.66 | 52 |
| 13 | M | 26 | 1.83 | 76 |
| 14 | F | 23 | 1.6 | 50 |
| 15 | F | 26 | 1.7 | 54 |
| 16 | F | 23 | 1.6 | 50 |
| 17 | M | 22 | 1.75 | 63 |
| 18 | F | 23 | 1.68 | 49 |
| 19 | F | 26 | na | na |
| 20 | F | 26 | 1.68 | 54 |
| 21 | M | 22 | 1.70 | 66 |
| 22 | F | 24 | 1.61 | 54 |
| 23 | M | 27 | 1.74 | 67 |
| 24 | M | 29 | 1.97 | 86 |
| 25 | F | 26 | na | na |
| 26 | F | 24 | 1.7 | 60 |
| 27 | F | 23 | 1.6 | 48 |
| 28 | M | 26 | 1.83 | 76 |
| 29 | M | 21 | 1.86 | 86 |
| 30 | M | 23 | 1.78 | 66 |
| 31 | F | [20;30] | na | na |

### 5.1.2 Experimental setup and experimental protocol

The Step32 multi-channel system (Medical Technology, Italy) was used to record surface electromyographic (sEMG) signals, with a sampling rate of 2000 Hz and a resolution of 12 bits. The target muscles were the Tibialis Anterior (TA), Lateral

Gastrocnemius (GL), Rectus Femoris (RF), Vastus Lateralis (VL), and Hamstrings (HAM), for both the right and left legs.

Electrodes were placed according to the SENIAM guidelines. Prior to application, the participants' skin was prepared by shaving, cleaning with abrasive paste, and disinfecting with alcohol to reduce impedance and improve signal quality. Fixed-geometry electrodes (Ag/AgCl, 4 mm diameter, 8 mm inter-electrode distance) were used for the Gastrocnemius, Tibialis Anterior, Hamstrings, Rectus Femoris and Vastus Lateralis.

The signal was amplified by a factor of 1000, and a high-pass filter at 10 Hz was applied to remove low-frequency noise, followed by a low-pass filter at 450 Hz to eliminate high-frequency interference.

For recording gait events, small footswitches (11×11×0.5 mm, activation force of 3 N) were placed under the heel, the first metatarsal, and the fifth metatarsal of both feet. These footswitches detected heel strike and toe-off, which were essential for segmenting the gait cycle. The electrogoniometers (accuracy of 0.5°) were placed laterally on both legs to monitor knee flexion angles in the sagittal plane, allowing for correlation between joint movements and muscle activity.

Participants were instructed to walk barefoot along a figure-eight-shaped path (Figure 21), which included both straight and curved sections. Each walking session lasted approximately 5 minutes, designed to allow participants to walk at their natural pace, providing complete data on muscle activity under various walking conditions [36] [2].

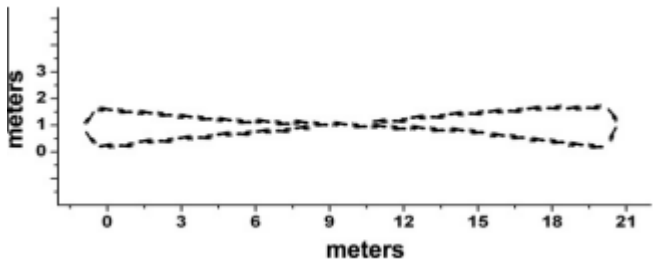



***Figure 21. Schematized representation of the path walked by the recruited subjects.***

## 5.2 EMG Signal Processing

Matlab2022b was used as the implementation environment for EMG signal processing. Pre-processing is performed to clean the signal from noise caused by various interferences.

### 5.2.1 EMG Signal Filtering and Noise Reduction

The first step was to find and extract each gait cycle for each of the subjects. This was done by respective correlation of the sEMG data with footswitches under the heels and metatarsals. These footswitches permitted the determination right toe off and heel strike, which are the events of each step. A gait cycle was determined from heel contact of one foot to heel contact of the same foot to ensure all muscle activation during one cycle is captured. For subject 22, the l final step which probably resulted from strange walking behavior was an outlier and was eliminated from analysis as it was irregular in length.

After performing the steps, the raw sEMG signals (Figure 22) were preprocessed to remove noise and other artifacts. Included was the use of a 50 Hz Notch filter which was meant to reduce powerline interference or distortion caused by electrical gadgets. Then, a 10 Hz high pass filter was further used to eliminate low frequency artefacts such as baseline drifts and movement related noise. Thereafter a 450 Hz low pass filter was used to cut out high frequency oscillations and preserve significant muscle activity. Upon applying the filters, the signals were rectified by converting all negative values to positive, enhancing the clarity of the muscle activation signals (Figure 23). Finally, the rectified signals were smoothed using a moving average filter to create the muscle activation envelope, providing a cleaner and more interpretable representation of muscle activity over time (Figure 24).

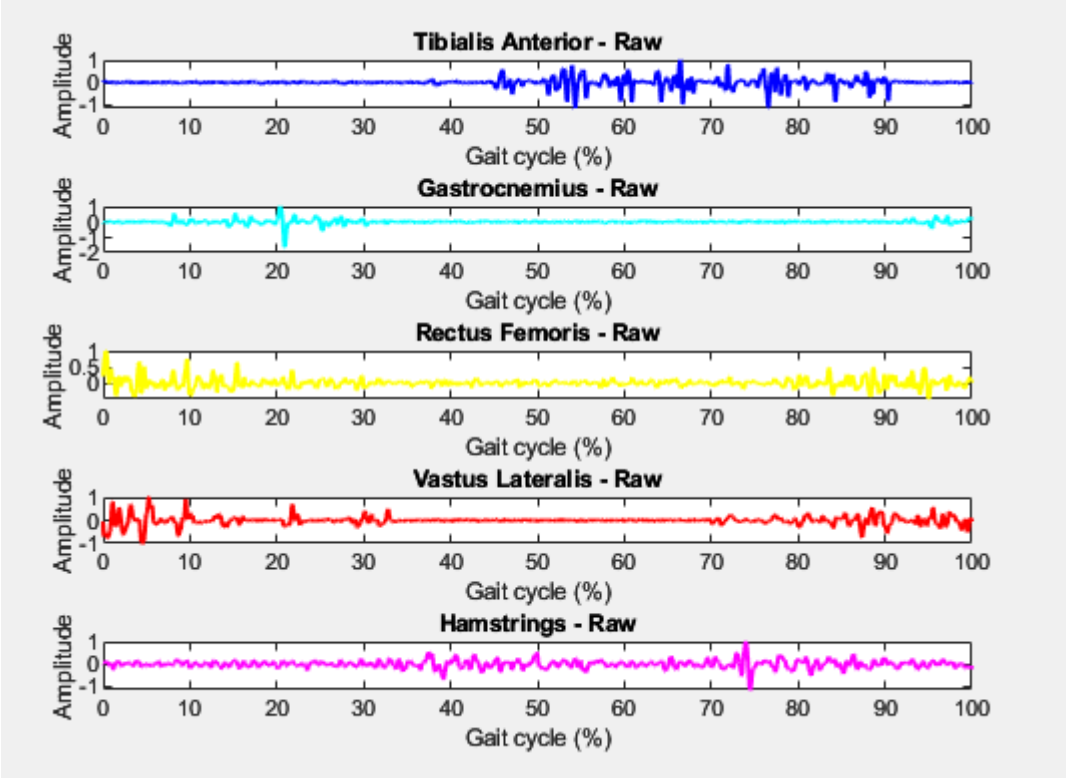



***Figure 21. Example of the raw signal example of step n° 85 of subject 1.***

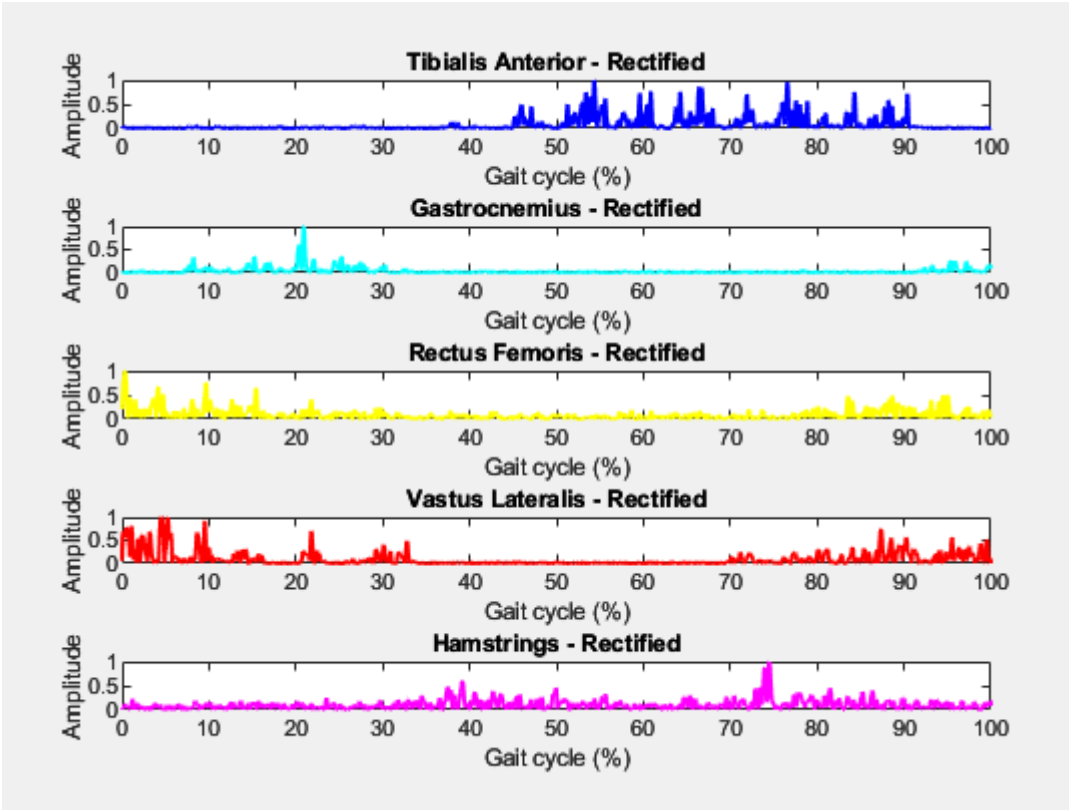



*Figure 22. Example of rectified signals example of step n° 85 of subject 1.*

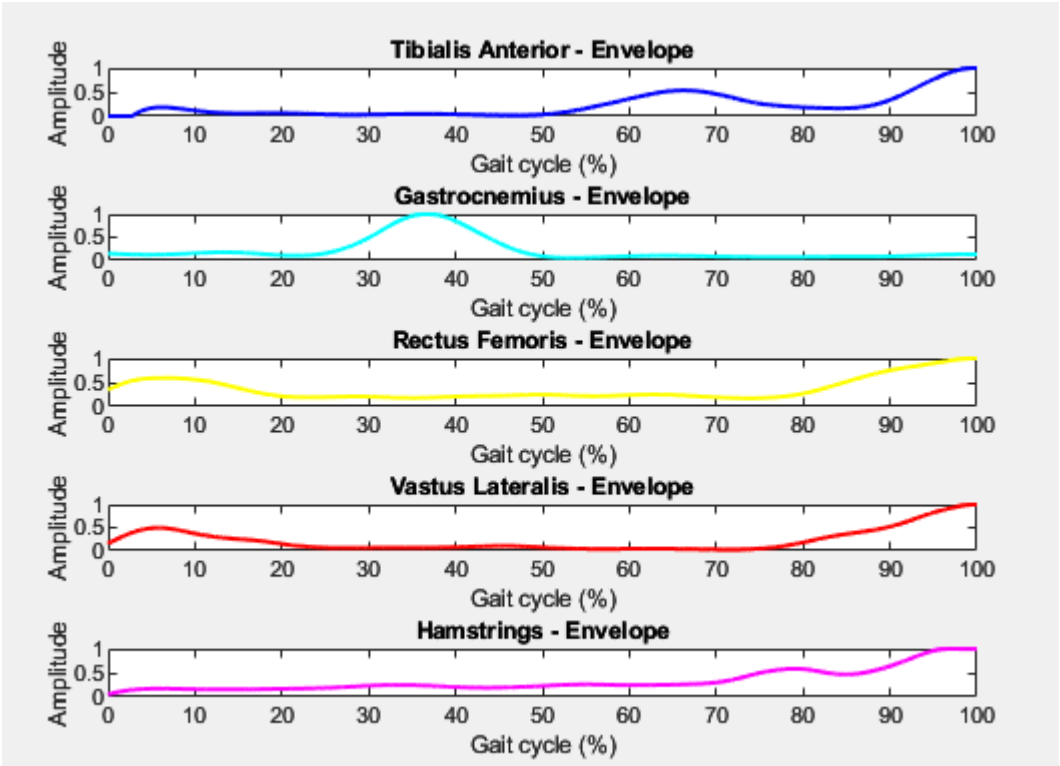



*Figure 23. Example of envelope signals of step n° 85 of subject 1.*

### 5.2.2 NMF

Following the preprocessing of sEMG signals, we constructed a matrix of muscle activation envelopes for each subject. This matrix consisted of five rows, one for each muscle: Tibialis Anterior, Lateral Gastrocnemius, Rectus Femoris, Vastus Lateralis, and Hamstrings, while the columns represented the steps of the gait cycle. This matrix served as the input for the Non-Negative Matrix Factorization (NMF) algorithm, which was used to extract muscle synergies.

Let's remember equation 5, in our study the NMF algorithm decomposes the original matrix *M* into two submatrices *W* and *C* as follows:

$$M=\mathrm{WC} \tag{6}$$

Where:

- *W* is the matrix of muscle synergy weights, where each column represents the contribution of a particular muscle to a given synergy.
- *C* is the matrix of time-varying synergy activation coefficients during the gait cycle. Each row in *C* describes how a specific synergy is activated over time.

The algorithm was run for 20 iterations with different random initializations to ensure robustness, and the solution with the highest coefficient of determination $R^2(i)$ was selected. The number of synergies *N* was varied between 1 and 5, and the optimal number was determined based on the proportion of explained variance, with a threshold of $R^2(i) \geq 0.9$.

After obtaining the number of modules for each subject, we analyzed the relative contributions of each muscle in the identified synergies. In this study, it was found that both the Rectus Femoris (RF) and Vastus Lateralis (VL) were frequently co-active in most subjects, and as a result, the corresponding synergy was calculated using the sum of the squared weights for these muscles. Once the synergy of interest was determined, the individual contributions of all five muscles were extracted, considering only those greater than 0.2 to isolate muscles with significant contributions. The choice of the 0.2 threshold

for determining significance was based on data analysis, in order to avoid including muscles that did not play a relevant role in most of the identified synergies, based on the amplitude of their contributions.

Contributions below 0.2 were considered negligible in the context of overall muscle activation or as possible artifacts, as they might simply reflect noise or low-level activations that were not relevant. By setting this threshold, the aim was to include only muscles with significant activation and avoid artificially inflating the number of EMG signals in a synergy. This cutoff was chosen to balance inclusivity and specificity, including only muscles that contributed significantly from a physiological perspective while excluding those with minimal impact. This strategy made it possible to delve deeper into the functional biomechanics of the main muscles during movement execution within the gait cycle. If a lower threshold had been used, the group of included muscles would have been broader and subject-dependent, making it difficult to identify common patterns across subjects.

Using a 20% threshold made it easier to identify the main co-activation patterns associated with the synergies and to identify the key muscles in each synergy, contributing to a better understanding of their role in movement coordination.

### 5.2.3 CWT-based scalogram and pooled scalogram

The time-frequency analysis of the muscles that composed each synergy was performed after processing sEMG signals and applying NMF for muscle synergies identification. Each raw sEMG signal from a muscle was then converted into a time-frequency representation using Continuous Wavelet Transformation (CWT), which enables a better illustration of activation changes in terms of both frequency and duration. This method was particularly useful for analyzing muscle behavior during different phases of the gait cycle. In the present work, the Daubechies wavelet (order 4) was applied, as it is successful in analyzing both rapid and slow variations in muscle activity.

The pooled scalogram proposed offers a new way to understand muscle synergy interactions. This method combined the wavelet coefficients of all muscle signals to investigate the time-frequency characteristics of multi-muscle co-activation. The following analysis is limited to five key muscles: Tibialis Anterior (TA), Lateral Gastrocnemius (LG), Rectus Femoris (RF), Vastus Lateralis (VL), and Hamstrings (HAM). The pooled scalogram was computed as the product of the wavelet coefficients for the muscles:

$$PSC_x(a,b) = [W_{x1}(a,b) \cdot W_{x2}^*(a,b)] \cdot W_{x3}^*(a,b) \quad (7)$$

Where $W_{x1}(a,b), W_{x2}(a,b)\ and\ W_{x3}(a,b)$ represent the wavelet coefficients for each of the three muscles, and the * symbol indicates the complex conjugate. This pooled scalogram made it possible to assess how these muscles collaborated at different moments in the gait cycle and across frequencies.

Following the computation of the pooled scalogram, data were standardized to facilitate subject-wise comparisons. The analysis provided further insight into specific time periods and frequency bins where muscle co-activation occurred, allowing a more thorough examination of how muscles are coordinated throughout the gait cycle. The pooled scalogram offered a direct view of the global muscle effort and coordination during walking, providing a deeper understanding of muscle synergies.

# 6 Results

In this chapter, the results of the analysis conducted on the data from all 31 subjects in the database [35] are presented. The primary aim of the analysis was to provide a comprehensive overview of the muscle synergies identified, detailing the contribution of each muscle within the synergies. Special focus was placed on the synergies where the Rectus Femoris (RF) and Vastus Lateralis (VL) exhibited greater co-activation, as these muscles played a particularly significant role in most subjects. For each of these synergies, the pooled scalogram was calculated, offering a time-frequency representation that visually captures the co-activation of the muscles involved.

The use of the pooled scalogram provides a detailed view of muscle behavior during the gait cycle. Unlike traditional studies that often rely on complex statistical analyses or clustering methods, this approach focused on the practical application of the pooled scalogram to deliver a more dynamic and visual interpretation of muscle synergies. Through concrete examples, the potential of this method to quantify and visualize muscle synergies was demonstrated, going beyond simple numerical analysis to highlight the interactions between muscles during movement. This approach offered detailed insights into how muscles co-activate, allowing a real-time visualization of their synergy during different phases of the gait cycle.

For each subject, the contributions of each muscle were analyzed, with particular attention to those muscles that demonstrated dominant activity within specific synergies. The results were then graphically represented through the pooled scalogram, allowing a clear visualization of how these synergies unfold in the time-frequency domain.

This helped to intuitively understand the muscle dynamics and how they contribute to coordinated movement, providing a richer understanding of the interplay between muscles as they work together during walking.

## 6.1 Results of 31 Subjects

The analysis conducted on all 31 subjects is presented in this section, with a focus on the number of muscle synergies (or modules) identified for each participant. Figure 25 below illustrates the distribution of participants according to the number of modules required to represent their muscle activation patterns during the gait cycle.

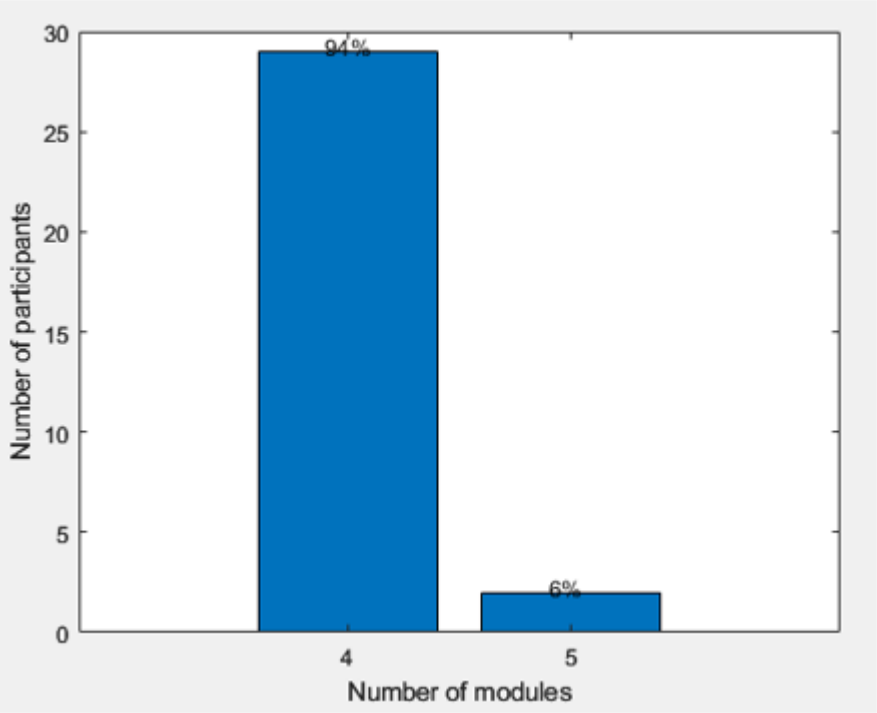



***Figure 24. Distribution of the number of modules across all participants.***

As the figure 25 shows, most participants (94%) required four modules to adequately capture their muscle activity patterns during walking. Only a small proportion (6%) needed five modules. This consistency suggests that four modules are generally sufficient to represent the muscle synergies during gait in most healthy subjects. The gait cycle, muscle synergies, and muscle behavior are represented in following figures, which include data derived from pooled scalogram settings. These graphs are designed to illustrate muscle activation over time and frequency, with a specific focus on five main muscles: Tibialis Anterior (TA), Lateral Gastrocnemius (LG), Rectus Femoris (RF), Vastus Lateralis (VL), and Hamstrings (HAM).

The following explanation applies to each figure for all subjects:

The synergy structure graph demonstrates the decomposition of electromyographic signals (sEMG) into muscle synergies using the Non-Negative Matrix Factorization (NMF) algorithm. At each level, muscle synergy weights are combined with time-varying activation coefficients to calculate the neural drive at the muscle level.

- Synergy Columns: The synergies are displayed as columns, with bars representing the relative contribution of each muscle to that synergy. This allows us to identify which muscles are most active during each phase of the gait cycle.
- Relative Contributions: The contribution of each muscle is shown as a percentage, indicating its importance within the synergy.

The Two-Dimensional (2D) Scalogram represents muscle behavior in both time and frequency throughout the gait cycle. It is computed using the Continuous Wavelet Transform (CWT), which allows the analysis of both fast and slow variations in muscle activity.

- Horizontal Axis: Represents the gait cycle (GC), divided into different phases such as stance and swing.
- Vertical Axis: Represents frequency bands, focusing on the most relevant ones for muscle activation (typically between 20 and 200 Hz).
- Color: The intensity of the color indicates muscle activation, with brighter colors representing higher levels of activation. This allows us to pinpoint the exact moments within the gait cycle when the highest levels of muscle activity occur.

The 2D scalogram is useful for identifying periods when individual muscles or groups of muscles are substantially activated, providing insights into muscle synergies during dynamic tasks and the Three-Dimensional (3D) Scalogram offers a more complete view of muscle activity by displaying both time and frequency data, along with an additional depth dimension.

- Temporal and Frequency Axes: Similar to the 2D scalogram, it displays muscle activation over time and frequency, with the addition of a third axis representing the amplitude of muscle activation.

- Activation Amplitude: The third dimension (height of the curves) represents the intensity of muscle activation and the level of co-activation between muscles. This allows for accurate visualization of how multiple muscles work together during different phases of the gait cycle.
- Muscle Co-Activation: This visualization is particularly useful for identifying patterns of muscle co-activation, helping to understand how different muscles work in synergy during the stance and swing phases of the gait cycle.

- **Subject 1**

In subject 1, synergy 1 is the one where the contributions of the Rectus Femoris (RF) and the Vastus Lateralis (VL) are greater with the contribution also of the Hamstrings (HAM) (Figure 26). In this synergy it can be observed that the activation takes place around 10% of the step cycle and then between 40% and 60%, subsequently, the activation gradually decreases before another peak between 80% and 90% (Figure 27). The pooled scalograms of synergy 1 (Figures 27, 28) highlight a small activation peak around 10% can be observed, followed by another between 40% and 60%, while the most pronounced activation occurs between 80% and 90%. These activations are mainly concentrated in the 30-50 Hz frequency band, with a higher intensity than in the other bands. The lower frequencies, between 10 Hz and 30 Hz, show less intensity, while those between 30 Hz and 50 Hz show more pronounced peaks. The predominant peak between 80% and 90% of the pitch cycle occurs mainly in the 30-50 Hz band. The activation peaks detected by the NMF, around 10% and between 80% and 90% of the pitch cycle, coincide with those observed in the pooled scalogram. The peak between 40% and 60% is also clearly visible, especially in the 3D pooled scalogram.

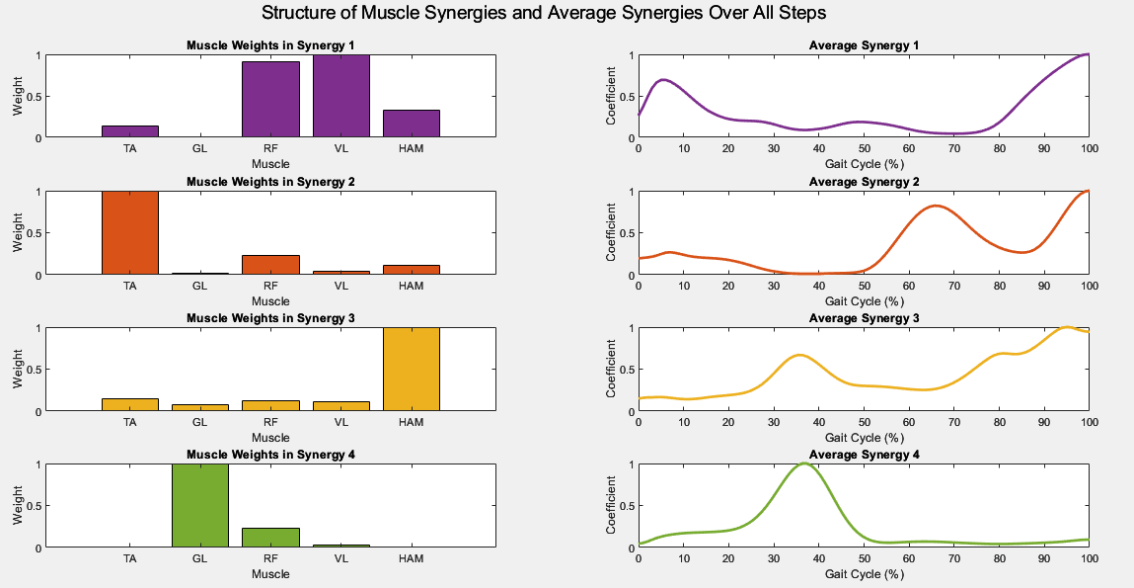



***Figure 25. Structure and Average Synergies Over All Steps for Subject 1.***

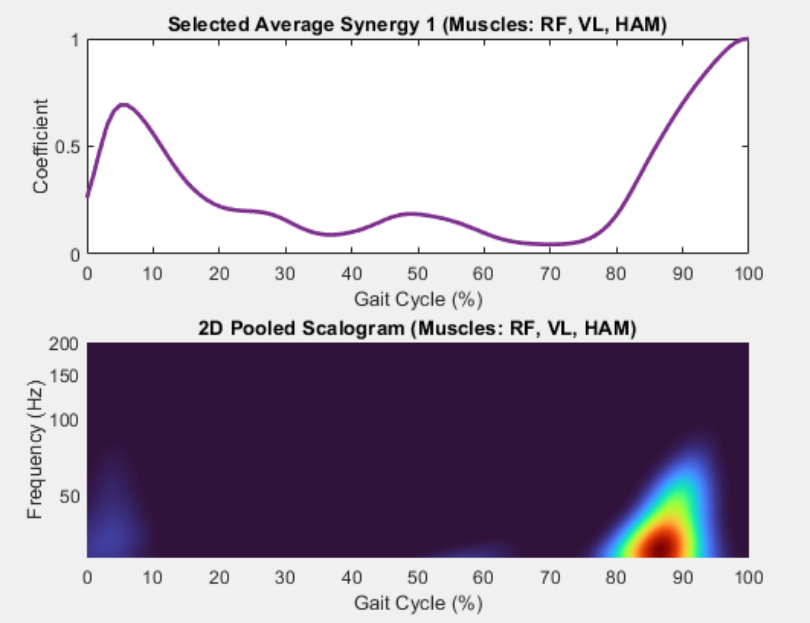



***Figure 26. Selected average synergy and 2D pooled scalogram for Subject 1.***

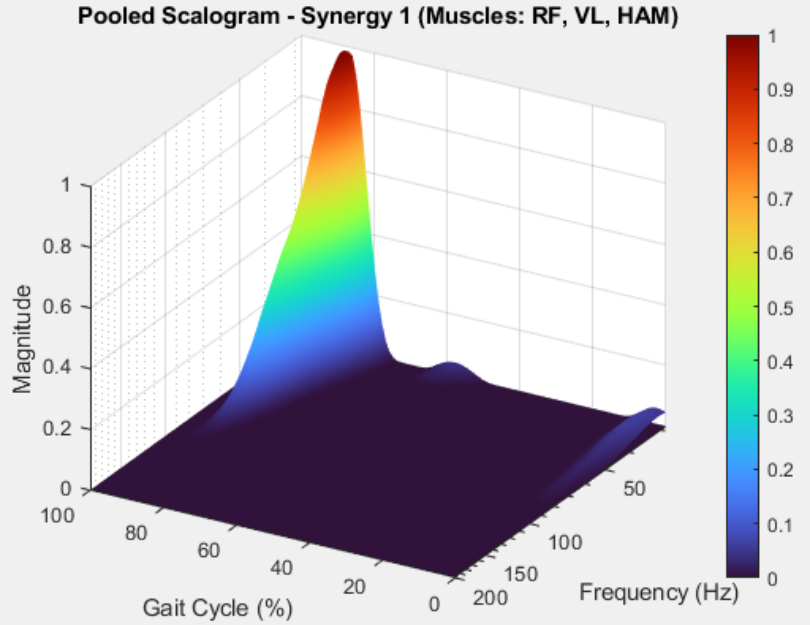



***Figure 27. 3D pooled scalogram for Subject 1.***

- **Subject 2**

In subject 2, the selected synergy is the second because it shows greater contributions of the Rectus femoris (RF), without having significant contributions from other muscles (Figure 29). There is continuous RF activation throughout the walking cycle, with distinct peaks in specific phases: about 5%, 55% and 100% of the walking cycle (Figure 30). The pooled scalograms (Figure 30, 31) of Synergy 2 have pronounced peaks at 5%, 55% and 100%, mainly concentrated in the frequency range 50-100 Hz. The first peak of activation, around 5%, shows the highest intensity, suggesting a rapid muscle response at the beginning of the walking cycle. The second peak, between 50% and 60%, shows a similar intensity, indicating sustained muscle effort, while the final peak at 100% represents preparation for the next step of the walking cycle. The lowest frequency bands (below 50 Hz) show minimal activation, while the 50 to 100 Hz band shows significant peaks. There is a good alignment of the activation peaks identified by NMF and those observed in the pooled scalograms.

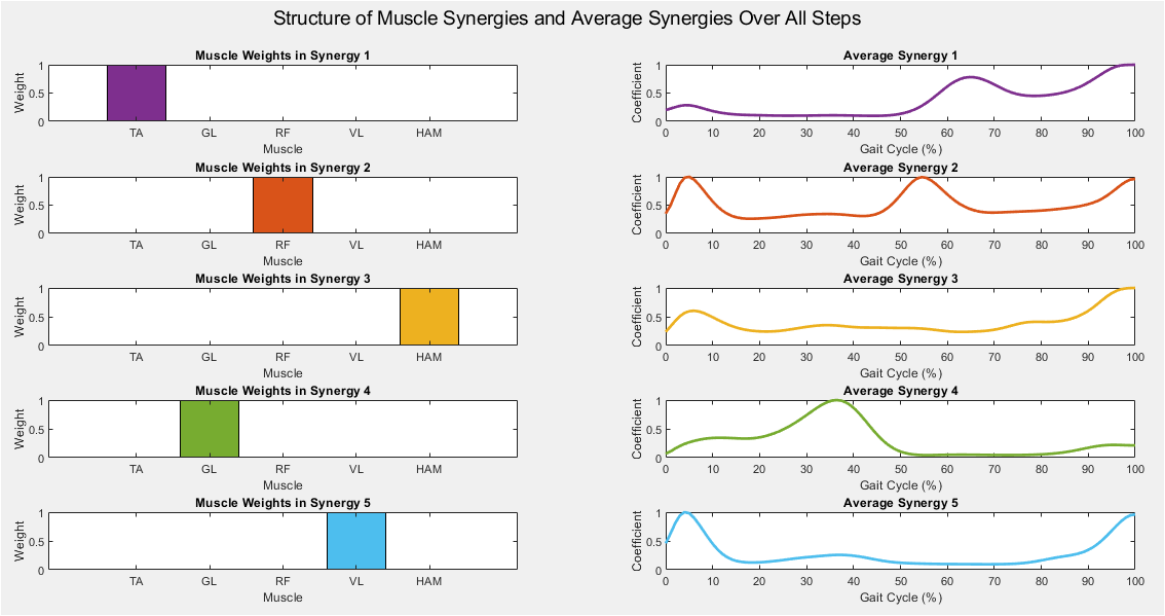



***Figure 28. Structure and Average Synergies Over All Steps for Subject 2.***

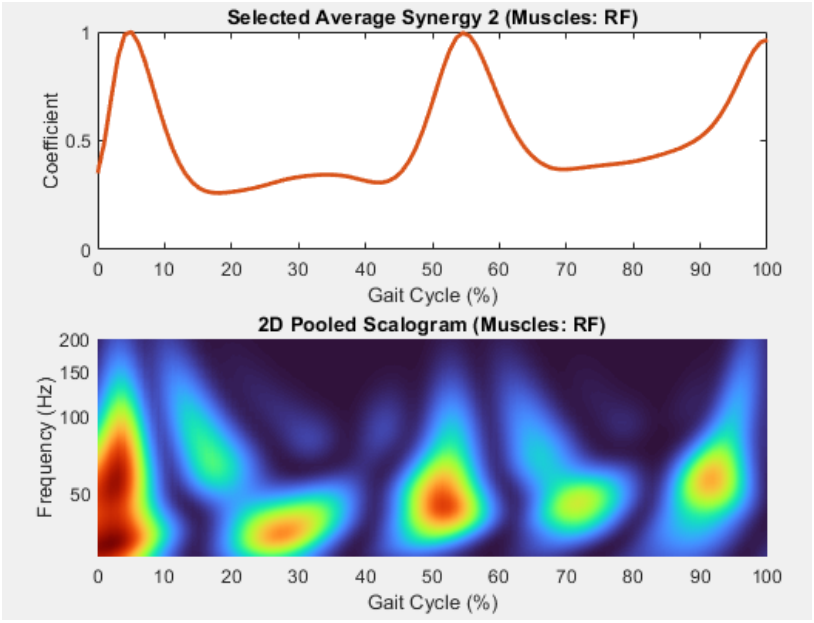



***Figure 29. Selected Average Synergy and 2D Pooled Scalogram for Subject 2.***

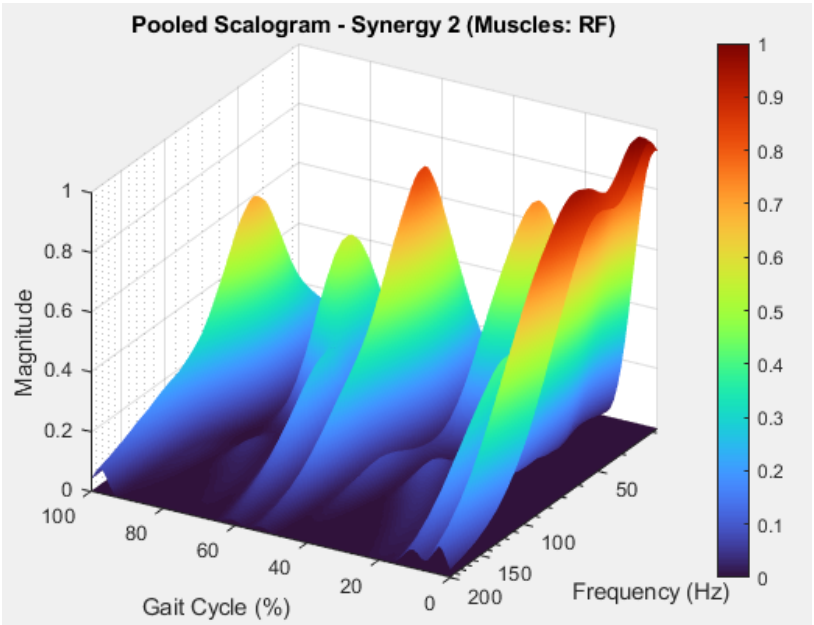



***Figure 30. 3D Pooled Scalogram for Subject 2.***

- **Subject 3**

In subject 3, the second synergy dominated by the Rectus Femoris (RF) is selected, with no significant contributions from other muscles (Figure 32). Continuous RF activation occurs throughout the walking cycle, with distinct peaks in specific phases: about 5%, 55% and 100% of the walking cycle (Figure 33). The pooled scalograms of Synergy 2 (Figures 33 and 34), provide information on frequency content and RF activation intensity, with pronounced peaks at 5%, 55% and 100%, mainly concentrated in the 50-100 Hz frequency range. The first peak of activation, around 5%, shows the highest intensity, suggesting a rapid muscle response at the beginning of the walking cycle. The second peak, between 50% and 60%, shows a similar intensity, indicating sustained muscle effort, while the final peak at 100% represents preparation for the next step of the walking cycle. The lowest frequency bands (below 50 Hz) show minimal activation, while the 50 to 100 Hz band shows significant peaks, underlining the role of RF in rapid contractions during key phases of the walking cycle. The alignment of the activation peaks identified by NMF and those observed in the pooled scalograms highlights critical moments of RF engagement.

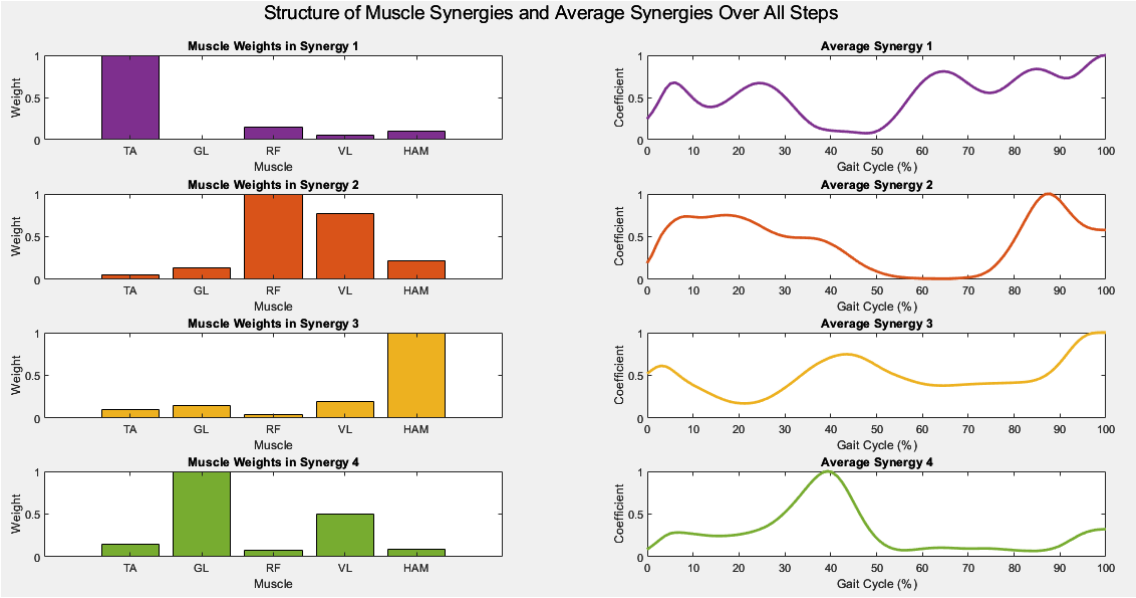



***Figure 32. Structure and Average Synergies Over All Steps for Subject 3.***

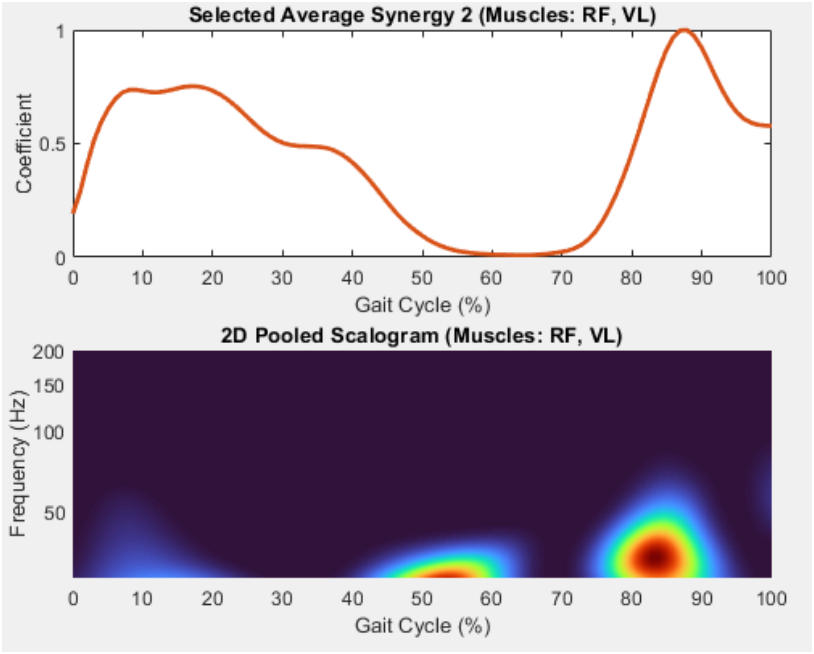



*Figure 33. Selected Average Synergy and 2D Pooled Scalogram for Subject 3.*

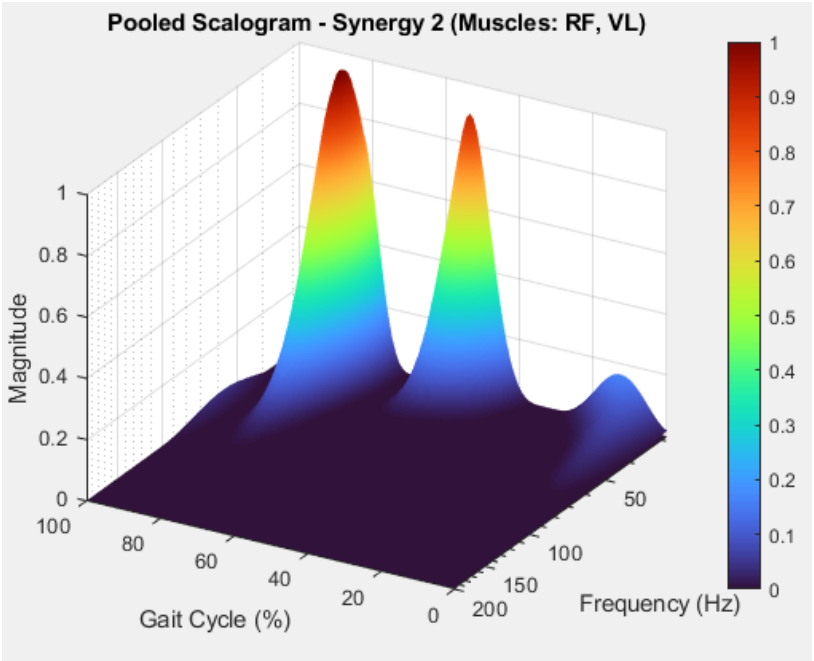



*Figure 34. 3D Pooled Scalogram for Subject 3.*

- **Subject 4**

In subject 4, synergy 3 is selected with a higher muscle contribution of the Vastus Lateralis (VL) without significant contributions from other muscles (Figure 35); The average temporal representation of Synergy 3 (Figure 36) confirms the activation pattern with an initial phase of high activity at 10%, followed by a decrease up to 60% in the walking cycle and then an increase between 80% and 90%. In the 2D pooled scalogram (Figure 36), significant activation is observed at 10%, with intermediate activation between 50% and 60%, and pronounced activation towards the end of the cycle, between 80% and 90%. The initial peak at 10% is concentrated between 35 and 55 Hz, while the intermediate activation from 50% to 60% covers a wider frequency range from 30 to 70 Hz. The final activation between 80% and 90% is also concentrated in the range of 35 to 55 Hz. In the 3D pooled scalogram (Figure 37), an additional activation is observed towards the end of the cycle (about 100%), characterized by higher frequencies, ranging from 60 to 90 Hz. The grouped scale indicates that the main activations are mainly concentrated between 35 and 55 Hz, with further contributions in higher frequency bands during specific phases of the gait cycle. The activation peaks identified by the NMF correspond well to those observed in the pooled scalograms for the initial phase at 10% and the final increase between 80% and 90%, while the intermediate activation between 50% and 60% shows a discrepancy, with less important activities in the NMF results.

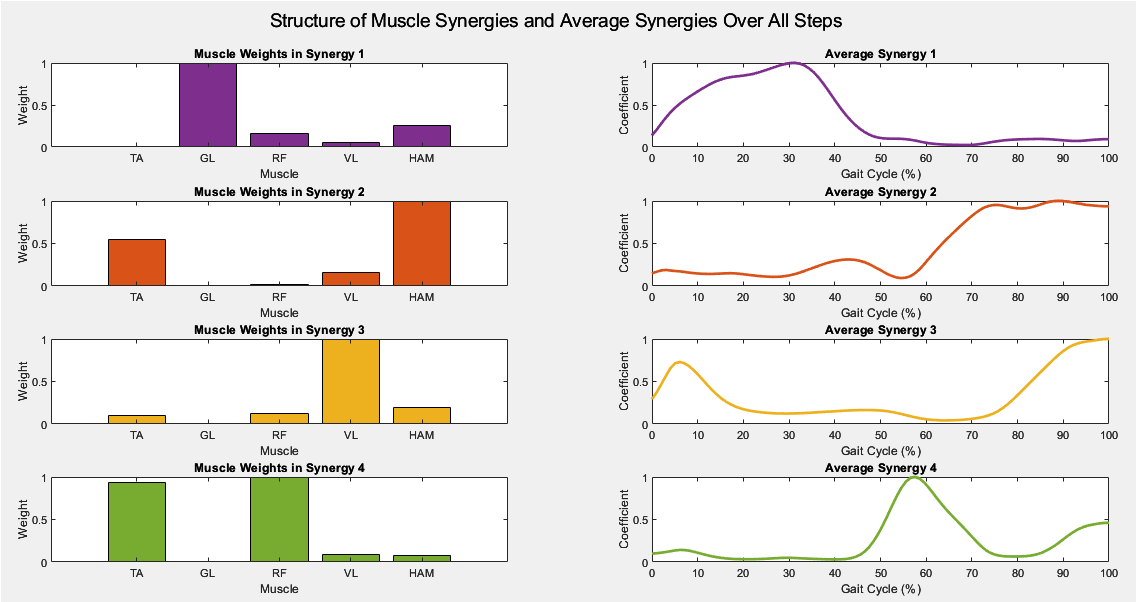



***Figure 35. Structure and Average Synergies Over All Steps for Subject 4.***

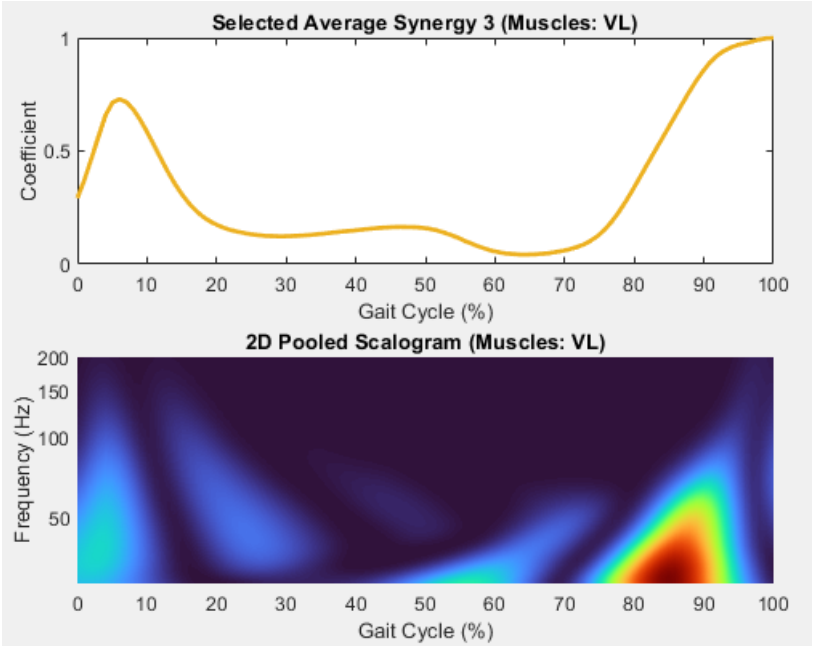



*Figure 36. Selected Average Synergy and 2D Pooled Scalogram for Subject 4.*

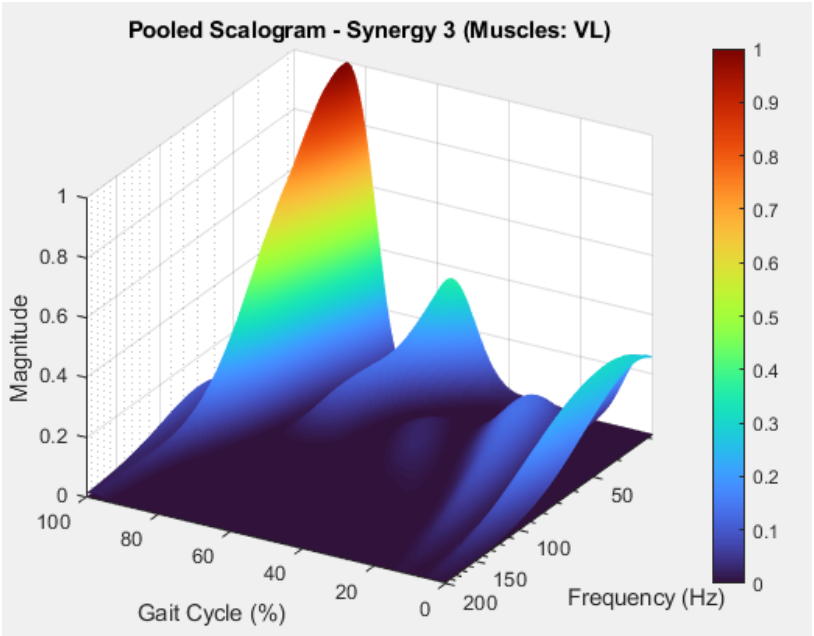



*Figure 37. 3D Pooled Scalogram for Subject 4.*

- **Subject 5**

In subject 5, the synergy in which the contributions of the Rectus Femoris (RF) and the Vastus Lateralis (VL) are most significant is the fourth with the contribution also of the Hamstrings (HAM) (Figure 38). In Figure 39, the average time representation of Synergy 4 shows an initial peak in activation around 8% of the gait cycle, followed by two minor peaks between 20% and 30% and 50% and 60%, The activation reaches its maximum amplitude towards the end of the walking cycle, between 80% and 100%. In the pooled scalograms (Figures 39, 40), a pronounced activation is observed between 80% and 100%, with an additional lower activation between 50% and 60%. In particular, the previous peaks identified by the NMF, around 8% and between 20% and 30%, are not clearly visible in the pooled scalograms, suggesting a partial alignment between the NMF results and the clustered frequency analysis. The pooled scalograms emphasize the frequency content of the activation, with the 80-100% peak showing significant intensity in the 30-50 Hz band, while the smaller activation between 50 and 60% also appears but less prominently.

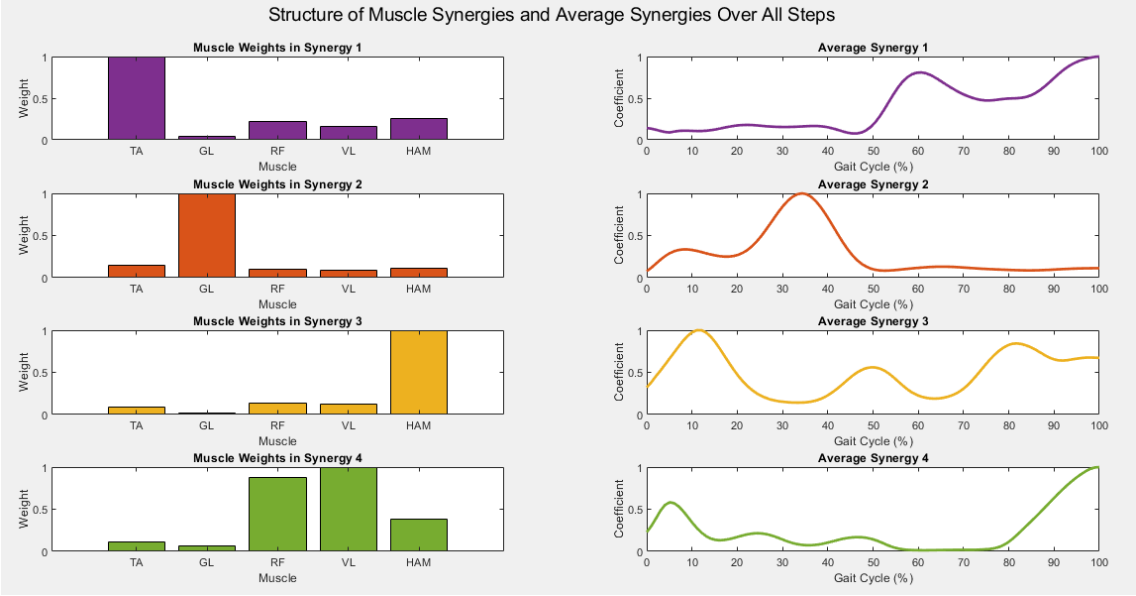



***Figure 38. Structure and Average Synergies Over All Steps for Subject 5.***

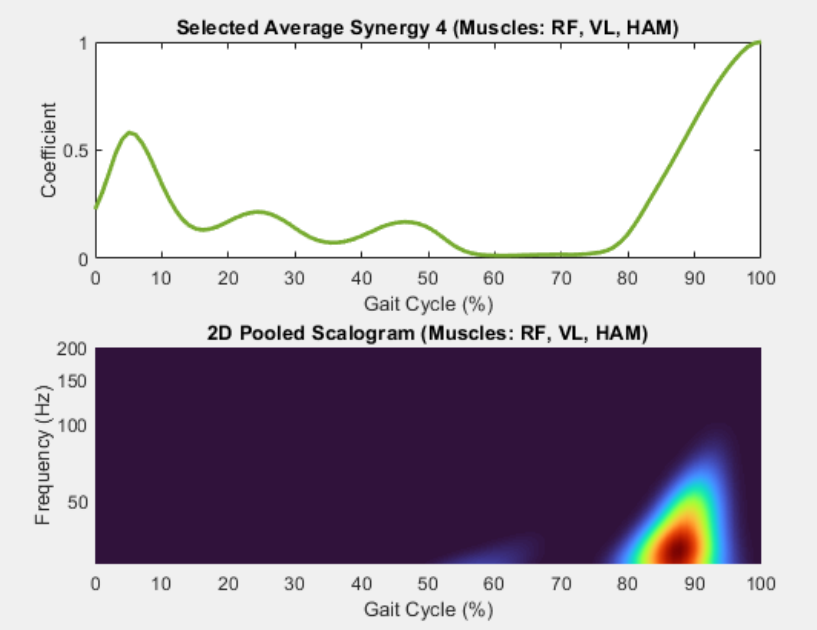



*Figure 39. Selected Average Synergy and 2D Pooled Scalogram for Subject 5.*

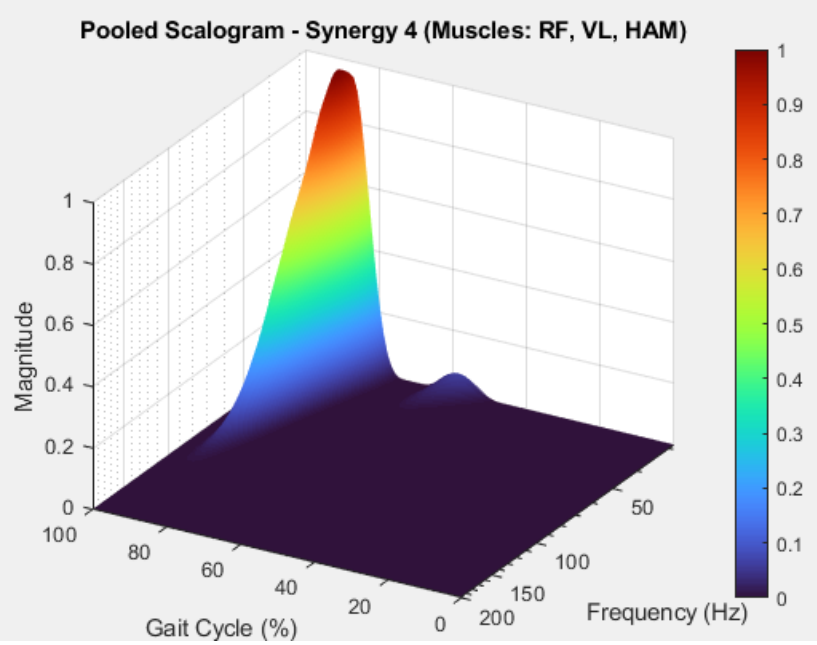



*Figure 40. 3D Pooled Scalogram for Subject 5.*

- **Subject 6**

In subject 6, the Rectus Femoris (RF) and the Vastus Lateralis (VL) are the main contributors to synergy 4 (Figure 41). The time-plot of Synergy 4 (Figure 42) reveals an initial peak of activation around 8% of the walking cycle, followed by smaller peaks between 20% and 30%, and at 50% a more pronounced increase in activation between 80% and 90%, corresponding to the terminal and oscillatory phases of the walking cycle. The pooled scalograms (Figures 42, 43) show a higher activation of around 8%, covering a wider frequency range than the subsequent peaks. Additional activations occur between 20% and 30%, and at 50%, with a pronounced final peak between 80% and 90% of the gait cycle. These activations are mainly concentrated in the frequency band 35-55 Hz, while the initial activation extends to lower frequencies, suggesting a more sustained effort. Alignment between the pooled scalograms activation models and NMF results indicates a consistent co-activation of RF and VL in key phases of the gait cycle.

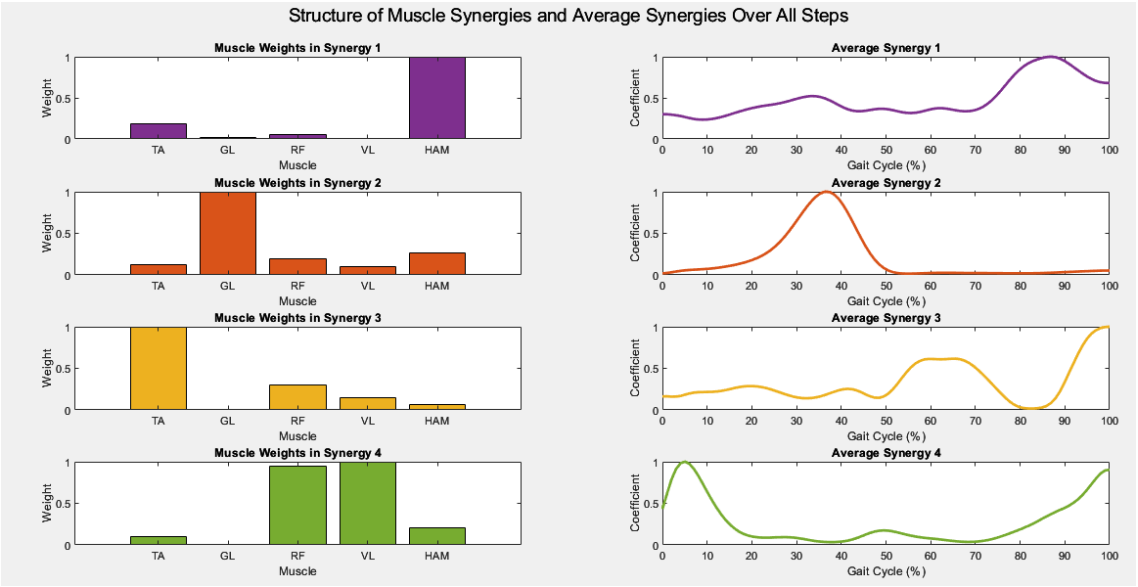



***Figure 41. Structure and Average Synergies Over All Steps for Subject 6.***

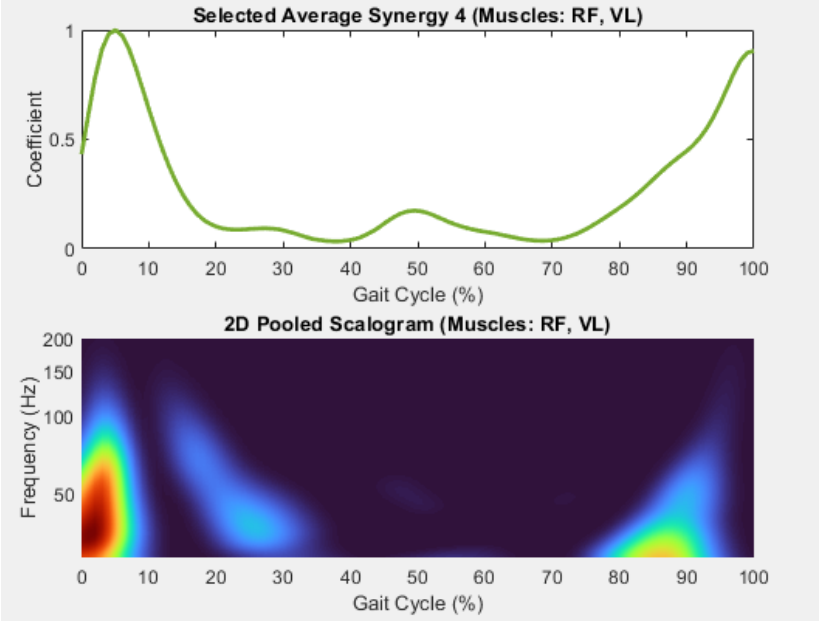



*Figure 42. Selected Average Synergy and 2D Pooled Scalogram for Subject 6.*

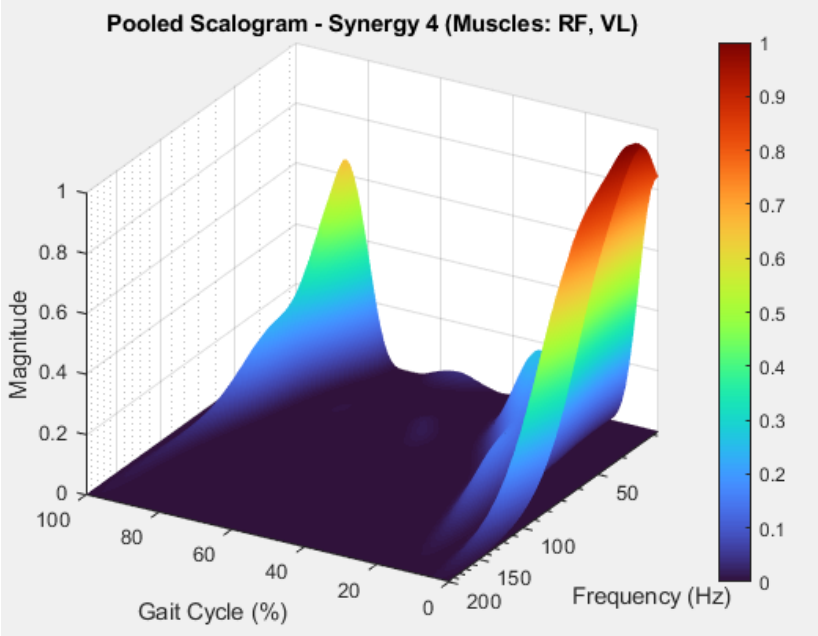



*Figure 43. 3D Pooled Scalogram for Subject 6.*

- **Subject 7**

In the fourth synergy of subject 7, high levels of activation are observed for the Rectus Femoris (RF) and Vastus Lateralis (LV) (Figure 44). The first peak occurs at about 8% of the running cycle, followed by an activation below 50%, and the most pronounced activity occurs during the terminal position, from 80% through the previous momentum (Figure 45). The pooled scalograms (Figures 45, 46) observe activations at 8%, 50% and during the second half of the position (80-100%), then the final activation has a wider frequency spectrum, centred around 30-50 Hz and ranging from 20 Hz to over 100 Hz. The 50% intermediate activation appears less pronounced than the NMF results but there is a good correspondence between the initial and final phases identified by the NMF and the pooled scalograms although the intermediate activation shows some differences between the two analyses.

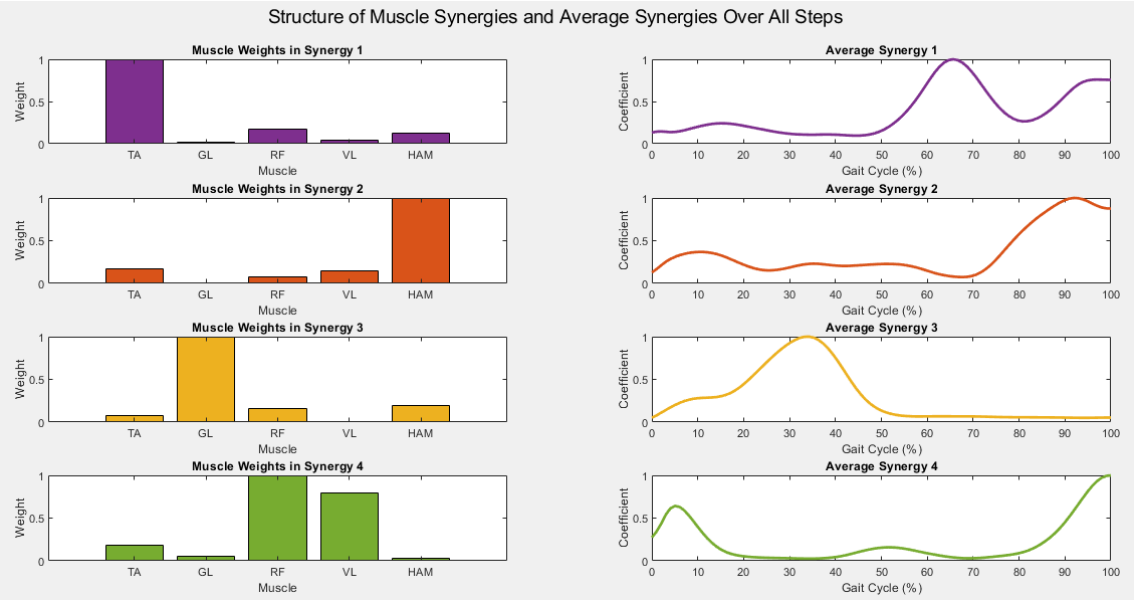



***Figure 44. Structure and Average Synergies Over All Steps for Subject 7.***

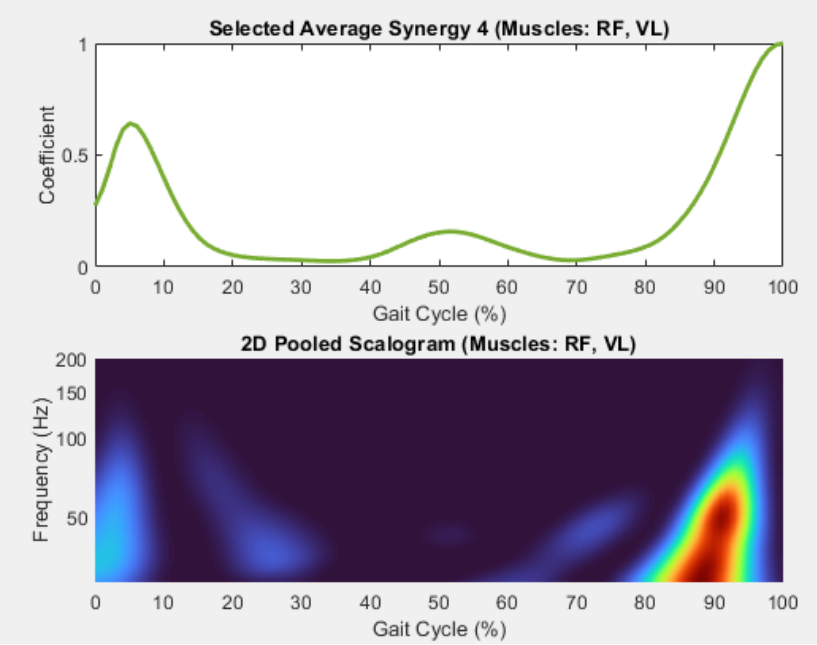



*Figure 45. Selected Average Synergy and 2D Pooled Scalogram for Subject 7.*

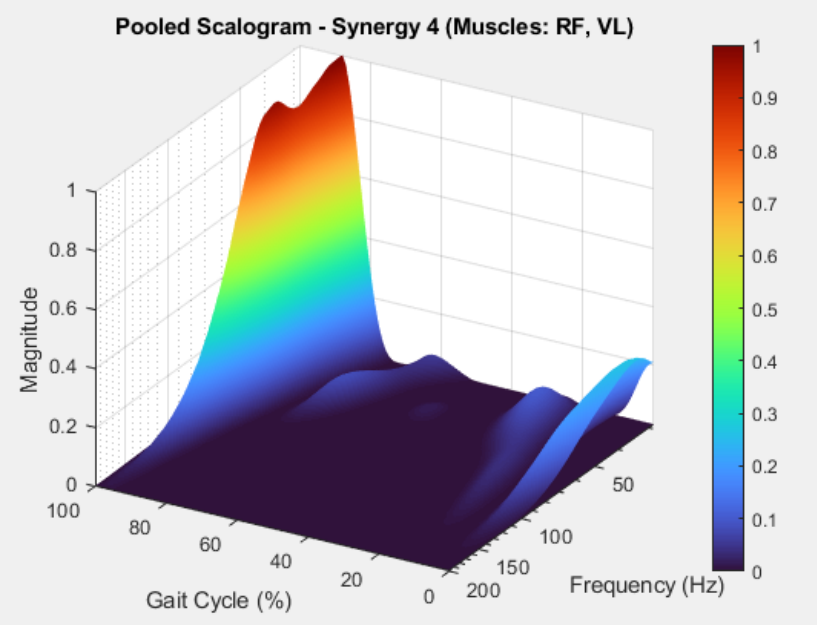



*Figure 46. 3D Pooled Scalogram for Subject 7.*

- **Subject 8**

In subject 8, the Rectus Femoris (RF) and Vastus Lateralis (VL) show significant activation in synergy 4 (Figure 47). The first major peak occurs between 10% and 20% of the gait cycle, corresponding to the initial loading phase, then there is a smaller activation follows between 20% and 30%, and another less intense phase is observed between 40% and 50%. There is also an activation between 55% and 65%, with the most prominent activation occurring between 80% and 100% of the gait cycle, which corresponds to the terminal stance and preparation for the swing phase (Figure 48). In the pooled scalograms (Figures 48, 49) an intense activation is visible between 0% and 10%, with frequencies spread across a broad range, extending beyond 100 Hz, indicating a rapid and variable muscle response. Another activation is seen between 20% and 30%, mainly concentrated in the 40 Hz to 70 Hz frequency range, followed by a less pronounced activation between 40% and 50%, with frequencies predominantly above 50 Hz. A further activation is detected between 55% and 65%, and finally, a very broad and significant peak occurs between 80% and 95% of the gait cycle, with frequencies centered between 30 Hz and 50 Hz, also extending beyond 70 Hz. There is a good correspondence between the peaks identified by NMF and those observed in the pooled scalograms for the initial and final phases of the gait cycle, however, there are some differences during the intermediate phases.

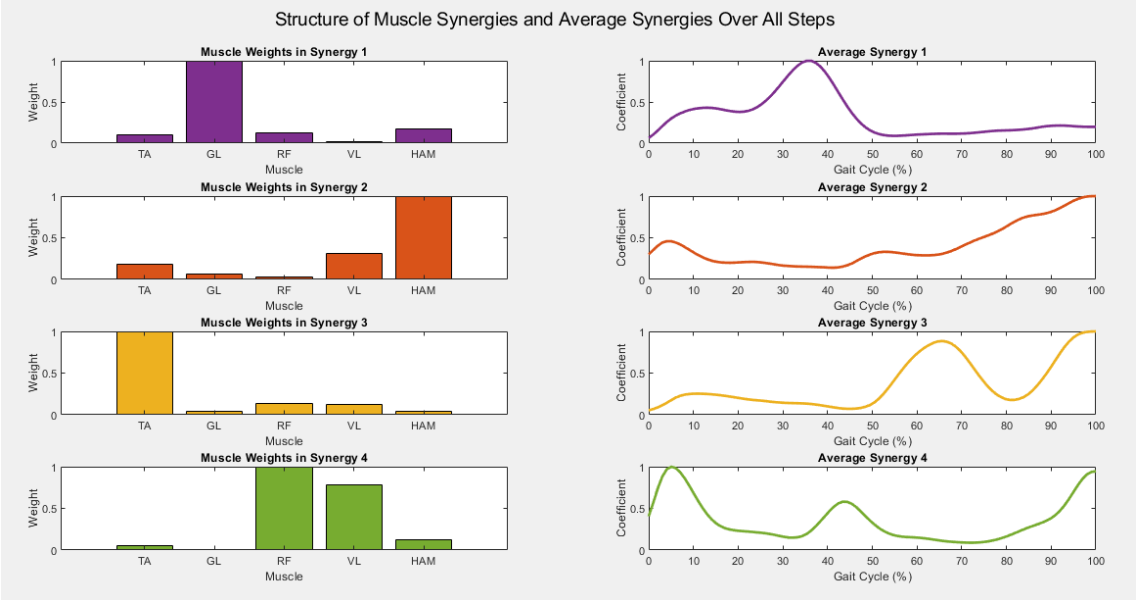



***Figure 47. Structure and Average Synergies Over All Steps for Subject 8.***

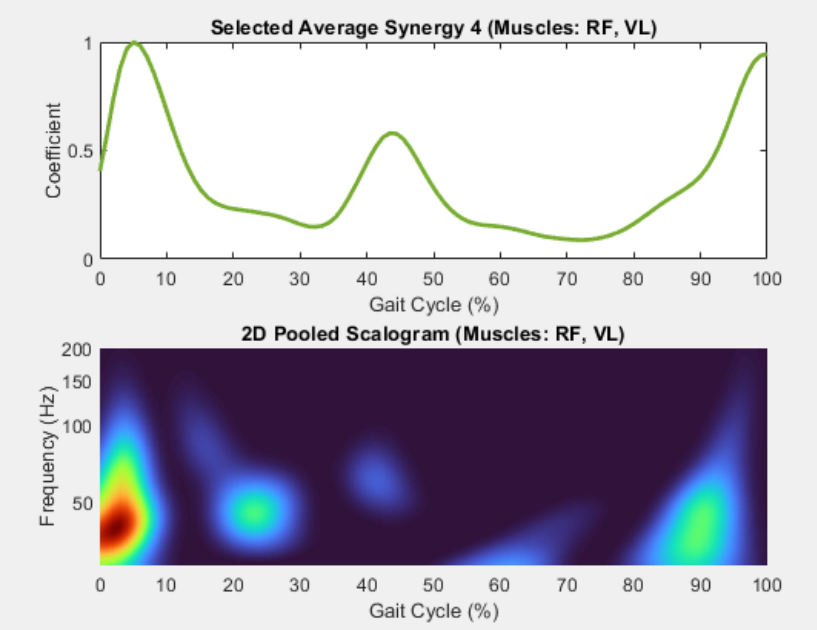



*Figure 48. Selected Average Synergy and 2D Pooled Scalogram for Subject 8.*

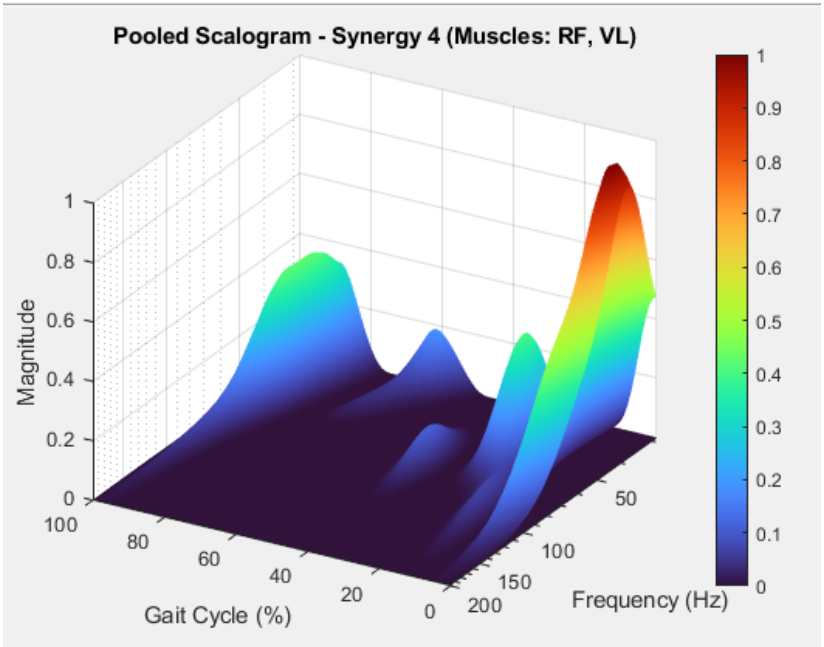



*Figure 49. 3D Pooled Scalogram for Subject 8.*

- **Subject 9**

In subject 9, the Rectus Femoris (RF) and the Vastus Lateralis (VL) have greater contributions to synergy 3 (Figure 50), in which a first significant activation is noted between 0% and 20% of the gait cycle, in line with the initial phase of the stance, then there is a minor activation is present around 40%, followed by a pronounced peak between 80% and 90%, corresponding to muscle activity during the terminal phase of the stance and preparation for the swing phase (Figure 51). Figures 51 and 52 illustrate the pooled scalograms of Synergy 3 with a concentration mainly in the 30-50 Hz frequency band. In the initial and final activations of the stride cycle, there are frequency ranges that extend beyond 50 Hz. It can be seen that an additional activation peak around 70% is evident in the pooled scalograms but not in the average Synergy 3 representation, suggesting variability in the co-activation pattern during this part of the stride cycle.

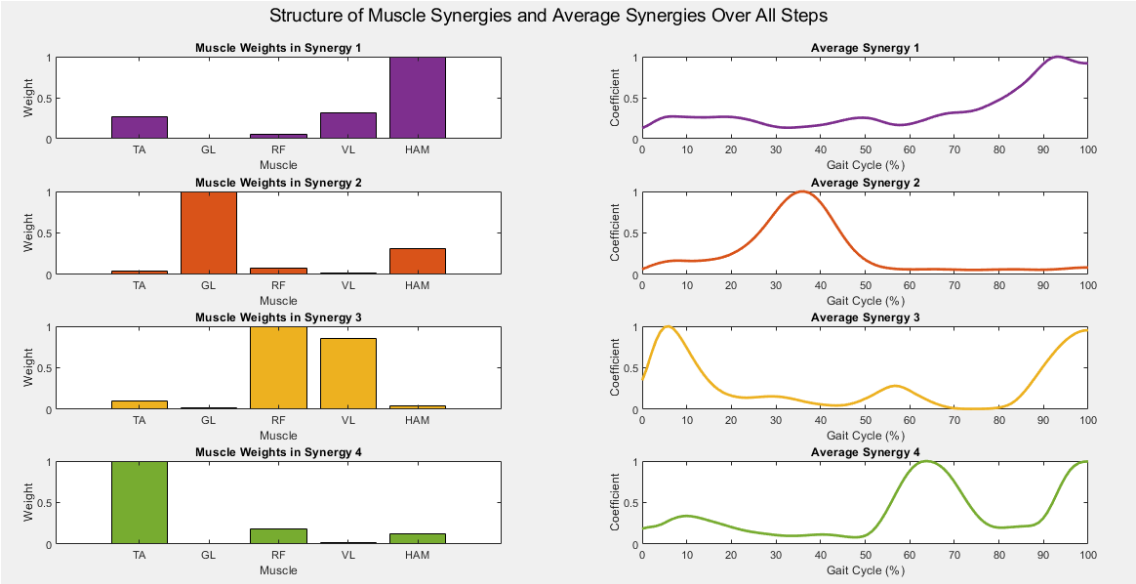



***Figure 50. Structure and Average Synergies Over All Steps for Subject 9.***

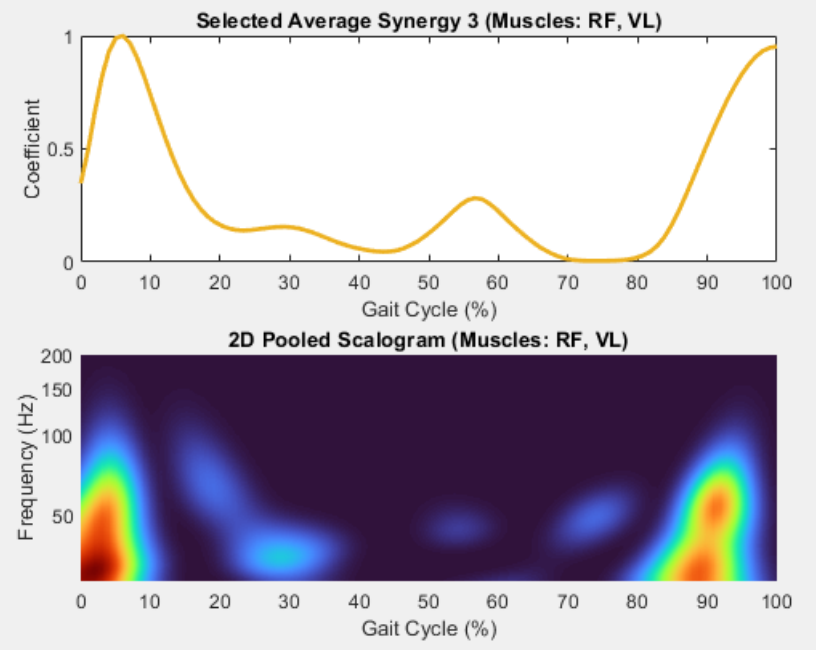



***Figure 51. Selected Average Synergy and 2D Pooled Scalogram for Subject 9.***

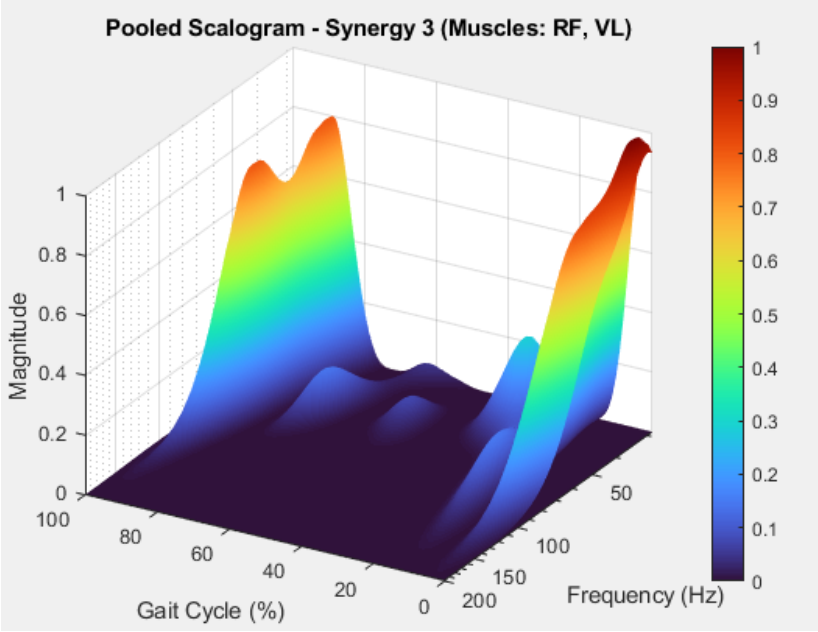



***Figure 52. 3D Pooled Scalogram for Subject 9.***

- **Subject 10**

In subject 10, the Rectus Femoris (RF), Vastus Lateralis (VL), and Hamstrings (HAM) show significant activation in the fourth synergy (Figure 53), where the primary activations are seen at the beginning of the gait cycle, between 0% and 10%, followed by a smaller, more diffuse activation between 40% and 70%, and finally, a pronounced peak towards the end, between 80% and 100%, which corresponds to the terminal stance as the leg prepares for the swing phase (Figure 54). Figures 54 and 55 present the pooled scalograms of Synergy 4, highlighting the main activations at the beginning and end of the gait cycle. These peaks are concentrated primarily in the 30-50 Hz frequency range, which indicates rapid muscle activation during these phases. A smaller peak can be observed at around 30% of the gait cycle, although this is less pronounced compared to the major peaks. The intermediate activation between 40% and 70% seen in the synergy is not clearly reflected in the pooled scalograms, suggesting limited correspondence between the NMF-derived synergy and the pooled frequency analysis for this phase.

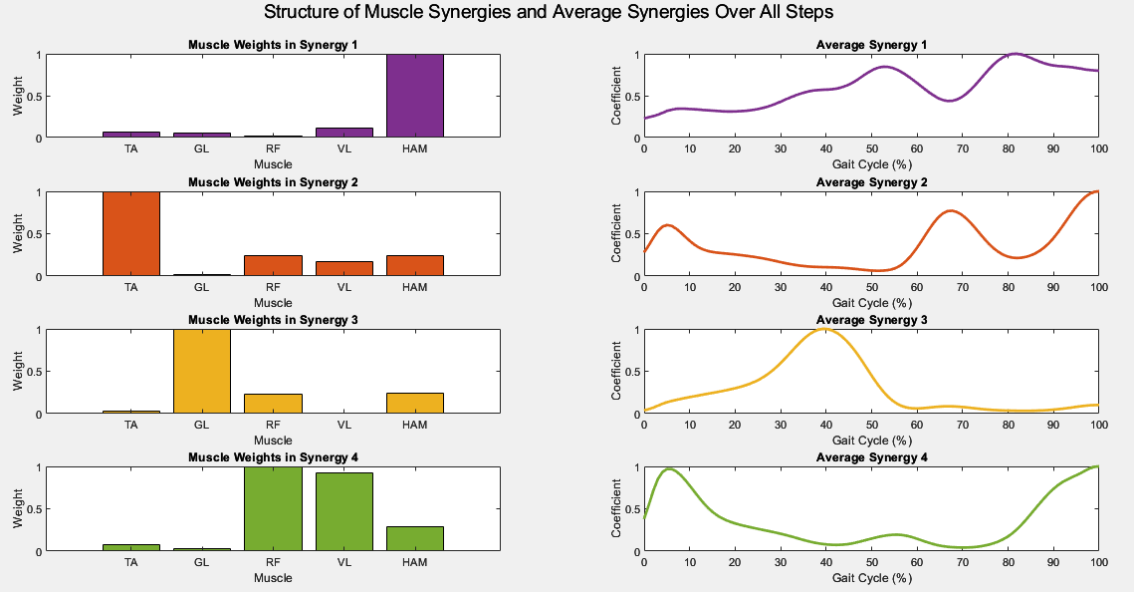



***Figure 53. Structure and Average Synergies Over All Steps for Subject 10.***

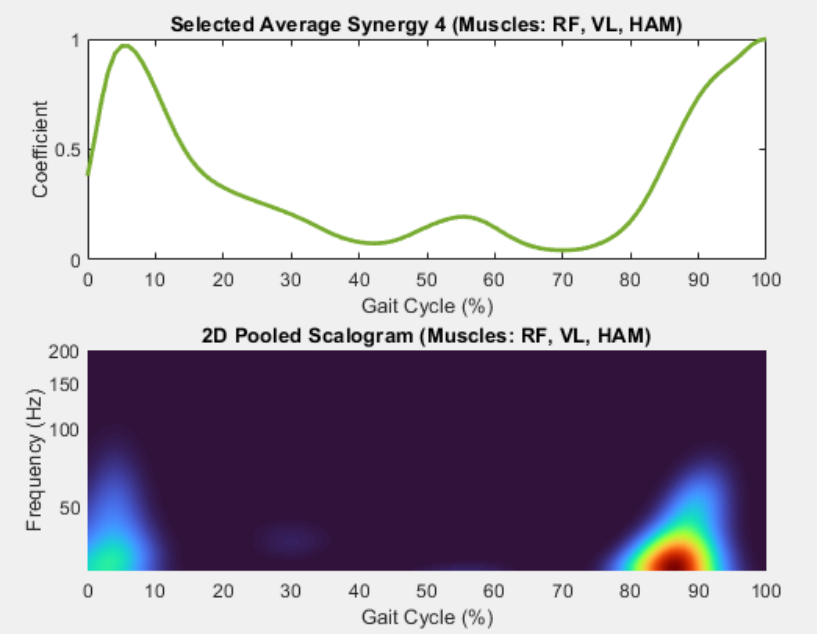



***Figure 54. Selected Average Synergy and 2D Pooled Scalogram for Subject 10.***

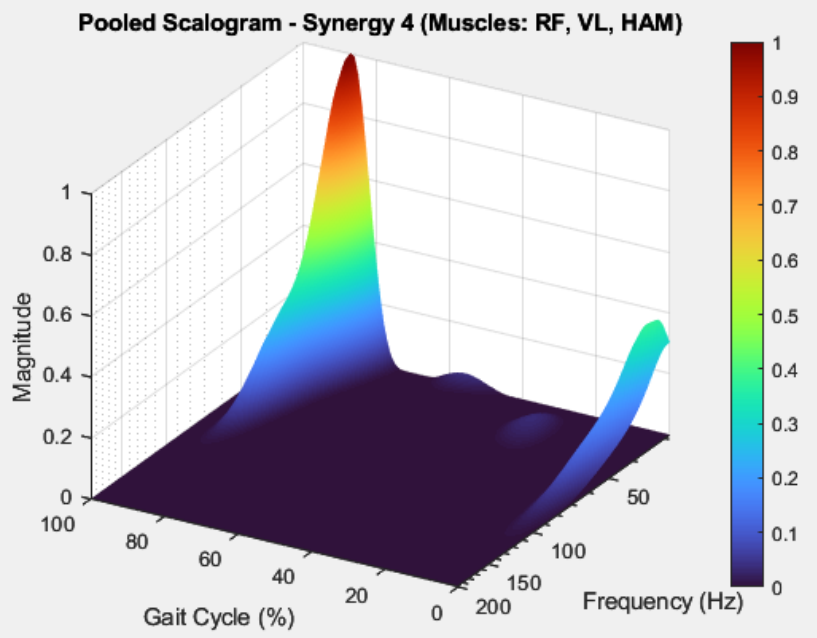



***Figure 55. 3D Pooled Scalogram for Subject 10.***

- **Subject 11**

In subject 11, the synergy in which Rectus Femoris (RF) and Vastus Lateralis (VL) are most active is the second one (Figure 56). This synergy shows continuous activation with distinct peaks occurring at approximately 10%, 55% and 100% of the gait cycle (Figure 57). The pooled scalograms (Figures 57, 58) reveal multiple patterns of activity within a frequency range of 20 Hz to 50 Hz, with high intensity observed around 55% and 90% extending to 100 Hz. There is a clear correspondence between the synergy and the pooled scalograms, as the peaks in the synergy align with the areas of highest intensity in the pooled scalograms, particularly at the 55% and 90% points of the gait cycle.

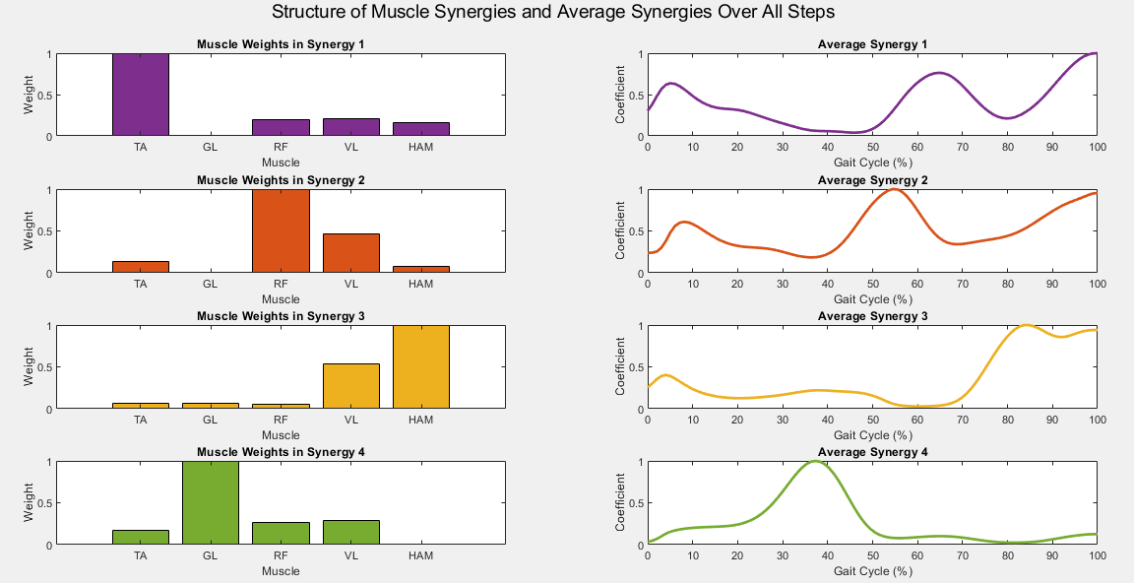



***Figure 56. Structure and Average Synergies Over All Steps for Subject 11.***

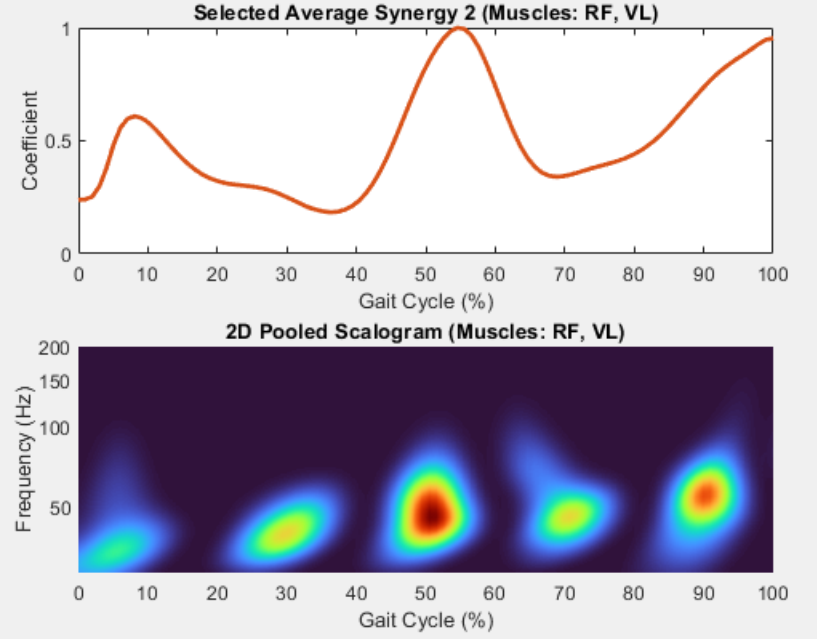



*Figure 57. Selected Average Synergy and 2D Pooled Scalogram for Subject 11.*

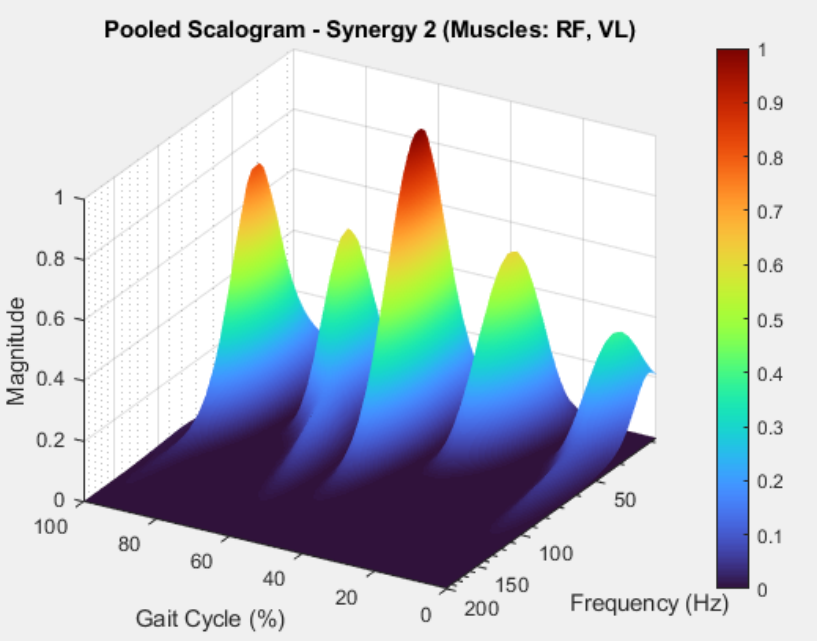



*Figure 58. 3D Pooled Scalogram for Subject 11.*

- **Subject 12**

In subject 12, the synergy in which Rectus Femoris (RF) and Vastus Lateralis (VL) are predominant is the fourth Synergy (Figure 59). A first activation around 8% of the step cycle, a second activation around 55% and a last activation at the end of the step cycle around 100% can be seen (Figure 60). In the pooled scalograms (Figure 60, 61) we notice higher intensity activities at the beginning of the step cycle with a higher frequency concentrated up to 50 Hz and lower intensity activities around 30%, 55% and 75% of the GC with frequencies concentrated in a range between 30 Hz and 55 Hz. At the end of the step cycle, we find an average intensity activation between 85% and 95% of the GC with frequencies that extend up to 100 Hz. We note correspondence between the moments of synergy activity and the pooled scalograms except for the activation present around 75% of the GC.

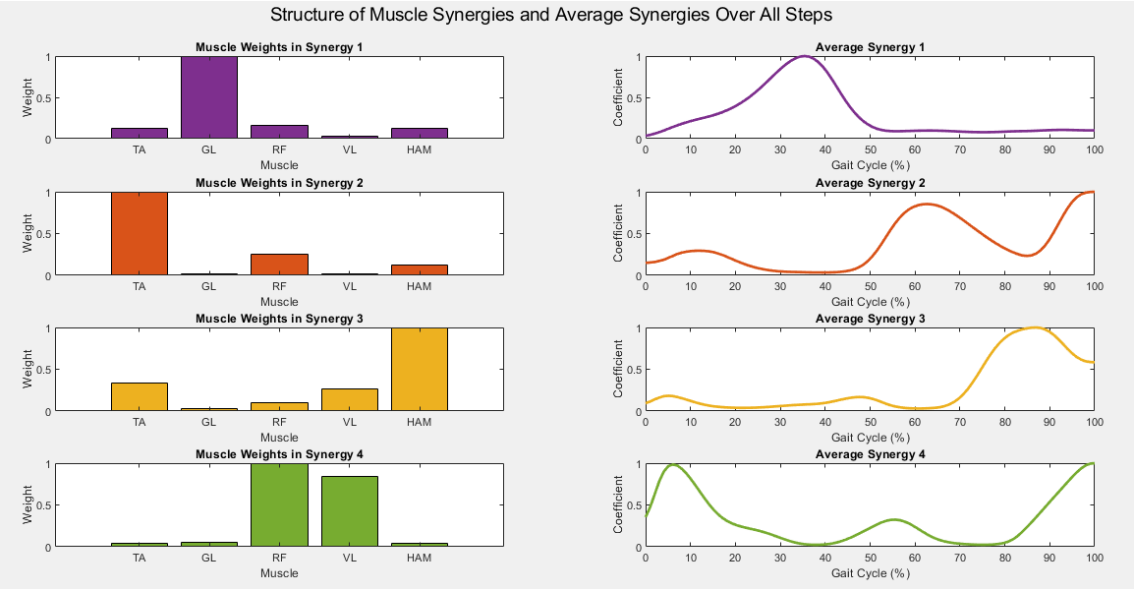



***Figure 59. Structure and Average Synergies Over All Steps for Subject 12.***

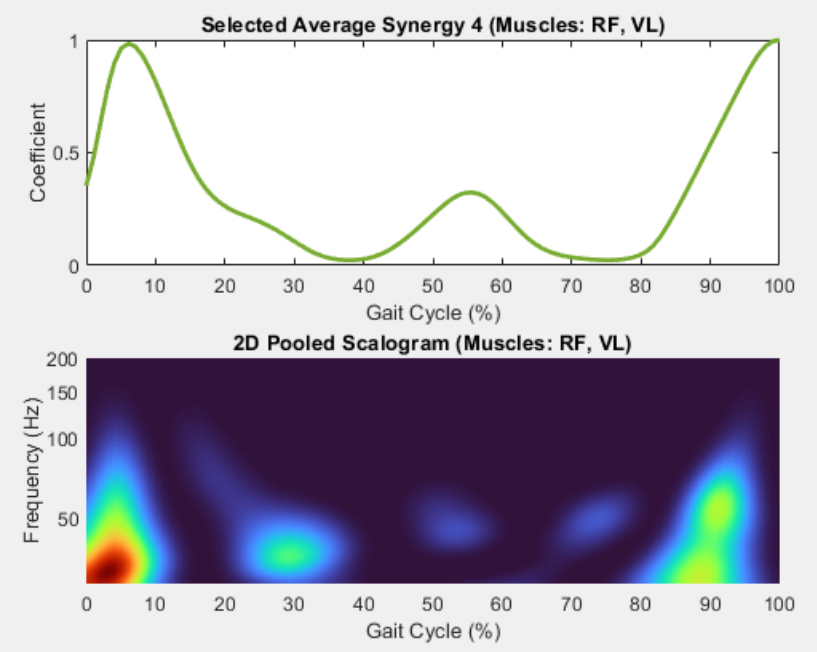



***Figure 60. Selected Average Synergy and 2D Pooled Scalogram for Subject 12.***

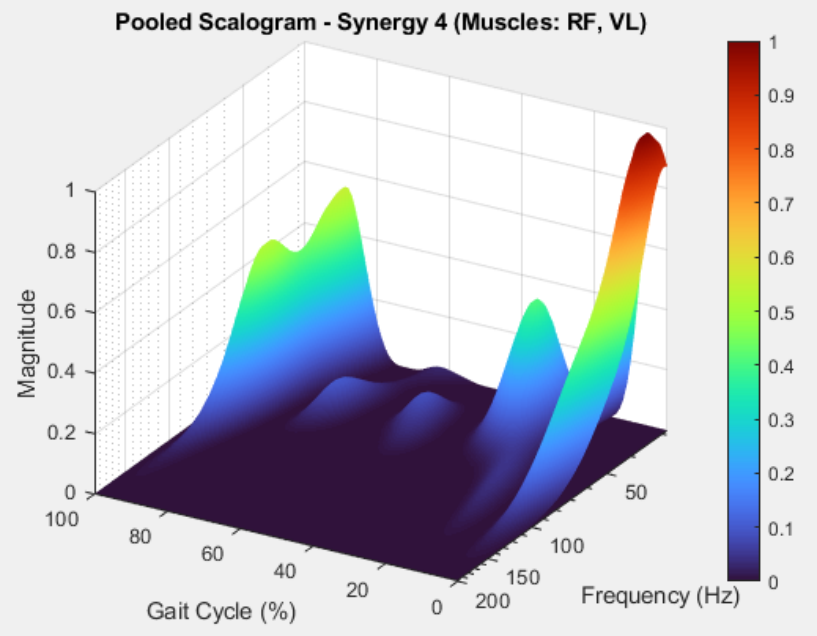



***Figure 61. 3D Pooled Scalogram for Subject 12.***

- **Subject 13**

In subject 13, the main contributions of Rectus Femoris (RF) and Vastus Lateralis (VL) identify synergy 3 (Figure 62), highlighting the dominant activation of RF, with secondary contributions by VL. This synergy shows a continuous activation throughout the walking cycle, with significant peaks in specific phases: about 10%, 50% and 90% of the walking cycle (Figure 63). In the pooled scalograms (Figures 63, 64) significant peaks of intensity below about 100 Hz are observed, with activity higher between 20 and 50 Hz. The most remarkable peak occurs around 85% of the walking cycle, while also minor intensity peaks around 25% and 70% of the GC are evident. The alignment of the activation peaks identified by Non Negative Matrix Factorization (NMF) with those observed in the clustered scalogram are consistent despite the lack of activity in the pooled scalograms around 50% of the step cycle.

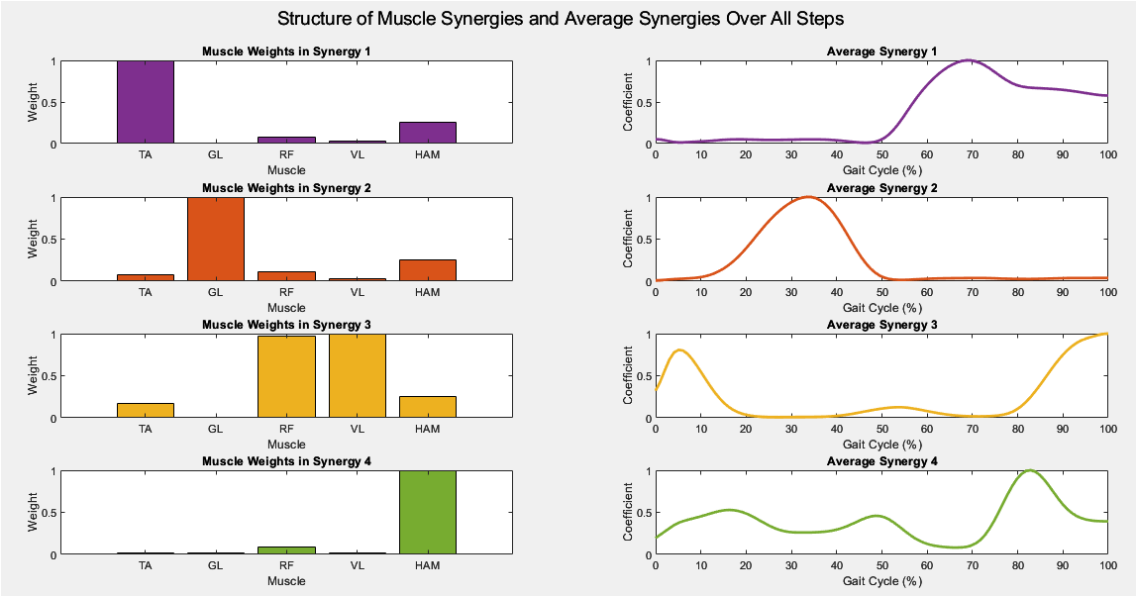



***Figure 62. Structure and Average Synergies Over All Steps for Subject 13.***

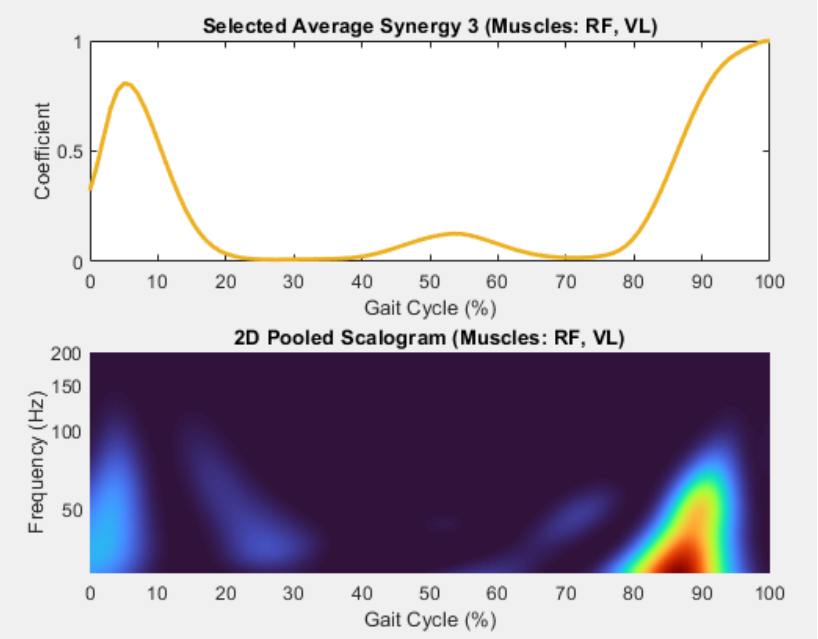



***Figure 63. Selected Average Synergy and 2D Pooled Scalogram for Subject 13.***

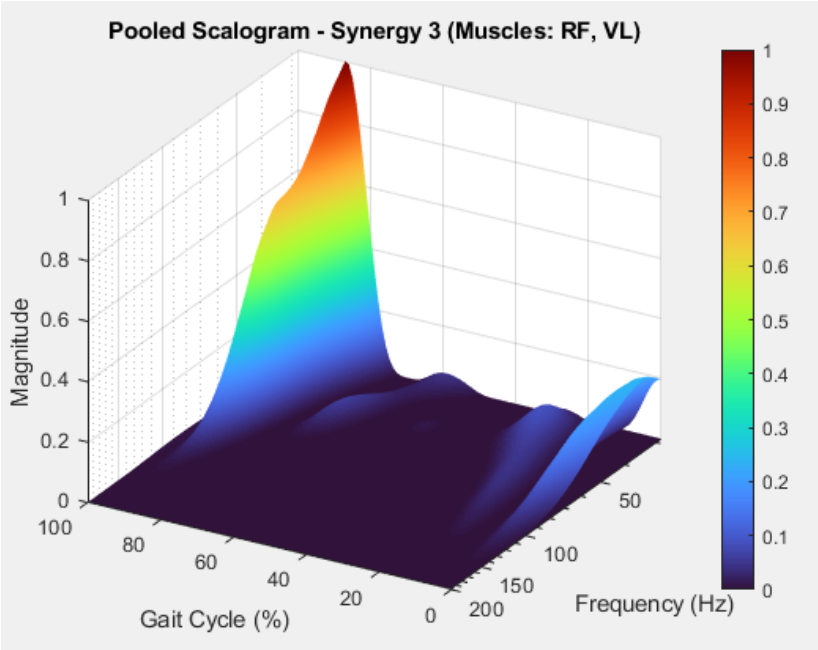



***Figure 64. 3D Pooled Scalogram for Subject 13.***

- **Subject 14**

In subject 14, synergy 2 is characterized by significant contributions from the Rectus Femoris (RF) and Vastus Lateralis (VL) (Figure 65), where there is continuous activation throughout the cycle, with notable peaks around 10%, 50% and 100% (Figure 66). The pooled scalograms (Figures 66, 67) reveal that most muscle activation is concentrated in the frequency range 50-150 Hz, with the most significant peak being around 90% at an intensity. There are additional lower intensity activations with a frequency range centered from 10 to 60 Hz. There is alignment of the activation peaks identified by NMF and those observed in the pooled scalograms.

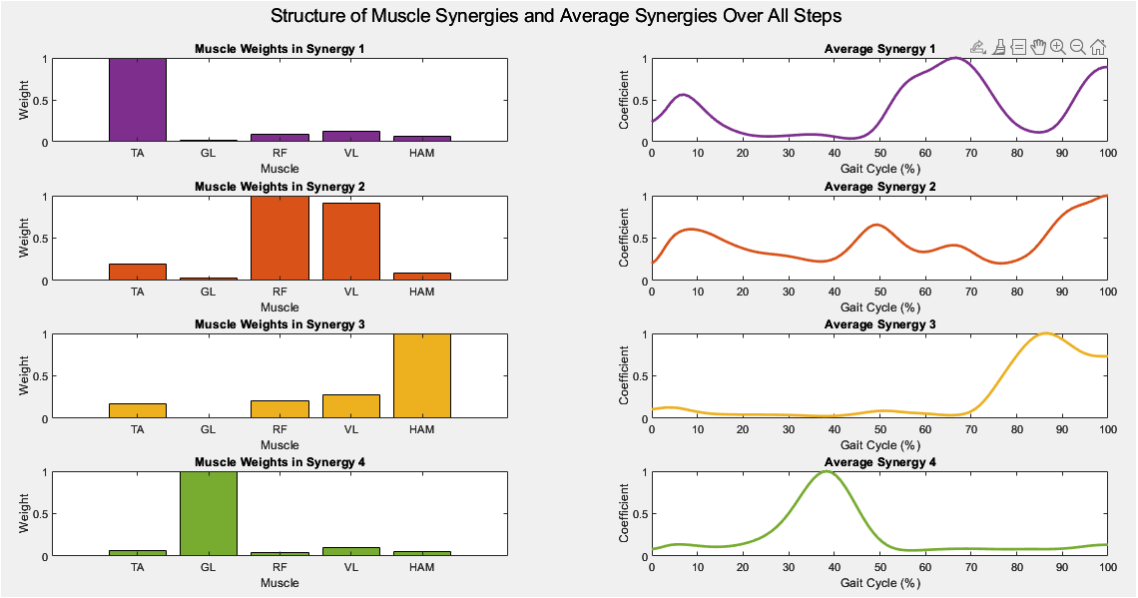



***Figure 65. Structure and Average Synergies Over All Steps for Subject 14.***

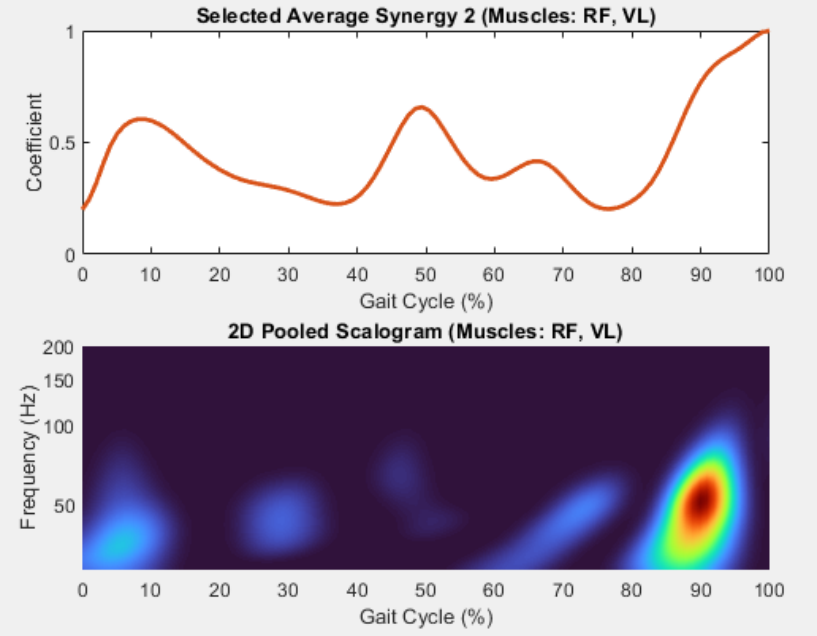



***Figure 66. Selected Average Synergy and 2D Pooled Scalogram for Subject 14.***

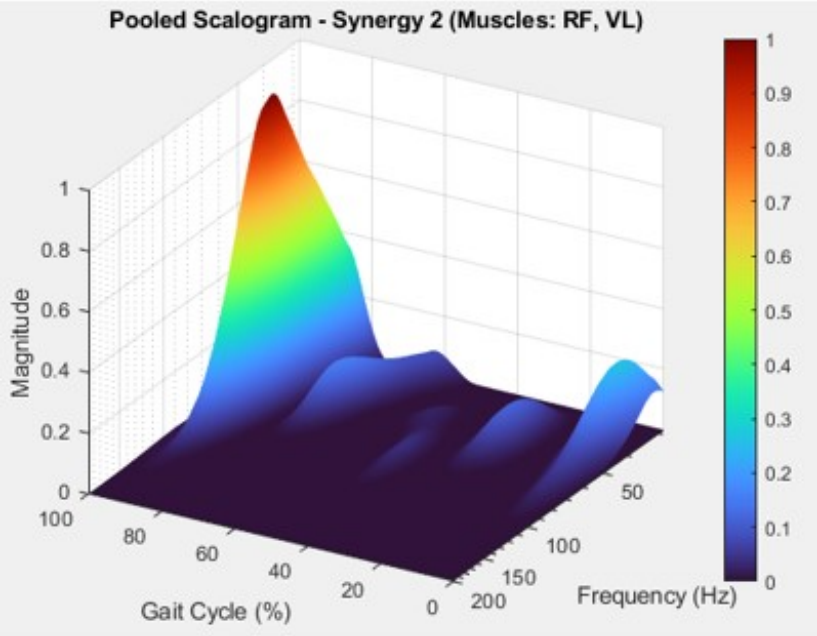



***Figure 67. 3D Pooled Scalogram for Subject 14.***

- **Subject 15**

In subject 15, synergy 4 is characterized by significant contributions from the Rectus Femoris (RF) and Vastus Lateralis (VL) (Figure 68). This synergy shows a continuous activation throughout the cycle, with significant peaks occurring at about 8%, 50% and 100% of the gait cycle (Figure 69). In the pooled scalograms (Figures 69, 70) most of the muscle activation occurs within the frequency range 20-150 Hz, with the most significant peak occurring around 90% of the gait cycle. Initially there is a peak of medium intensity, then there are peaks of lower intensity concentrated around 50 Hz. There is a perfect alignment of the activation peaks identified by the NMF with those shown in the pooled scalograms.

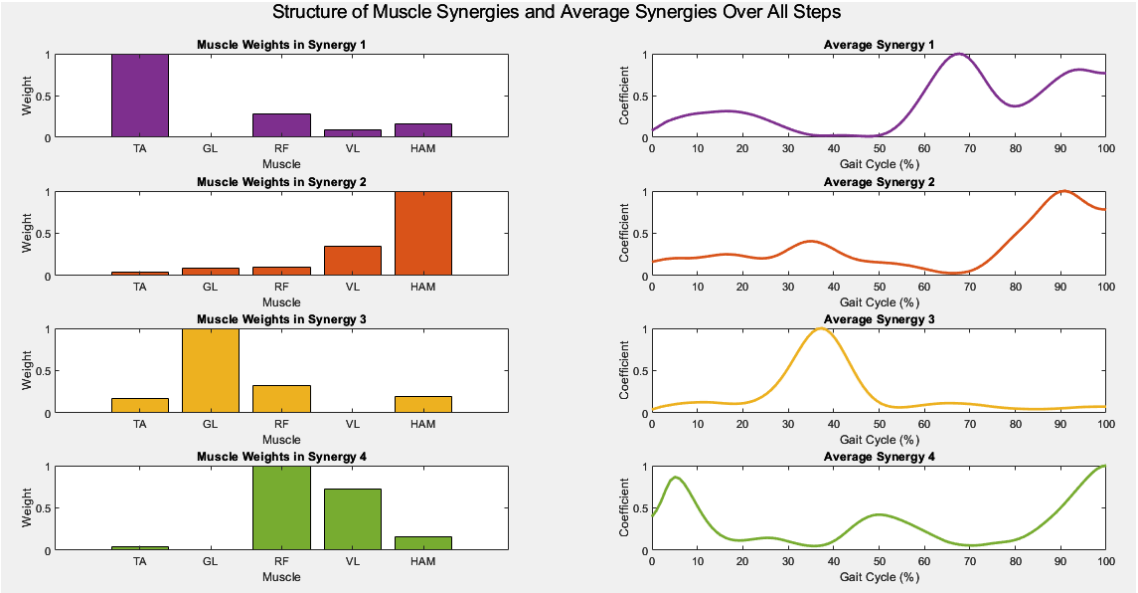



***Figure 68. Structure and Average Synergies Over All Steps for Subject 15.***

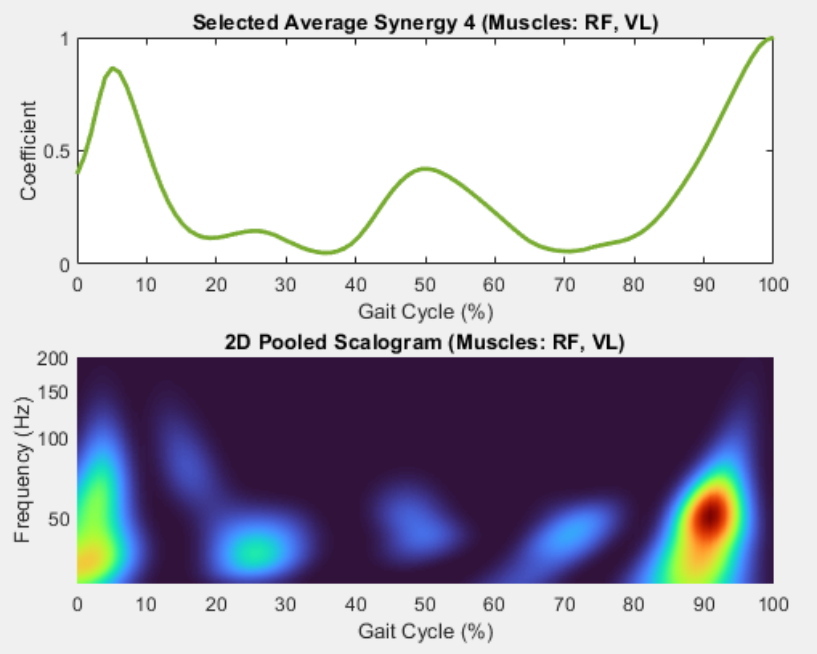



*Figure 69. Selected Average Synergy and 2D Pooled Scalogram for Subject 15.*

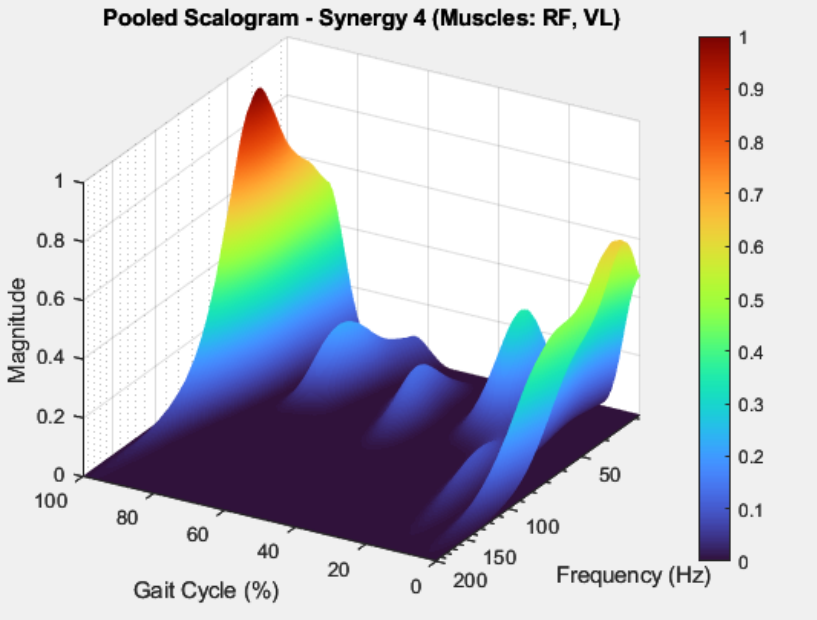



*Figure 70. 3D Pooled Scalogram for Subject 15.*

- **Subject 16**

In subject 16, figure 71 illustrates the muscle weights where the major contribution of the muscles Rectus Femoris (RF) and Vastus Lateralis (VL) is in the fourth synergy, in which there is continuous activation up to 70%, with peaks occurring around 8% and 50% of the step cycle with a subsequent decrease to have an increase in GC around 100% (Figure 72). In the pooled scalograms (Figure 72, 73) most of the muscle activation occurs mainly in the frequency range 50-100 Hz, with the most significant peak occurring around the 8% of the walking cycle, then there is a peak at 90% medium intensity with a frequency range of 50 to 70 Hz and further low intensity activations. There is a good alignment of the activation peaks identified by the NMF with those observed in the grouped scalogram except for the activation of the pooled scalograms at 70%.

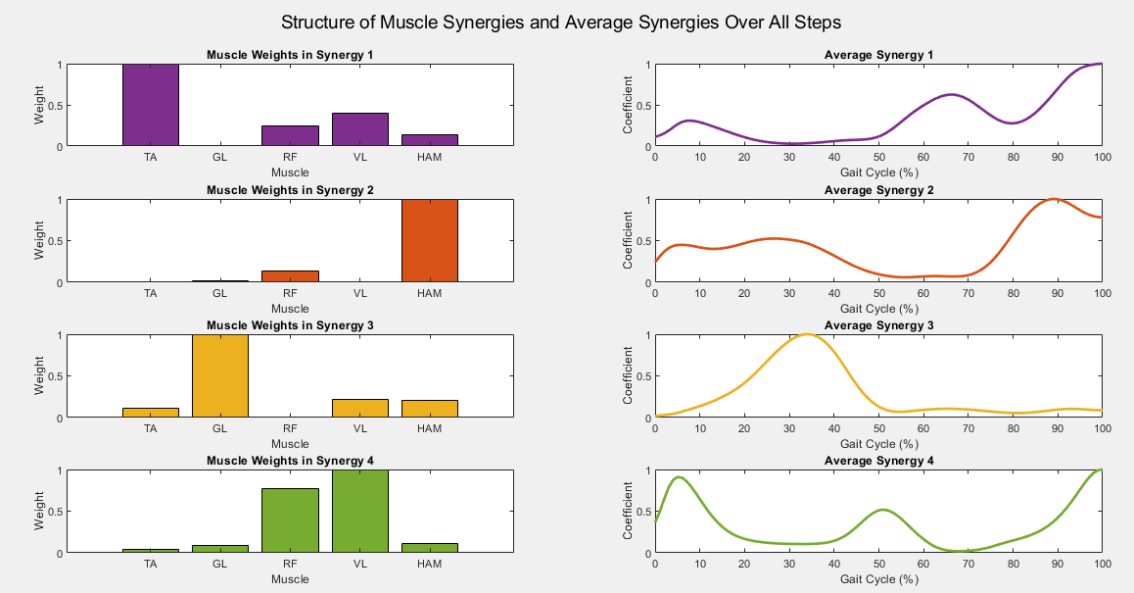



***Figure 71. Structure and Average Synergies Over All Steps for Subject 16.***

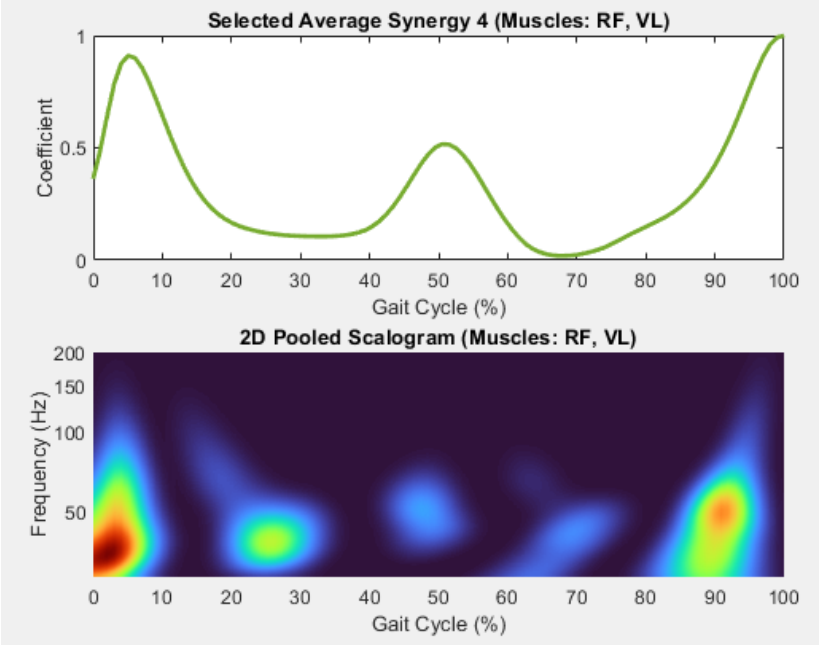



*Figure 72. Selected Average Synergy and 2D Pooled Scalogram for Subject 16.*

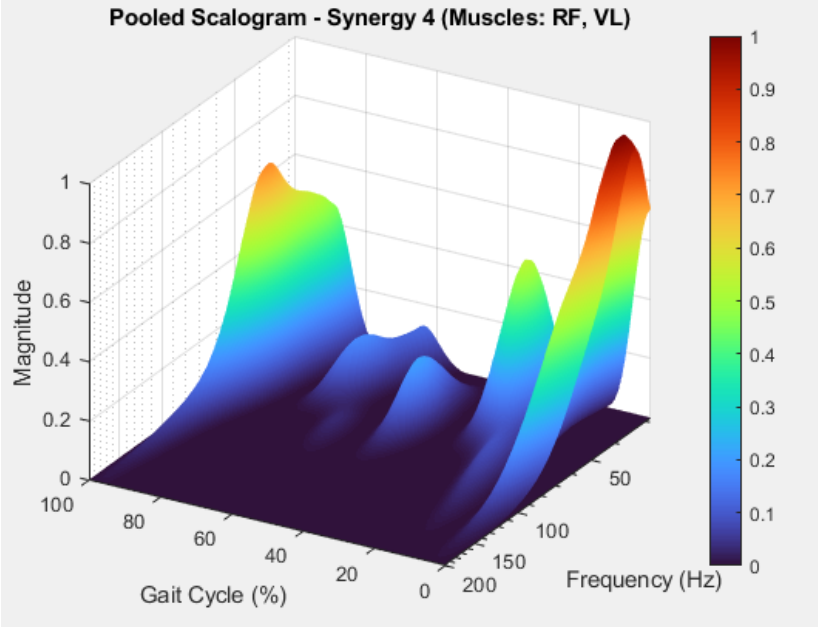



*Figure 73. 3D Pooled Scalogram for Subject 16.*

- **Subject 17**

In subject 17, Femoris (RF) and Vastus Lateralis (VL) identify synergy 3 as the one where these muscles have greater contributions (Figure 74). This synergy shows a continuous activation throughout the cycle, with distinct peaks occurring around 8%, 50% and 100% of the gait cycle (Figure 75). In the pooled scalograms (Figures 75, 76), most muscle activation is concentrated mainly in the frequency range 50-100 Hz, with the most significant peak occurring between 80-90% with a higher intensity concentrated within 50 Hz. Further activations are present with lower intensity around 8%, 30% and 60% of the step cycle. There is a match between the activation peaks identified by the NMF and those identified by the pooled scalograms except for the activation around 50% which in the pooled scalogram is around 60%.

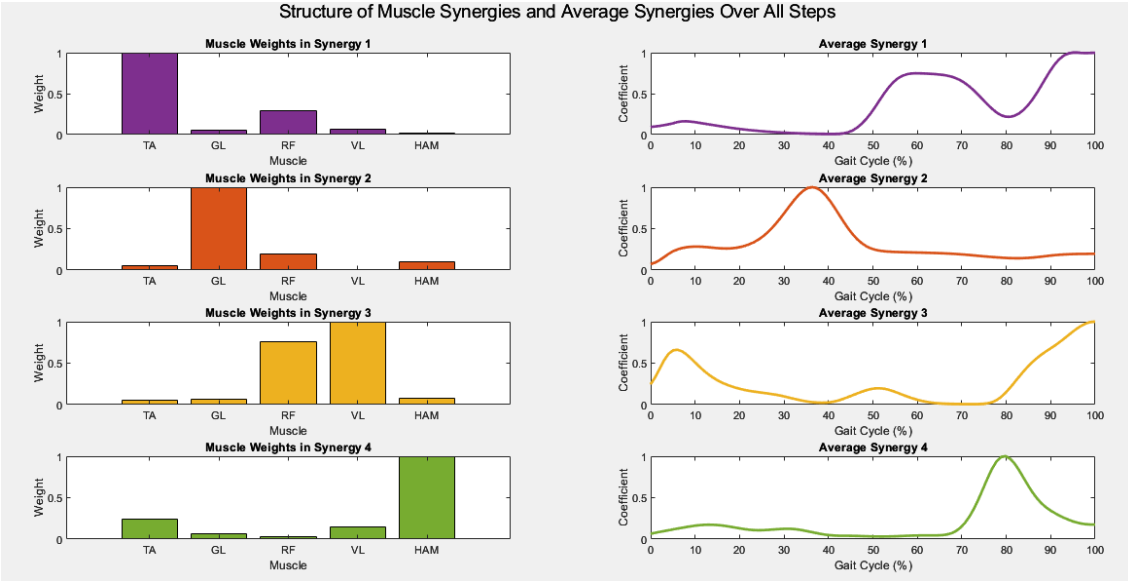



***Figure 74. Structure and Average Synergies Over All Steps for Subject 17.***

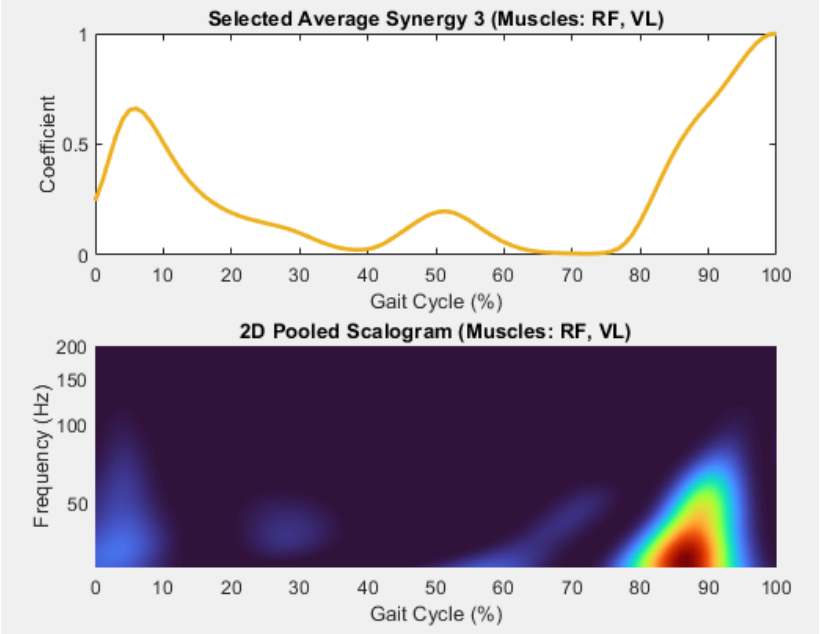



***Figure 75. Selected Average Synergy and 2D Pooled Scalogram for Subject 17.***

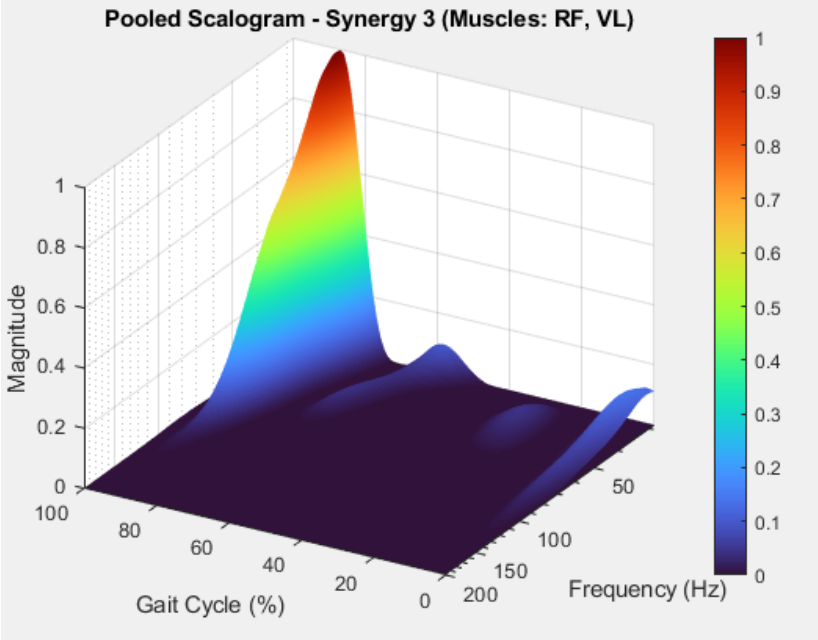



***Figure 76. 3D Pooled Scalogram for Subject 17.***

- **Subject 18**

In subject 18, synergy 2 is characterized by significant contributions from the Rectus Femoris (RF), as evidenced in muscle weights (Figure 77). This synergy shows a continuous activation throughout the walking cycle, with pronounced peaks occurring at about 8%, 55% and 88% of the walking cycle (Figure 78). In the pooled scalograms (Figures 78, 79) most of the muscle activation takes place in the frequency range 50-150 Hz. The most significant peak appears around 50% of the gait cycle with several medium intensity peaks around 5%, 30%, 90%. The frequency range is from 10 Hz to 150 Hz with a gradual increase during the step cycle, in fact the first activation at 5% is concentrated from 10 Hz to 40 Hz and ending with the last one that concentrates from 50 Hz to 100 Hz. There is a good alignment of the activation peaks identified by the NMF with those observed in the pooled scalograms.

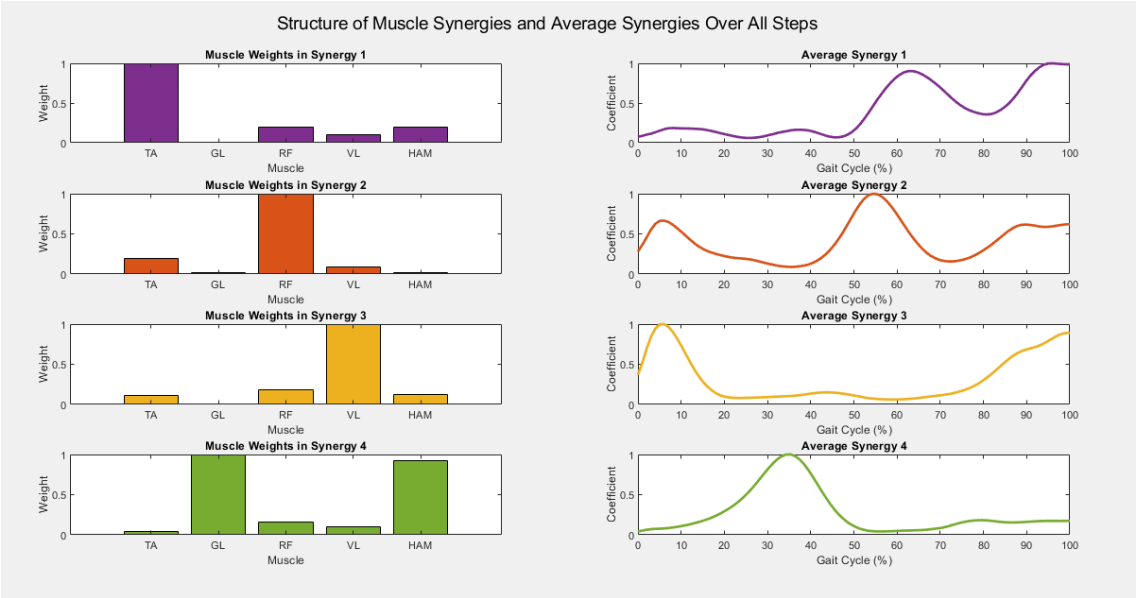



***Figure 77. Structure and Average Synergies Over All Steps for Subject 18.***

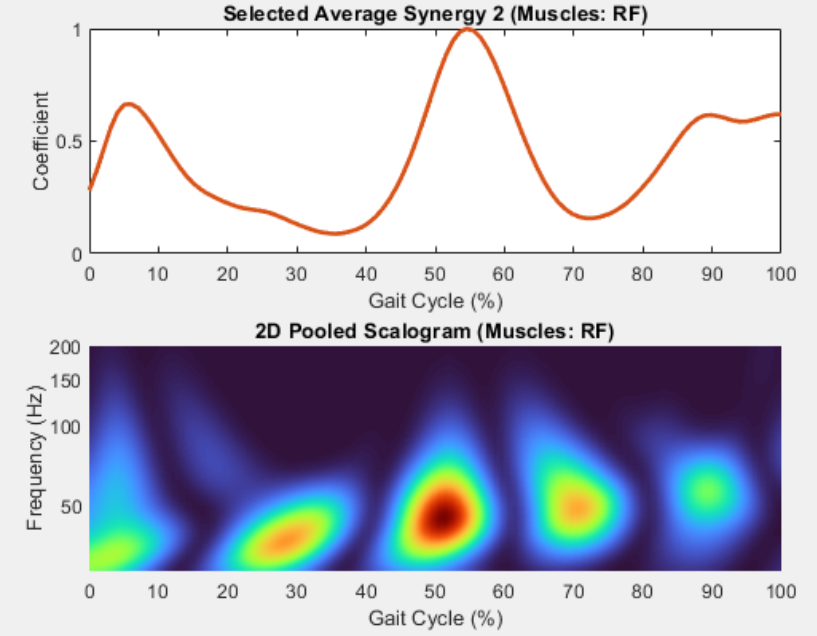



*Figure 78. Selected Average Synergy and 2D Pooled Scalogram for Subject 18.*

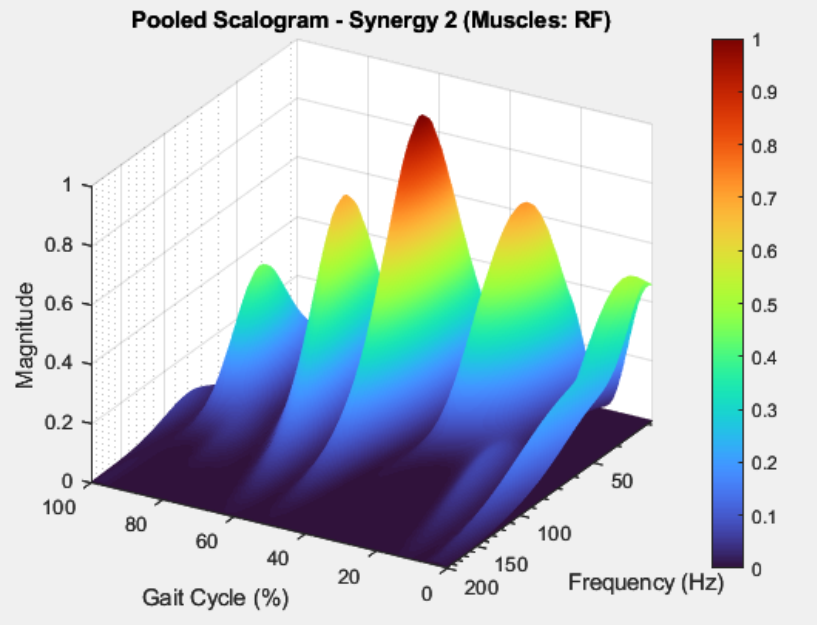



*Figure 79. 3D Pooled Scalogram for Subject 18.*

- **Subject 19**

In subject 19, synergy 2 is identified in which there is a great contribution of the Vastus Lateralis (VL) and also of the Hamstrings (HAM) while the contribution of the Rectus Femoris (RF) is absent (Figure 80). We have a continuous activation up to 55% where there is a first peak around 8% of the GC and another between 23% and 55% of the step cycle, then we have a last increase in activity between 80% and 100% of the GC (Figure 81). In the pooled scalograms (Figures 81, 82) the peak of higher intensity is detected between 89% and 95% of the GC, with a frequency band below 80 Hz and a lower peak of intensity around 60% concentrated below 50 Hz. There is a partial alignment of the activation peaks identified by the NMF with those observed in the pooled scalograms since the first two peaks are not identified but only the peak of greater intensity at the end of the GC.

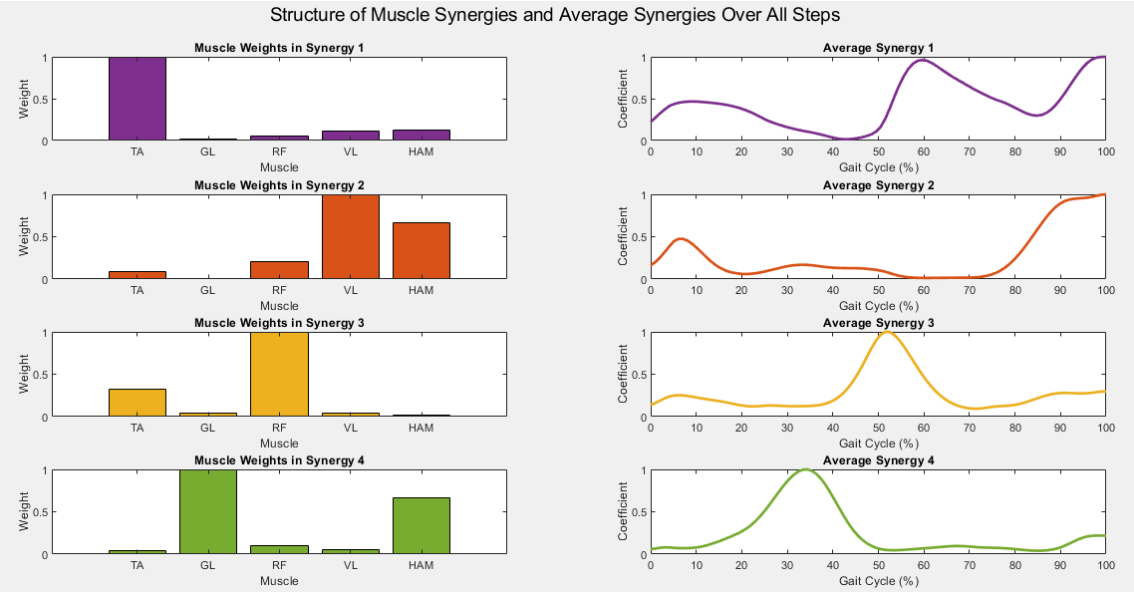



***Figure 80. Structure and Average Synergies Over All Steps for Subject 19.***

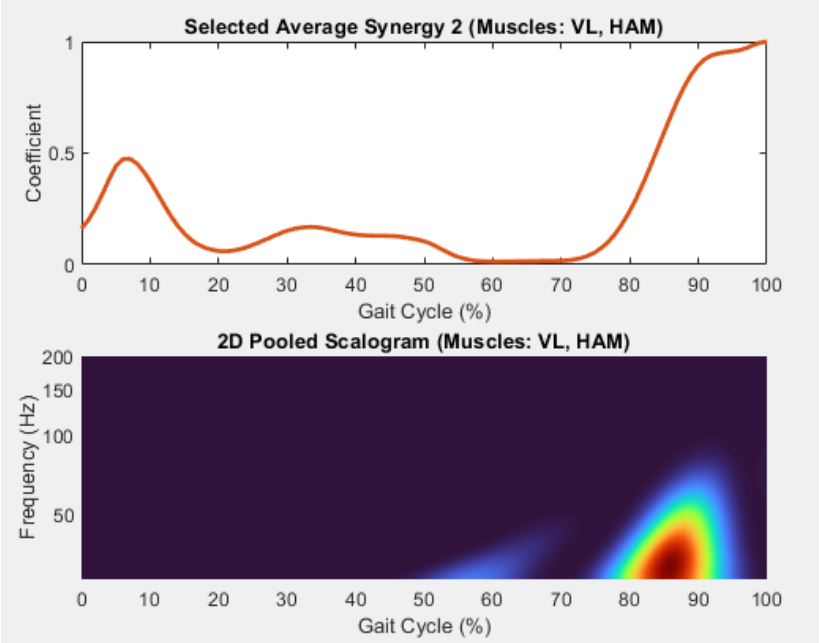



*Figure 81. Selected Average Synergy and 2D Pooled Scalogram for Subject 19.*

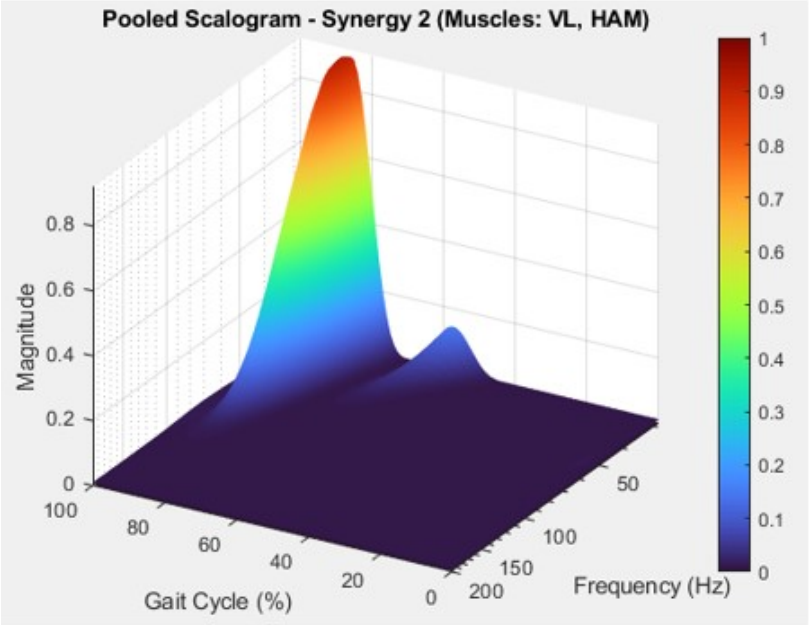



*Figure 82. 3D Pooled Scalogram for Subject 19.*

- **Subject 20**

In subject 20, the third synergy is characterized by the increased muscle weights of the Rectus Femoris (RF) and Vastus Lateralis (VL) and also the contribution of the Tibialis Anterior (TA) cycle (Figure 83), where there is a continuous activation with obvious peaks around 8% and 90% of the gait cycle (Figure 84). In the pooled scalograms (Figures 84, 85), most muscle activation occurs mainly in the frequency range 10-100 Hz, with a significant peak around 5% of the walking cycle, and a peak at 90% which has a higher intensity detected around 30 Hz. Low activity occurs at about 25% of the CG. There is a good match between the NMF results and the pooled scalograms except for this event which occurs around 25% of the gait cycle.

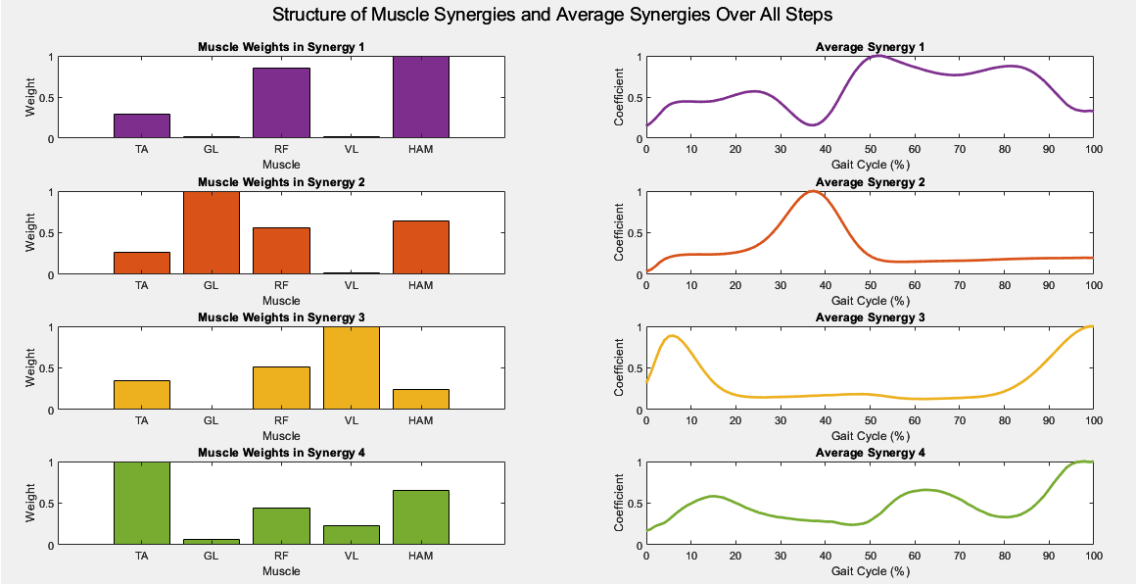



***Figure 83. Structure and Average Synergies Over All Steps for Subject 20.***

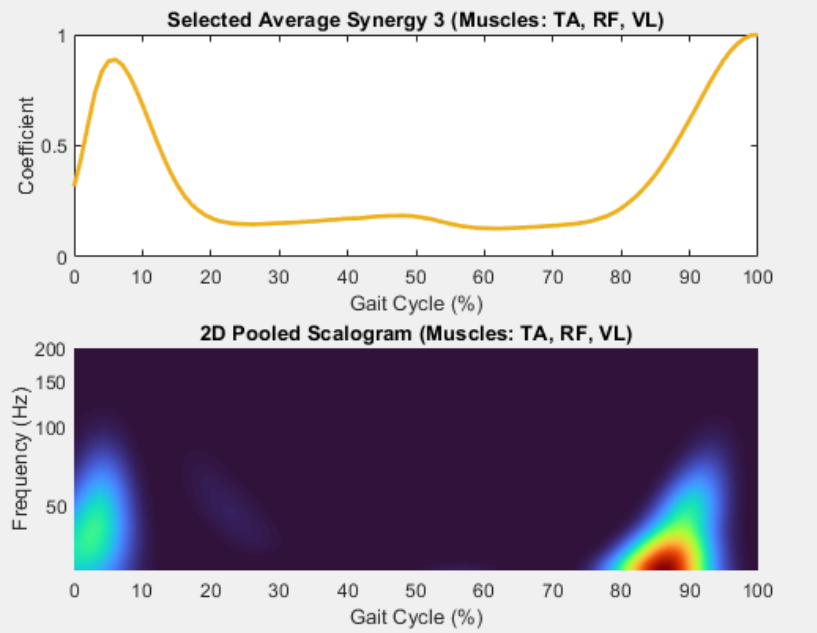



***Figure 84. Selected Average Synergy and 2D Pooled Scalogram for Subject 20.***

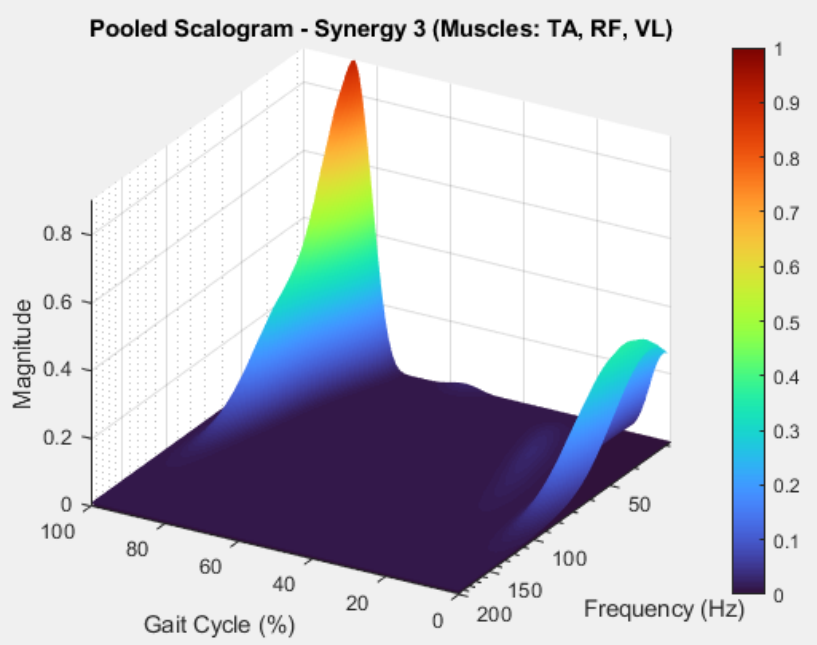



***Figure 85. 3D Pooled Scalogram for Subject 20.***

- **Subject 21**

In subject 21, the third synergy shows significant activation of the Rectus Femoris (RF) and Lateralis Vastus (VL) (Figure 86). The first peak occurs between 0% and 10% of the walking cycle, with a minor but significant activation between 40% and 50%. A second peak is observed between 80% and 90%. (Figure 87). In the pooled scalograms (Figures 87, 88), most of the muscle activity occurs in the 10Hz -70 Hz, with a prominent peak at about 10% of the walking cycle and another peak at 90% also there are peaks of lower intensity around 25%, 50% and 65%. Overall, the NMF results align well with the pooled scalograms results.

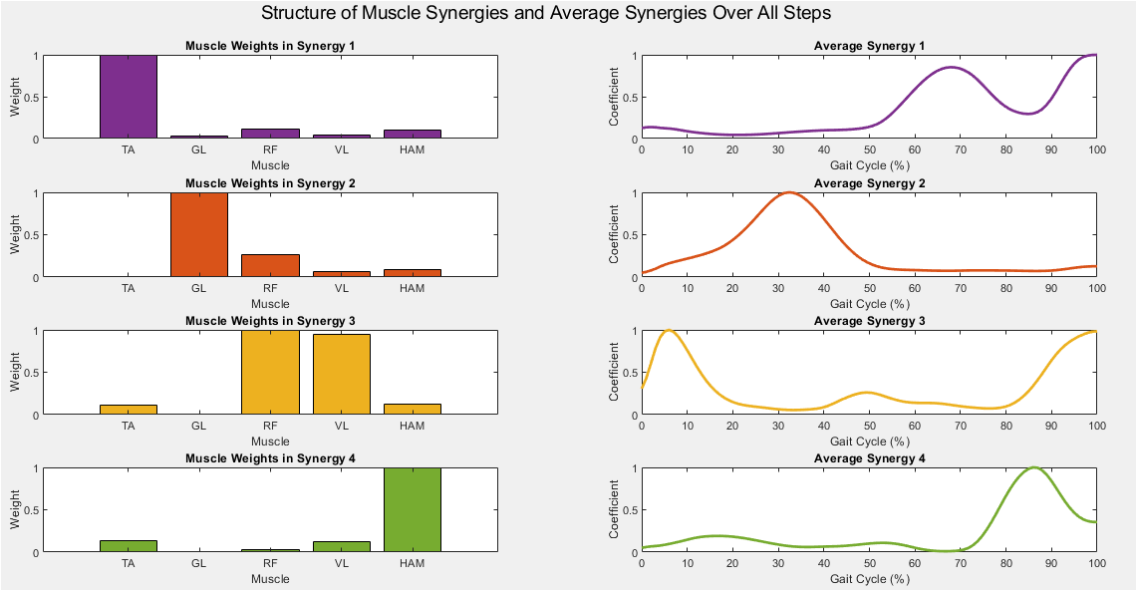



***Figure 86. Structure and Average Synergies Over All Steps for Subject 21.***

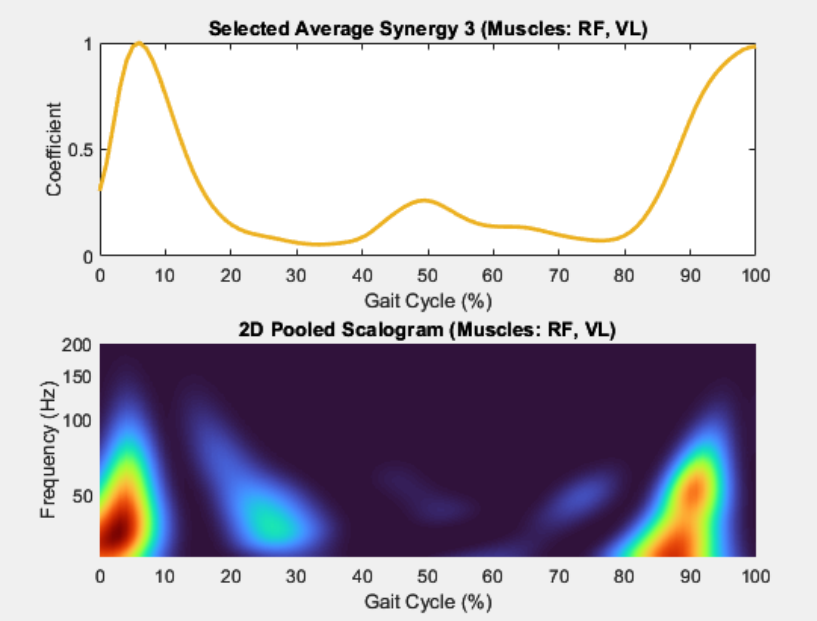



*Figure 87. Selected Average Synergy and 2D Pooled Scalogram for Subject 21.*

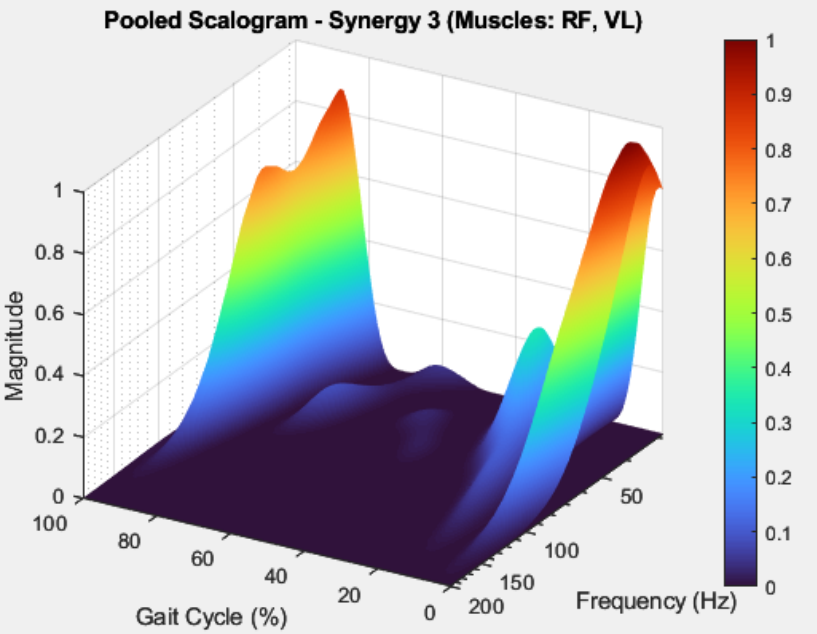



*Figure 88. 3D Pooled Scalogram for Subject 21.*

- **Subject 22**

In subject 22, contributions of the Rectus Femoris (RF) and Vastus Lateralis (VL) are greater in the third synergy (Figure 89), where muscle activation shows distinct peaks around 8% to 40% and 100% of the walking cycle (Figure 90). The pooled scalograms (Figures 90, 91) indicates that several activations from 0 to 10%, 20%, 40% 50% to 60% and finally from 80% to 90% of the step cycle, where they have a small intensity except the last small one which has a higher intensity and concentrates within 60 Hz. The activation patterns identified by the NMF correspond well to the data of the pooled scalograms except for the activation present in the latter from 50% to 60% of the gait cycle.

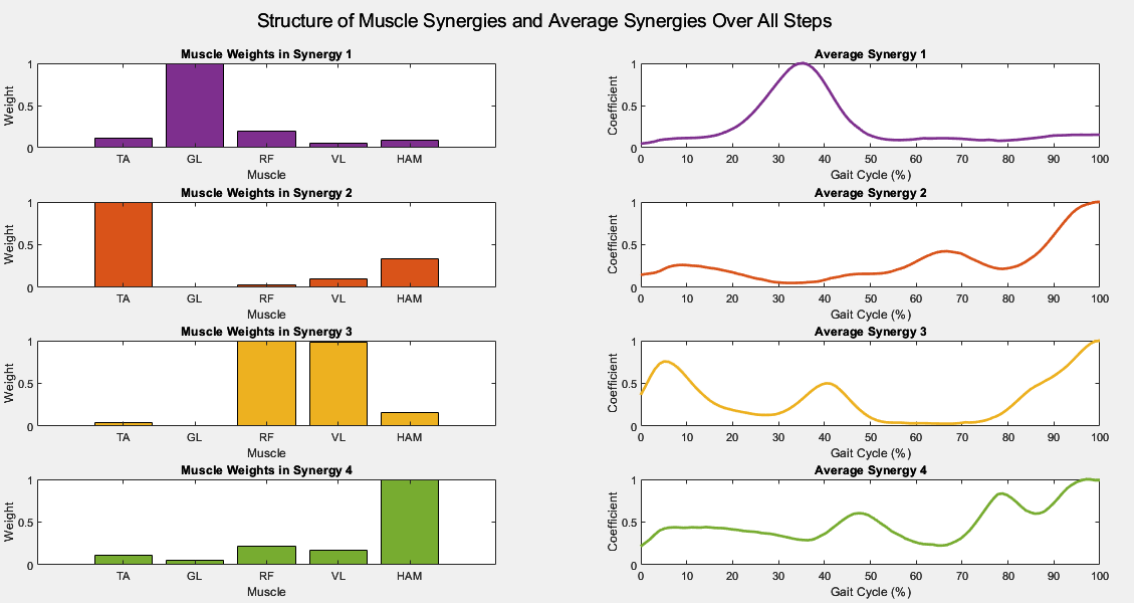



***Figure 89. Structure and Average Synergies Over All Steps for Subject 22.***

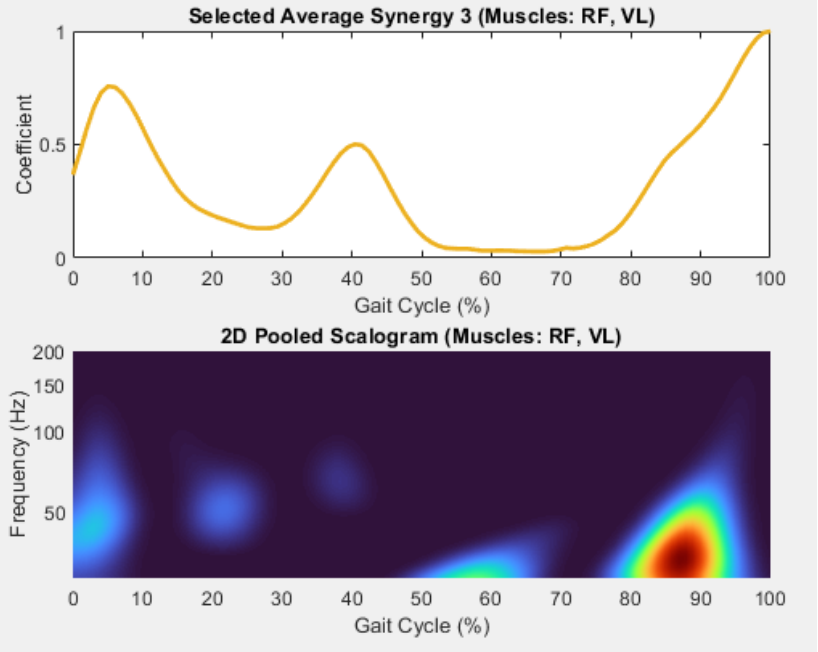



***Figure 90. Selected Average Synergy and 2D Pooled Scalogram for Subject 22.***

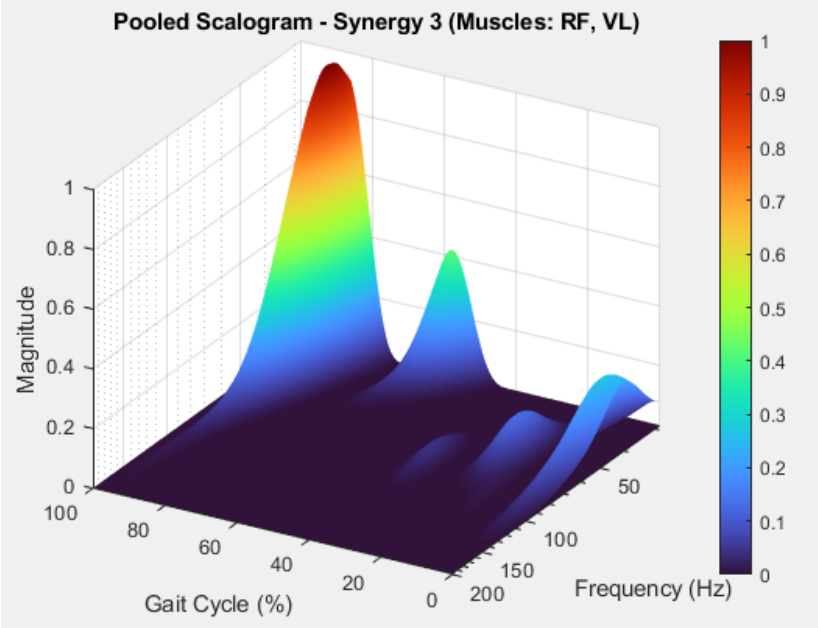



***Figure 91. 3D Pooled Scalogram for Subject 22.***

- **Subject 23**

In subject 23, the third synergy presents substantial contributions from the Rectus Femoris (RF) and Vastus Lateralis (VL), and there is also the presence of the contribution of the Hamstrings (HAM) (Figure 92). There is an activation around 8% of the walking cycle with a decrease in activity until the second peak around 100% of gait cycle (Figure 93). The pooled scalograms (Figures 93, 94) show that most muscle activity occurs mainly in the 50 Hz frequency range, with a higher peak near 8% of the walking cycle and a secondary peak is also noted at 85% where a higher intensity is present around 30 Hz, while the minimum activation is seen at 40%. The results of the NMF match well with the pooled scalograms.

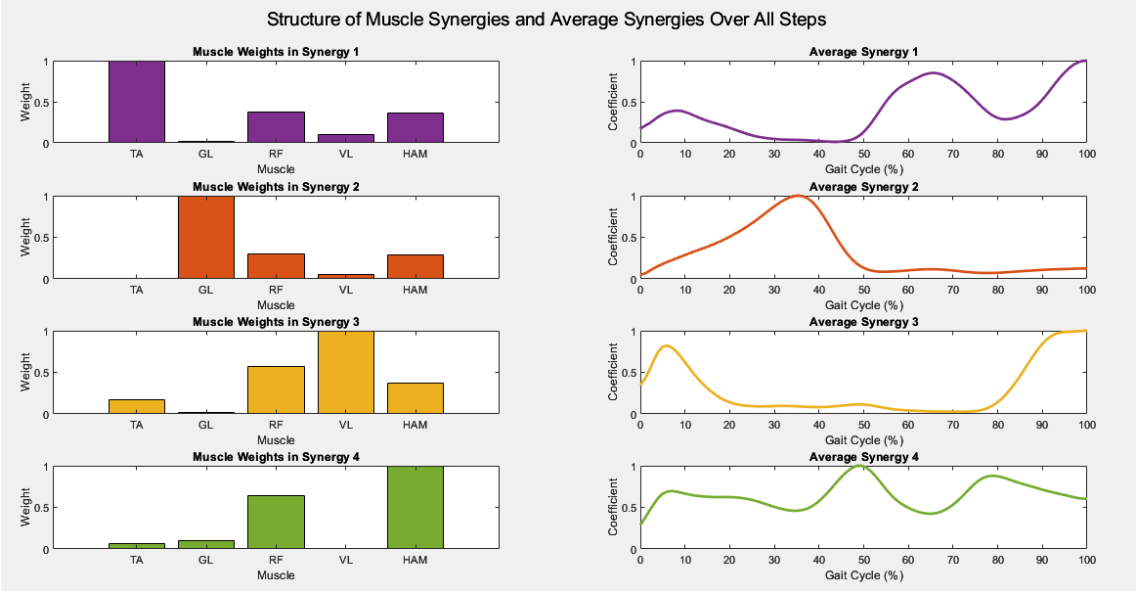



***Figure 92. Structure and Average Synergies Over All Steps for Subject 23.***

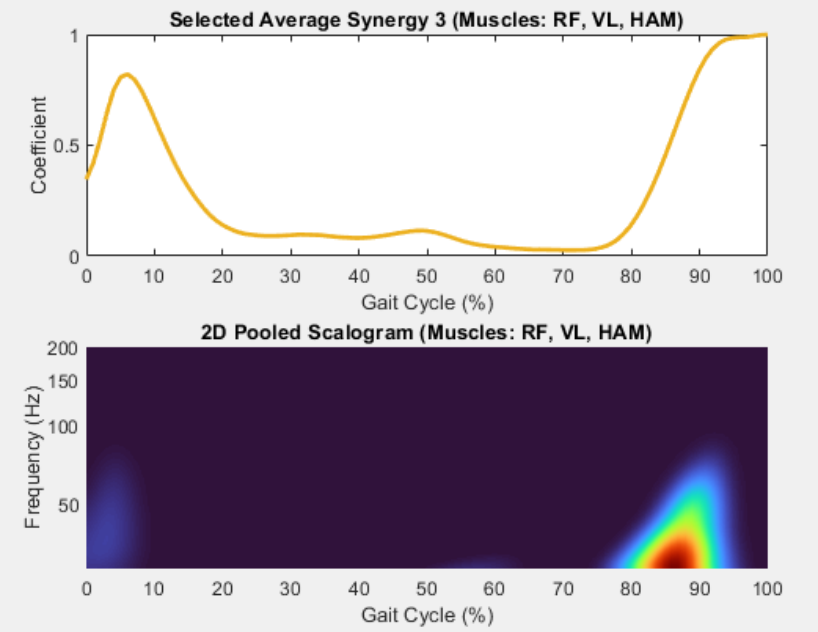



*Figure 93. Selected Average Synergy and 2D Pooled Scalogram for Subject 23.*

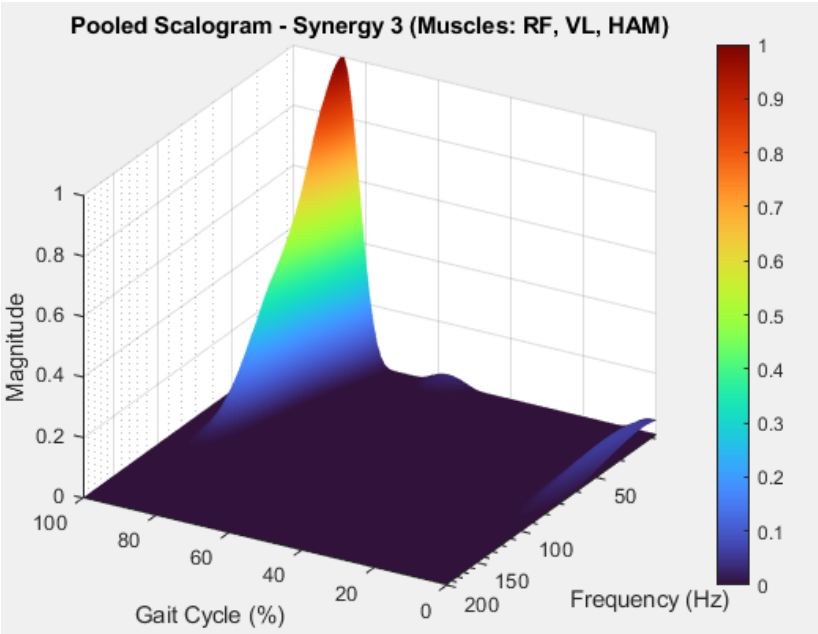



*Figure 94. 3D Pooled Scalogram for Subject 23.*

- **Subject 24**

In subject 24, the third synergy is the major muscle contributions of the Rectus Femoris (RF) and Vastus Lateralis (VL) (Figure 95). There are significant activation peaks at about 8%, 55% and 100% of the gait cycle (Figure 96). The pooled scalograms (Figures 96, 97) indicate that most muscle activation occurs in the 10-190 Hz frequency range with obvious peaks around 8% and 90%. Additional activity is detected between 20% and 30% of the GC, around 50% of the GC and 70% to 80% of the GC. The alignment between the NMF results and the pooled scalograms is good, except for the detection of activity between 70%-80% of the GC.

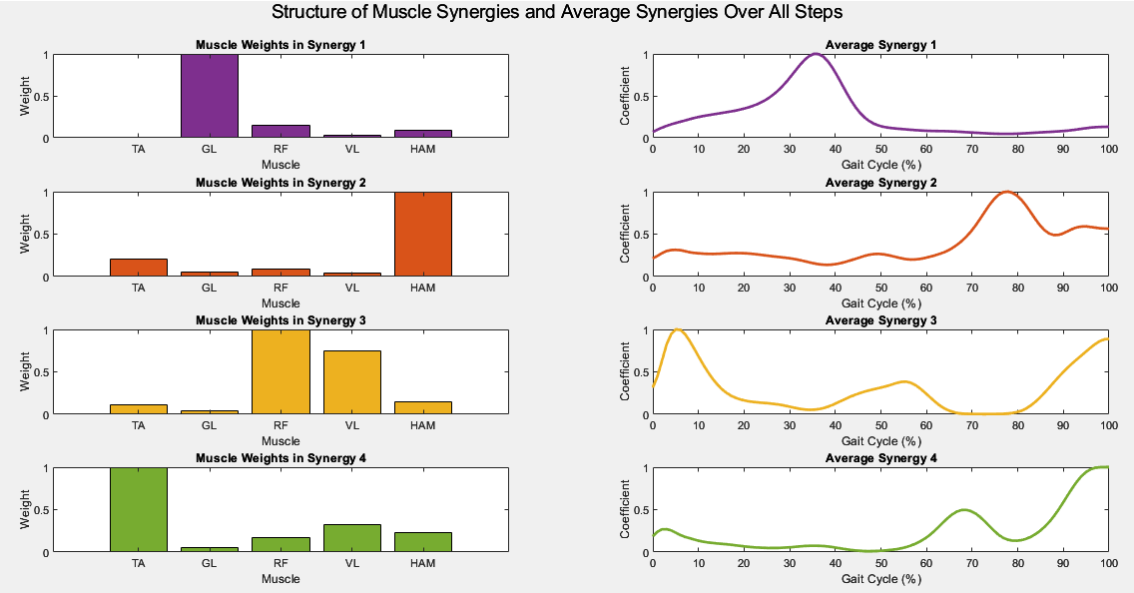



***Figure 95. Structure and Average Synergies Over All Steps for Subject 24.***

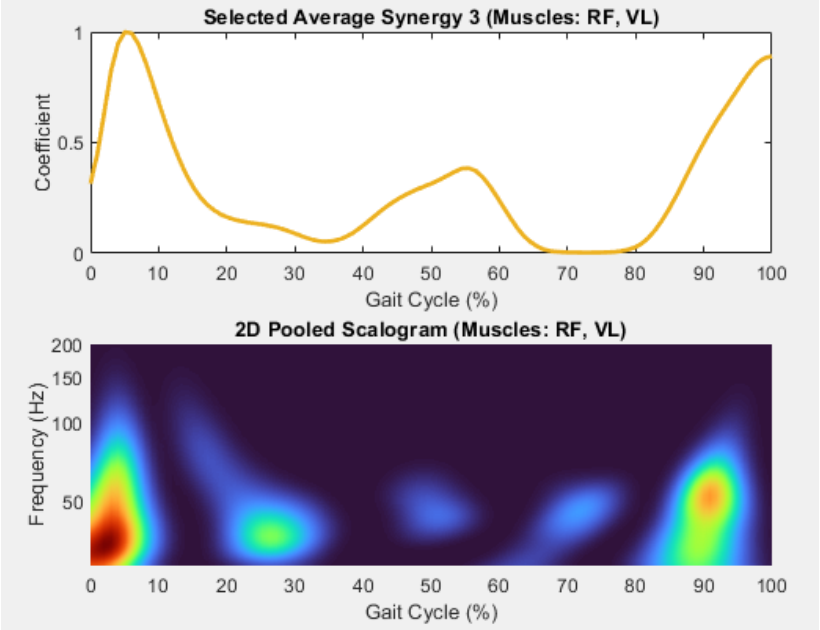



*Figure 96. Selected Average Synergy and 2D Pooled Scalogram for Subject 24.*

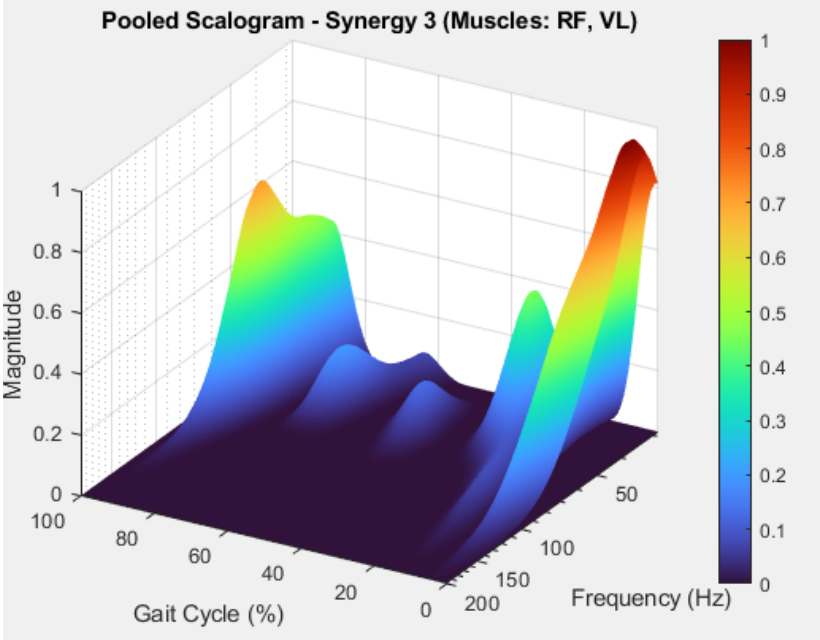



*Figure 97. 3D Pooled Scalogram for Subject 24.*

- **Subject 25**

In subject 25, the Rectus Femoris (RF) and Vastus Lateralis (VL) show their maximum activation in the second synergy with the contribution of the Tibialis Anterior (TA) (Figure 98). A noticeable peak occurs between 0% and 8% of the walking cycle, followed by another peak between 40% and 70% and at the end of the walking cycle around 100% (Figure 99). The pooled scalograms (Figures 99, 100) show low intensity activations at the beginning of the step cycle, around 30% and 70% of the GC where they have a frequency range of about 50 Hz; at the end of the gait cycle there is a high peak between 80% and 90%, in the frequency range from 10 Hz to 100 Hz. There is a good correspondence between the NMF results and pooled scalograms even if the peak evidenced in the time-response of the synergy between 40% and 70% of the GC is not present in the pooled scalograms.

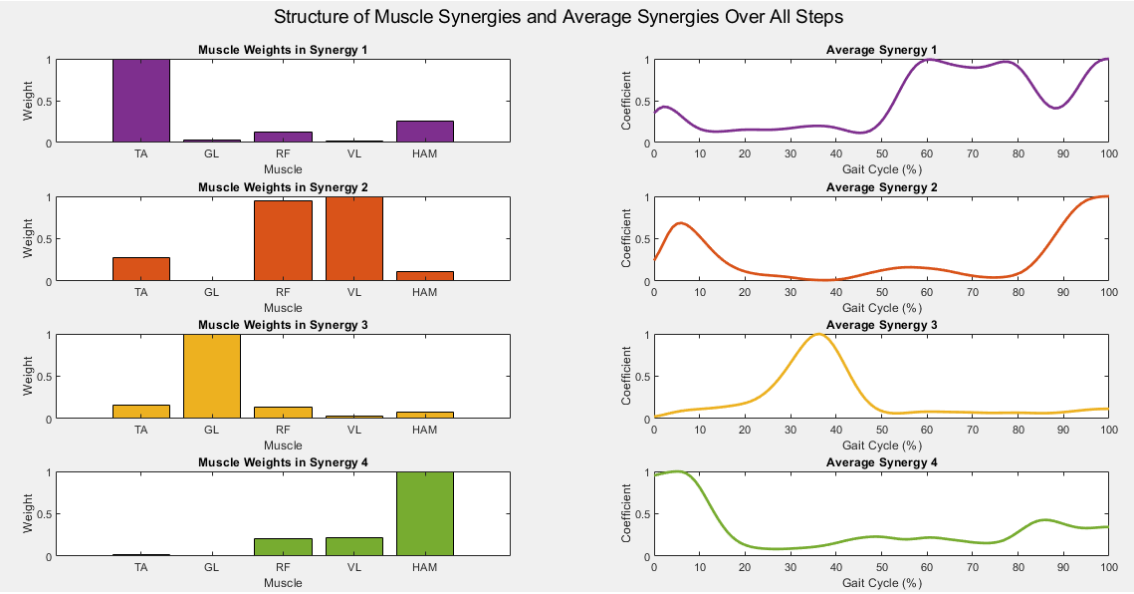



***Figure 98. Structure and Average Synergies Over All Steps for Subject 25.***

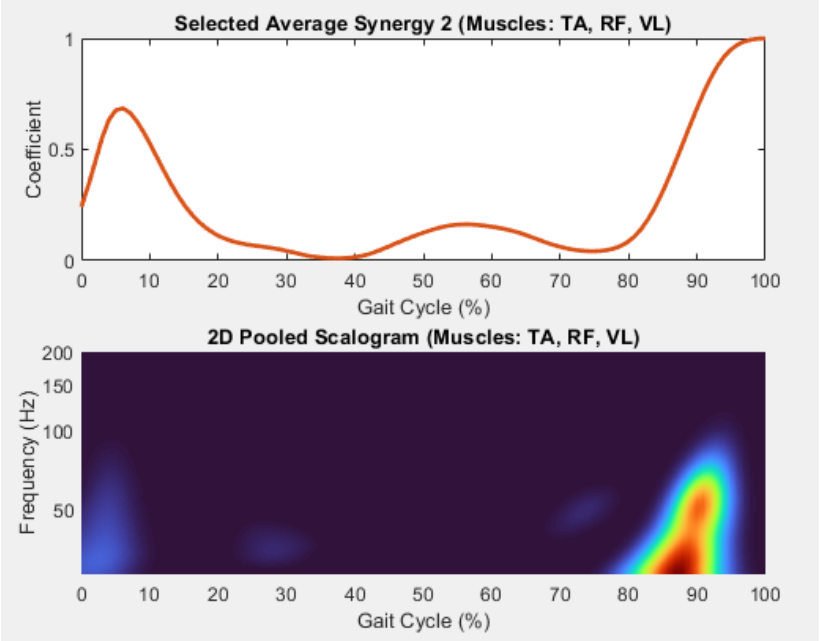



***Figure 99. Selected Average Synergy and 2D Pooled Scalogram for Subject 25.***

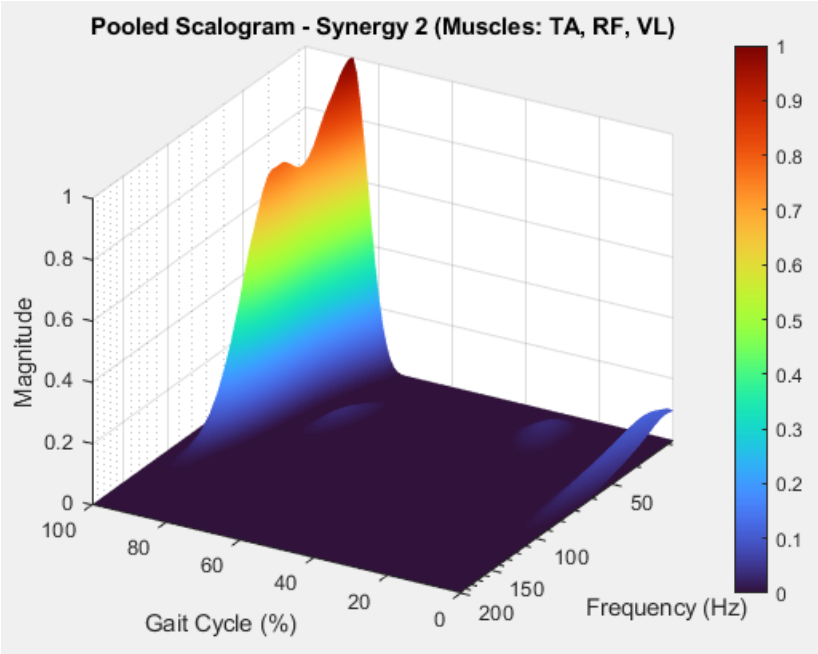



***Figure 100. 3D Pooled Scalogram for Subject 25.***

- **Subject 26**

In subject 26, the fourth synergy is chosen because a significant increase of muscle weights of the Rectus Femoris (RF) and Vastus Lateralis (VL) (Figure 101), where there is continuous activation with peaks at 8%, 40% and 100% of the step cycle, is observed (Figure 102). The pooled scalograms (Figures 102, 103) show that the majority of muscle activation occurs mainly in the frequency range 10-150 Hz. There is a low intensity peak concentrated below 50 Hz at 50-60% of the step cycle and another between 20% and 30% of the GC where we have a higher frequency range between 40 Hz and 100 Hz. Concentrated around 30 Hz. In general, the NMF results align very well with the various pooled scalograms.

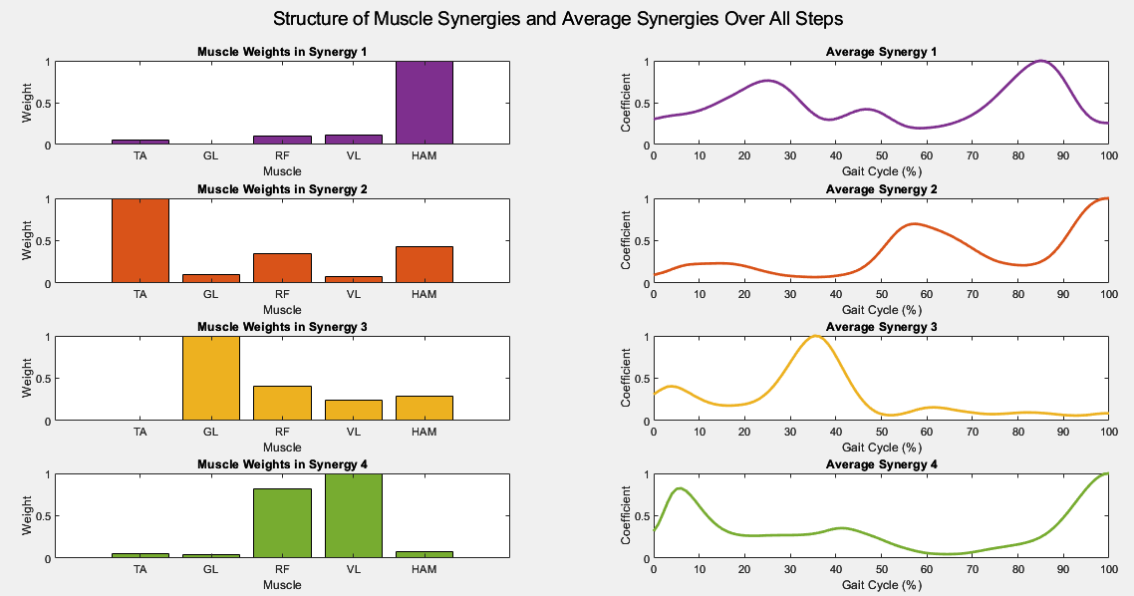



***Figure 101. Structure and Average Synergies Over All Steps for Subject 26.***

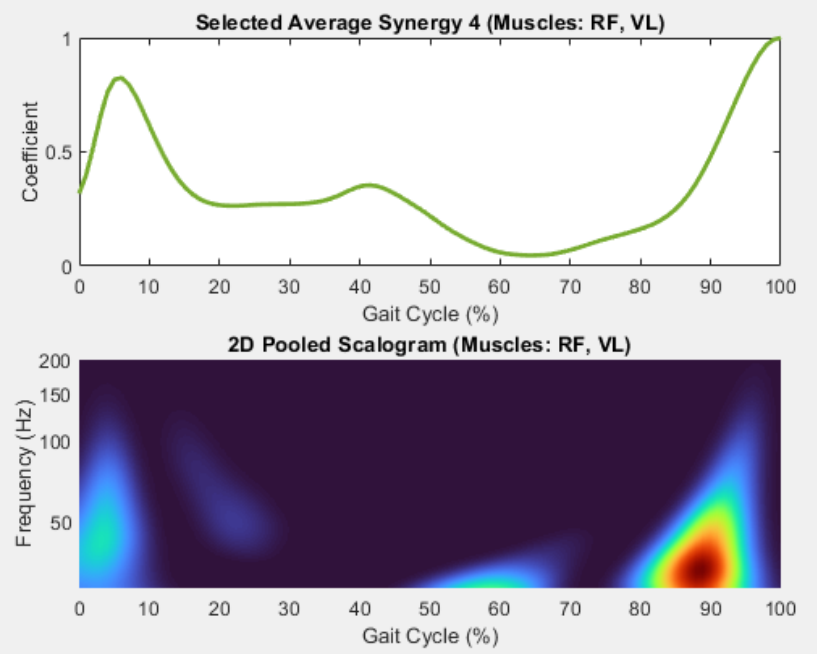



***Figure 102. Selected Average Synergy and 2D Pooled Scalogram for Subject 26.***

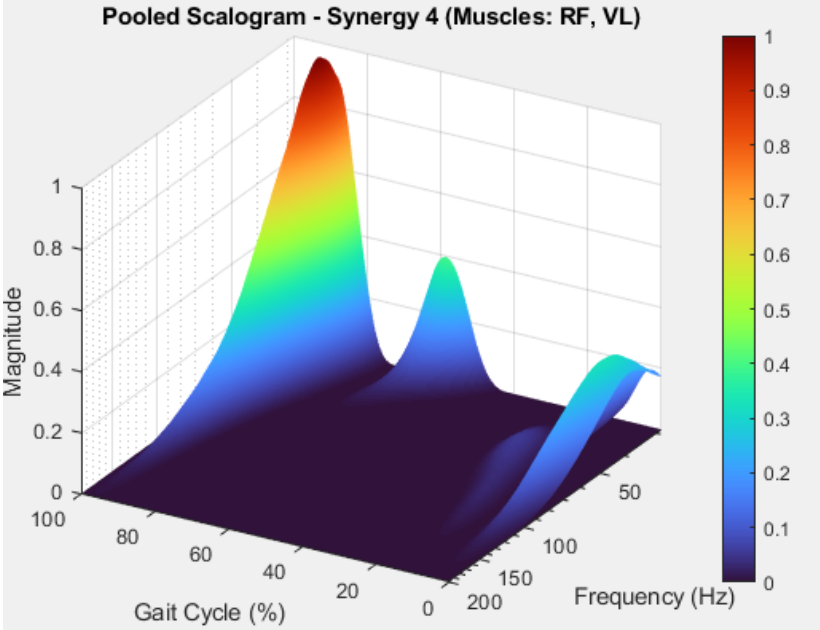



***Figure 103. 3D Pooled Scalogram for Subject 26.***

- **Subject 27**

In subject 27, the chosen synergy is the first and is characterized by the contribution of only the Rectus Femoris (RF) (Figure 104). In this synergy there are almost always activations with a large peak ranging from 0% to 60% of the step cycle, with a subsequent decrease in activation and then increase again around the end of the step cycle (Figure 105). Pooled scalograms (Figures 105, 106) show that muscle activation occurs mainly in the 10-frequency range100 Hz, in particular there are two peaks of higher intensity between 0% and 15% of the GC and between 55% and 75% of the step cycle which both have frequencies concentrated within 50 Hz and a further peak with frequencies extending up to 100 Hz at 100% of the step cycle. Overall, there is a strong alignment between the results of non-negative matrix factorization and pooled scalograms.

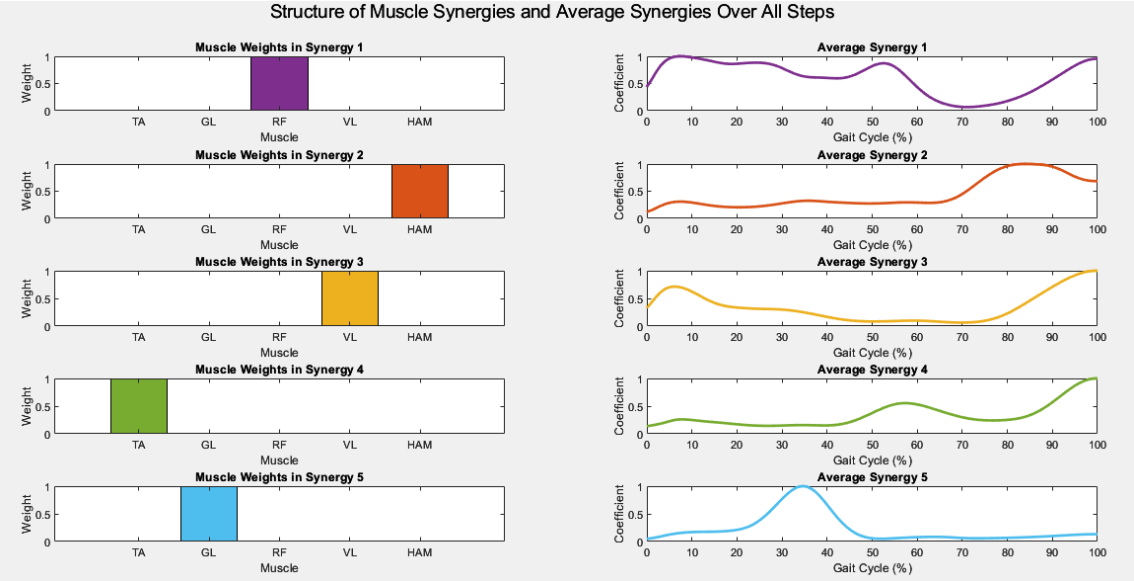



***Figure 104. Structure and Average Synergies Over All Steps for Subject 27.***

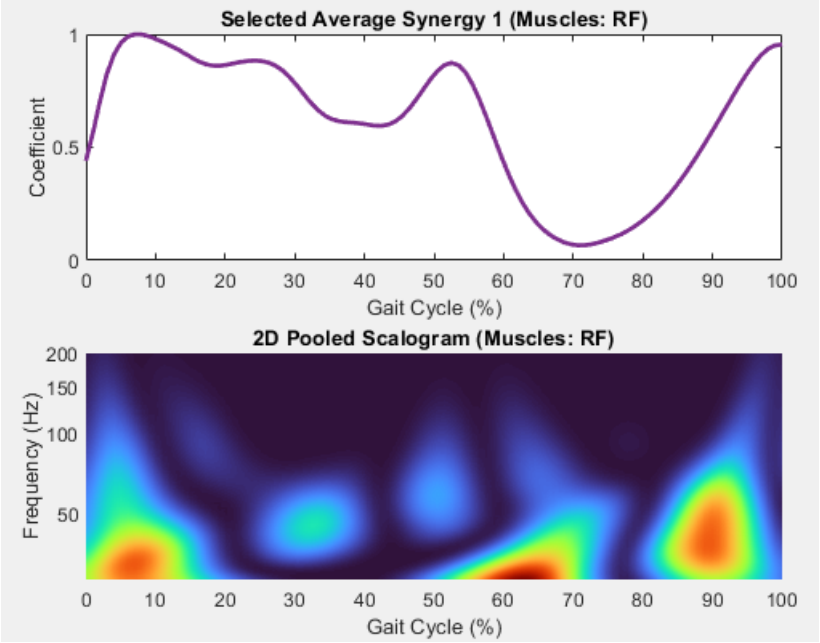



*Figure 105. Selected Average Synergy and 2D Pooled Scalogram for Subject 27.*

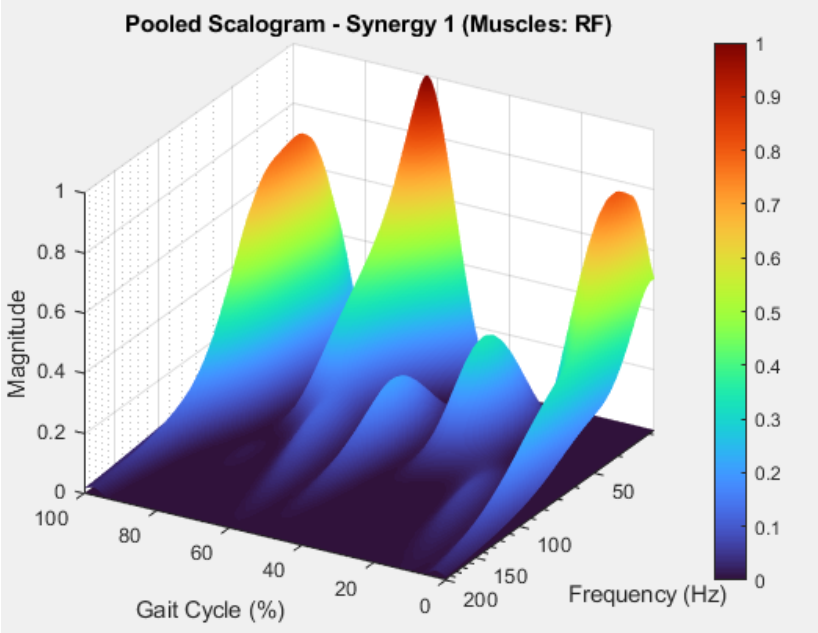



*Figure 106. 3D Pooled Scalogram for Subject 27.*

- **Subject 28**

In subject 28, the fourth synergy showing prominent activation of the Rectus Femoris (RF) and Vastus Lateralis (VL) (Figure 107). There are two obvious activation peaks around 8% and 100% of the step cycle, while one is detected at a lower intensity activity close to 55% of the GC (Figure 108). The pooled scalograms (Figures 108, 109) reveal that most muscle activations occur predominantly in the 10-100 Hz frequency range as peaks at the beginning and end of the step cycle where the step has a higher intensity in the 10-50 Hz range. Low muscle activity is observed between 20% and 30% of the gait cycle and around 65% of the step cycle. There is a strong correlation between the NMF results and the pooled scalograms for the higher intensity activations but there are some discrepancies as the pooled scalograms do not detect the minor activity that occurs near 55% of the GC in the course time of the synergy but instead are detected activities of low intensity not present.

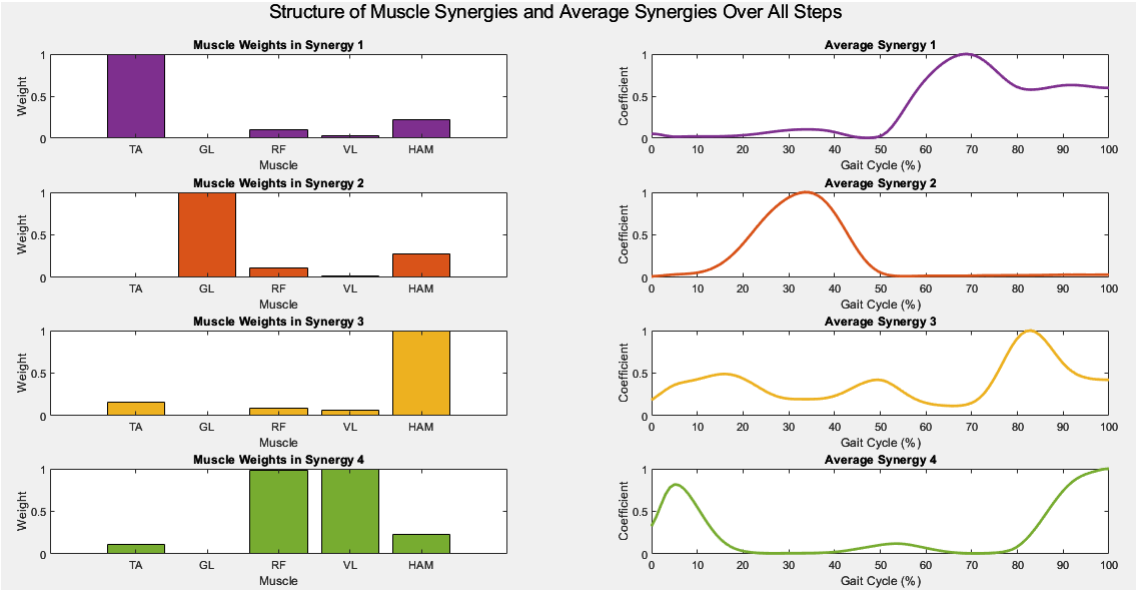



***Figure 107. Structure and Average Synergies Over All Steps for Subject 28.***

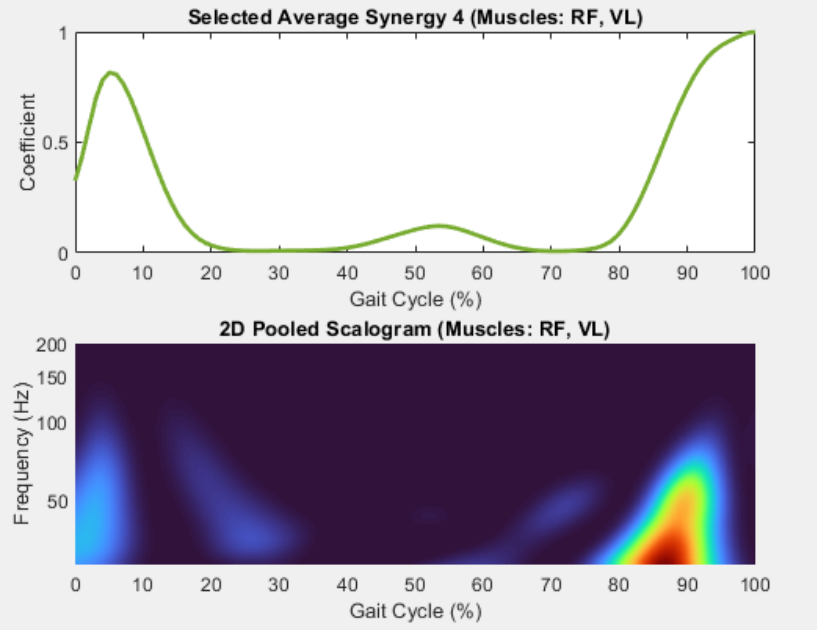



*Figure 108. Selected Average Synergy and 2D Pooled Scalogram for Subject 28.*

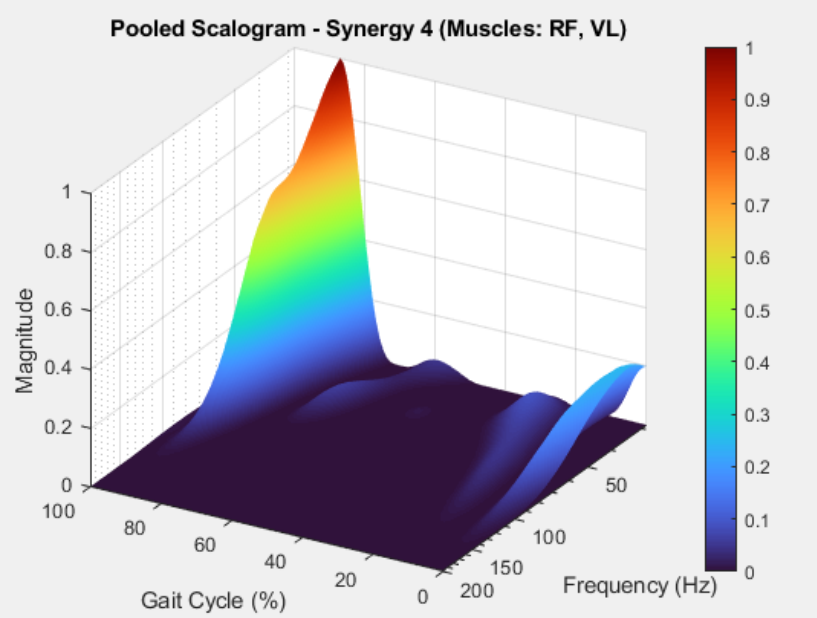



*Figure 109. 3D Pooled Scalogram for Subject 28.*

- **Subject 29**

In subject 29, the fourth synergy is selected, being characterized by substantial contributions of the muscles of the Rectus Femoris (RF) and Vastus Lateralis (VL) (Figure 110). The latter has almost always continuous activity with remarkable activation peaks around 8%, 58% and 100% of the gait cycle (Figure 111). In pooled scalograms (Figures 111, 112), the predominant frequency range for muscle activation is between 10 and 150 Hz. A significant peak occurs from 0% to 10% of the gait cycle, next to another remarkable peak from 80% to 90% of the step cycle with higher intensity at frequencies contained in the 50 Hz. Minimum activity is observed at about 30, 50% and 70% of the walking cycle. The results of the Non Negative Matrix Factorization (NMF) align well with pooled scalograms.

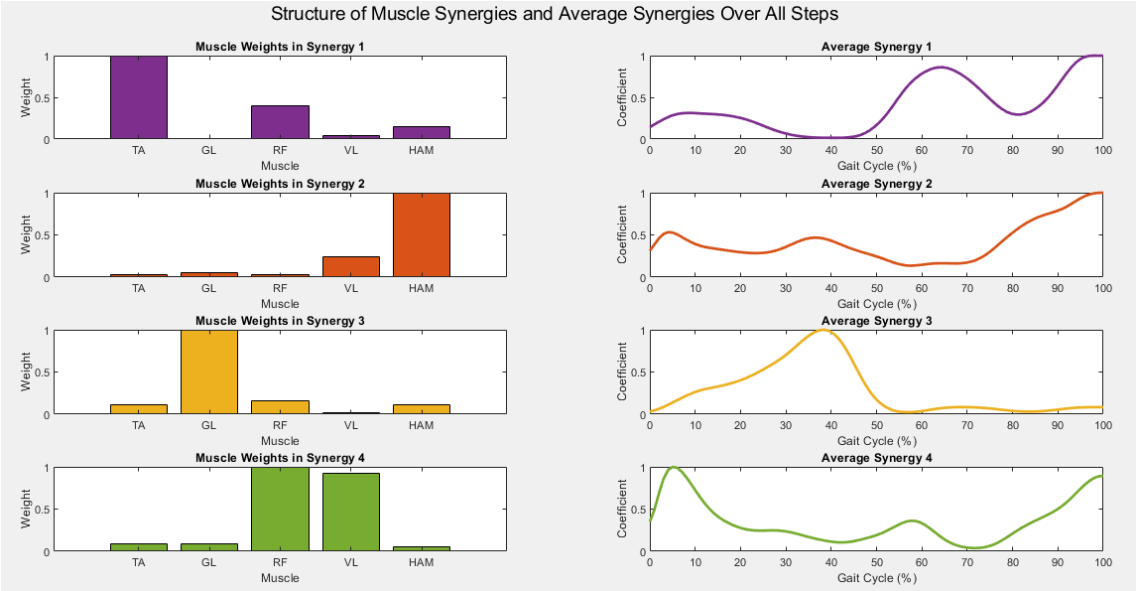



***Figure 110. Structure and Average Synergies Over All Steps for Subject 29.***

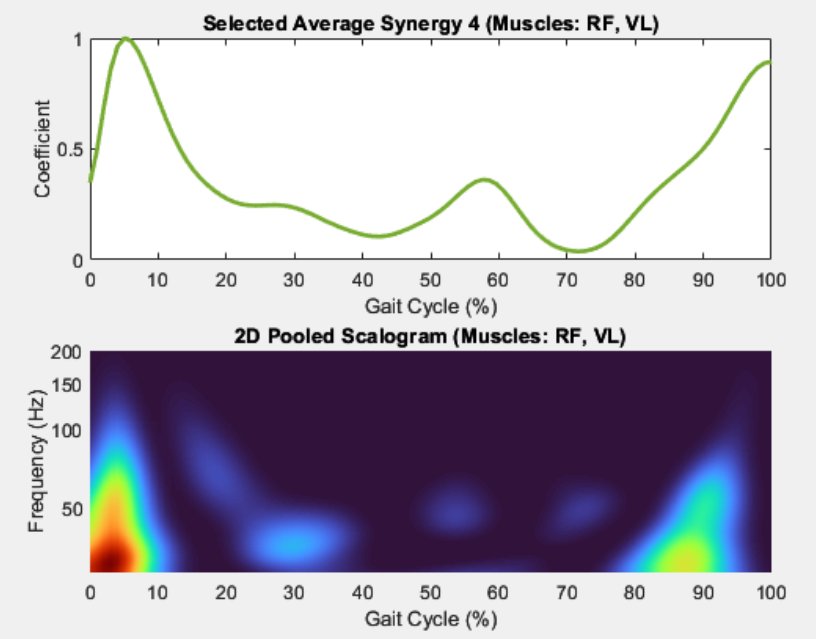



*Figure 111. Selected Average Synergy and 2D Pooled Scalogram for Subject 29.*

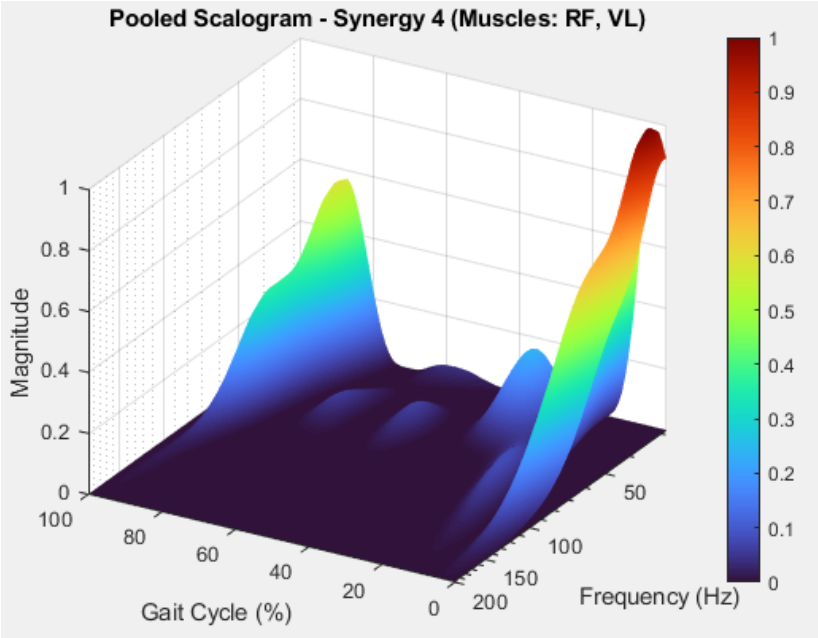



*Figure 112. 3D Pooled Scalogram for Subject 29.*

- **Subject 30**

In the analysis of subject 30, the third synergy is that which shows greater muscle weights of the Rectus Femoris (RF) and Vastus Lateralis (VL) (Figure 113). A significant peak is observed between 0% and 20% of the walking cycle, followed by a minor activation around 43%, and another peak occurs between 80% and 100% of the walking cycle (Figure 114). The pooled scalograms (Figures 114, 115) show an average activation between 0% and 10% of the GC, with another peak of strong activation occurring between 80% and 90% of the GC, predominantly in the frequency range from 10 Hz to 50 Hz. A low frequency activation is also observed around 20% - 30% of the GC, mainly below 50 Hz and another around 60% of the GC below 30 Hz. There is a strong alignment between the results of the Non negative Matrix Factorization (NMF) and the pooled scalograms, except for the low activities observed around 25% and 60% of the walking cycle.

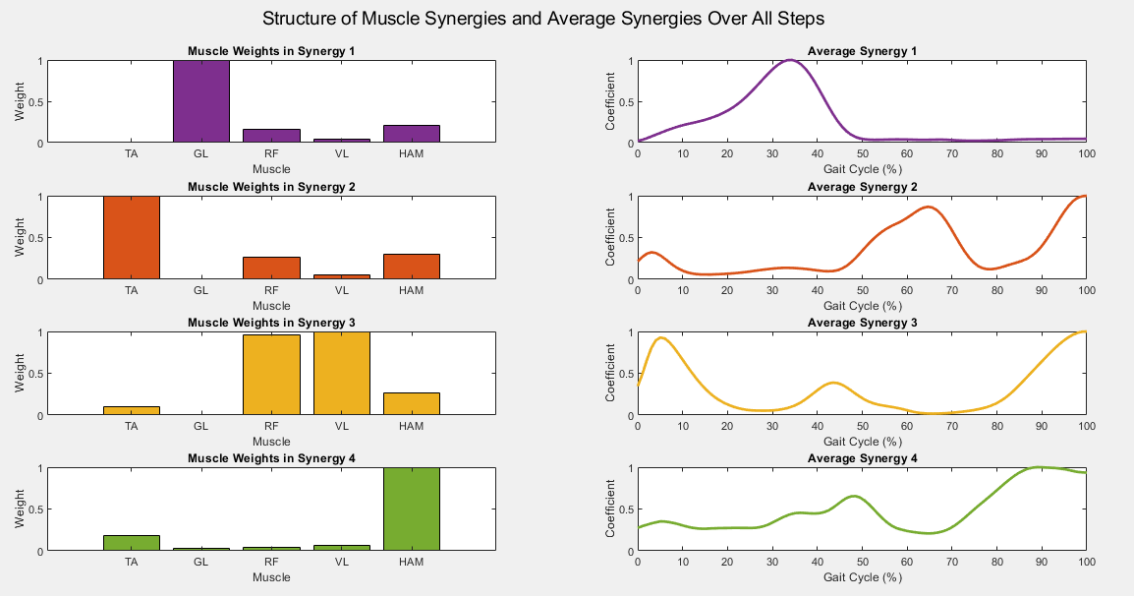



***Figure 113. Structure and Average Synergies Over All Steps for Subject 30.***

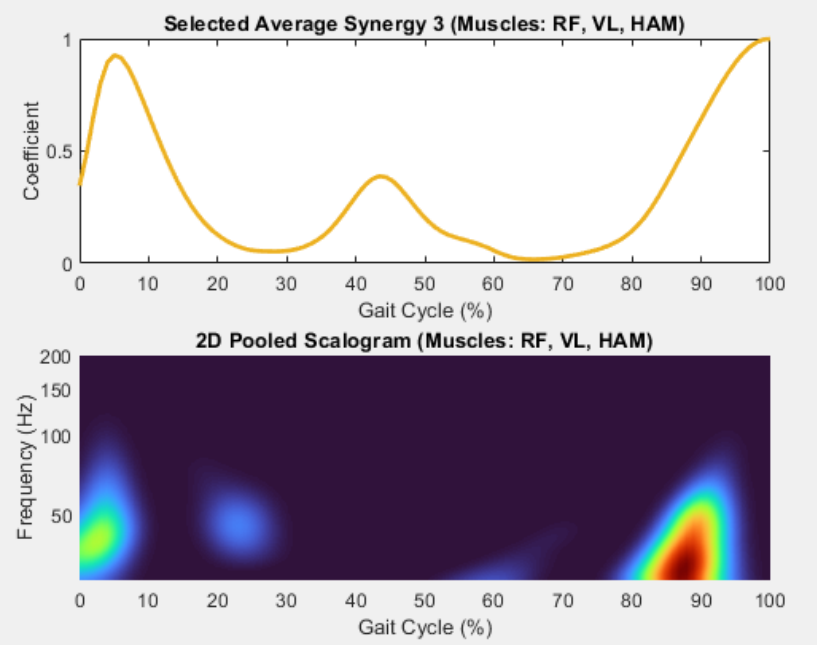



*Figure 114. Selected Average Synergy and 2D Pooled Scalogram for Subject 30.*

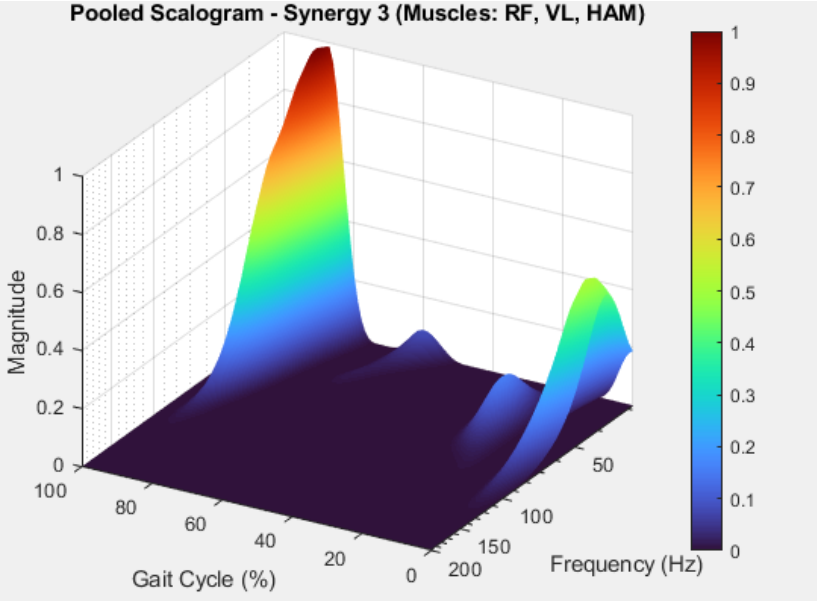



*Figure 115. 3D Pooled Scalogram for Subject 30.*

- **Subject 31**

In subject 31, muscle activation analysis shows that the Rectus Femoris (RF) and the Vastus Lateralis (VL) have their maximum activation in the fourth synergy (Figure 116), in particular there are three clear peaks around 8%, 46% and 100% of the step cycle (Figure 117). The pooled scalograms (Figures 117,118) also reveal that there are activation events around 0 to 10%, between 20 and 30%, between 40 and 50%, between 58 and 78% of the step cycle which are all of low intensity and have a frequency range around 50 Hz, While there is a last activation between 80% and 98% of the step cycle showing more intense activity with frequencies concentrated between 30 Hz and 70 Hz. Except for the peaks between 58% and 78% of the step cycle present in pooled scalograms, there is a good match between the results of the latter and the NMF.

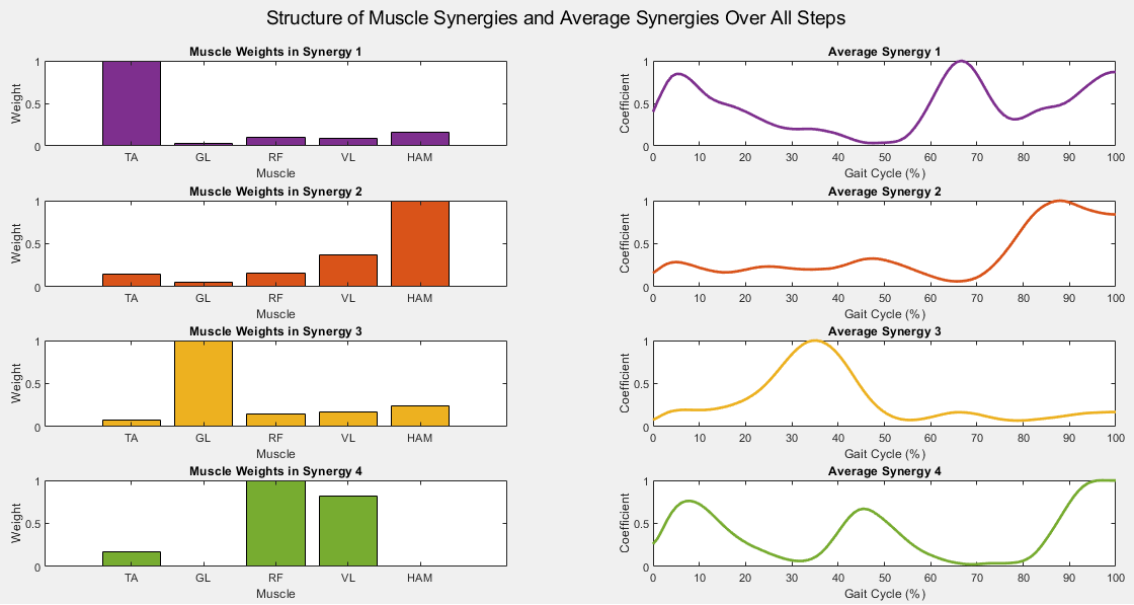



***Figure 116. Structure and Average Synergies Over All Steps for Subject 31.***

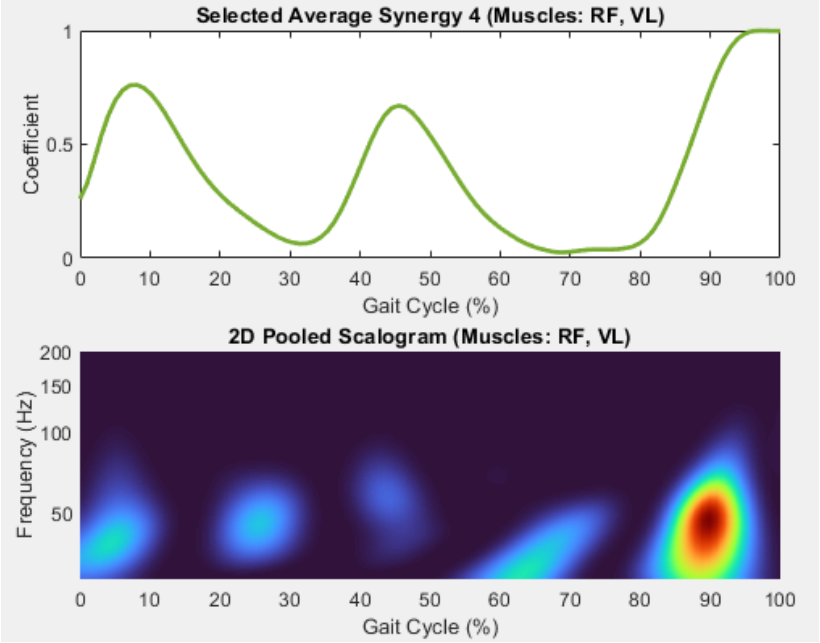



***Figure 117. Selected Average Synergy and 2D Pooled Scalogram for Subject 31.***

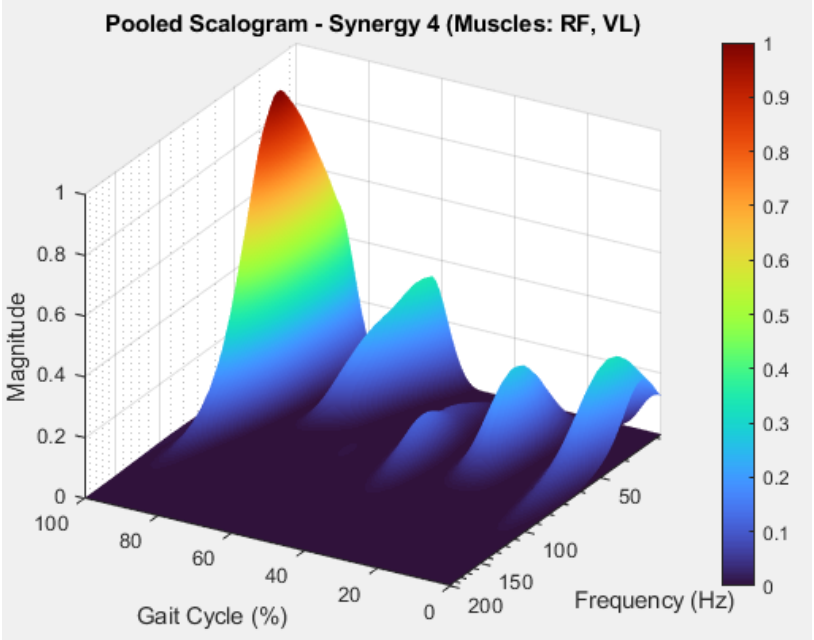



***Figure 118. 3D Pooled Scalogram for Subject 31.***

# 7 Discussion

The present analysis was performed to validate the applicability to walking of a recently developed approach, the pooled scalogram [2], based the assessment of CWT cross-energy localization to quantify the muscle synergy in the time-frequency domain through. The validation during walking of this novel approach was performed by direct comparison with the outcomes achieved by applying the NMF, one of the most used techniques to assess muscle synergies [6]. Indeed, NMF is a well-established technique used for extracting muscle synergies from sEMG signals, breaking down complex muscle activation picture into a smaller set of synergistic components over time. The results of this study provided significant insights into the complexity and organization of muscle synergies during walking, focusing particularly on the synergies identified through pooled scalogram analysis. In the majority of the subjects analyzed (94%), four muscle synergies were identified by NMF, while only two subjects (6%) exhibited five synergies. This finding suggests that the central nervous system (CNS) uses different strategies based on individual characteristics to optimize motor control. Previous studies have highlighted the role of muscle synergies in simplifying motor control, making the management of complex movements more effective [37] [38].

Subjects 2 and 27, who exhibited five synergies, offer an interesting perspective on individual variability in motor control. The presence of an additional synergy could indicate a higher level of complexity in control strategies, potentially due to specific biomechanical characteristics or a greater need for motor adaptation. Moreover, previous research suggests that adding synergies may be a strategy to compensate for neuromuscular limitations or enhance motor control precision in specific scenarios [39]. This adaptation could be related to factors such as increased joint stability demands, greater muscle flexibility, or the need for more precise movement control [40]. The presence of five synergies might also reflect a higher capacity of the CNS to modulate responses in more complex motor situations, as observed in other studies on motor coordination [11] [41]. The additional synergy could also represent an attempt by the neuromuscular system to compensate for asymmetries or inefficiencies in gait biomechanics, showcasing the diverse adaptive strategies available to the CNS.

The database used in this study [35] included sEMG signal from only five muscles: Rectus Femoris (RF), Vastus Lateralis (VL), Tibialis Anterior (TA), Hamstrings (HAM),

and Lateral Gastrocnemius (GL). The most frequently observed muscle synergies involving RF, VL, TA, and HAM in various combinations among the subjects. The synergy between RF and VL consistently emerged during phases requiring knee extension and stabilization, particularly during the stance phase of the gait cycle. The physiological significance of this muscle combination lies in the synergistic role of RF and VL in providing both stability and propulsion, ensuring effective knee joint control [42]. These muscles contribute to force production and joint stability, allowing the body to maintain balance and progress during walking. This coordination reflects an efficient strategy employed by the CNS to address the biomechanical challenges of balance and movement. The synergy between VL and HAM was particularly interesting. It was active primarily during the transition between the stance and swing phases, playing a crucial role in knee stability and hip extension control, thereby allowing a smooth transition between different gait phases [15]. The involvement of HAM reflects the need to coordinate knee extension and hip flexion control to prepare the limb for the swing phase. This activation pattern highlights the importance of effective coordination between muscle groups to ensure efficient and uninterrupted movement, which is key to understanding how the CNS manages the transition between loading and propulsion phases while balancing stability and movement. Another significant combination is the one involving RF, VL, and TA. This synergy was particularly active during the foot advancement phase and initial contact with the ground. The Tibialis Anterior plays a crucial role in lifting the forefoot during the swing phase, preventing foot drag and facilitating ground contact. The co-activation with RF and VL suggests a strategy to enhance knee stability during the preparation for impact and control the foot's lowering, ensuring a smooth and safe transition to the stance phase [9]. This synergy is essential for managing ground reaction forces and maintaining balance during the initial phases of foot contact. The combination of RF, VL, and HAM was observed during the transition from the stance to the swing phase. This activation pattern suggests that the CNS uses a coordination strategy involving knee extension and hip extension, providing both stability and propulsion. Specifically, RF and VL stabilize the knee, while HAM contributes to hip extension, facilitating body weight transfer and preparing the limb for the swing phase [44]. This combination represents an effective adaptation to optimize movement during the gait cycle, enabling an efficient transition between different phases. The synergy involving only the Vastus Lateralis is noteworthy for its role in maintaining lateral knee stability during the stance phase, particularly in the

medio-lateral direction. This isolated activation could indicate a CNS strategy to ensure joint stability during single-limb support, which is crucial for maintaining balance [43]. The action of VL in this phase is indispensable for counteracting destabilizing forces and ensuring a stable posture throughout the support period.

Across all subjects, the quantification of synergies achieved using the pooled scalogram closely matched the outcomes from NMF, both in terms of synergy activation timing. The results reported in each single subject, indeed, showed very similar temporal activation patterns reported by NMF and the pooled scalogram approaches. This alignment between the two methods reinforces the reliability of the pooled scalogram for time-domain synergy analysis and supports its use in dynamic tasks such as walking. The pooled scalogram added a valuable layer of frequency-domain analysis, which NMF does not provide. For example, it revealed that the most significant muscle activations occurred in the 30–50 Hz range during key phases of the gait cycle, such as early stance and terminal swing, showing how muscles coordinate not just in time but across specific frequency bands. This frequency information adds a new dimension to the understanding of muscle synergies, potentially offering insights into muscle force generation and control strategies that are missed by NMF. One of the main limitations of this study concerns the database used, which included only five muscles: Rectus Femoris, Vastus Lateralis, Tibialis Anterior, Hamstrings, and Lateral Gastrocnemius. This limitation may reduce the ability to fully understand the contribution of other important muscles involved in motor control, such as hip or trunk stabilizers, which play a crucial role in maintaining posture and balance during walking. This limitation restricts the possibility of obtaining a complete picture of muscle synergies during walking, as other important muscles for movement control may not have been considered. The choice to analyze only five muscles was dictated by the need to limit data complexity, but it remains a significant restriction for the generalizability of the obtained results. In the future, it would be desirable to extend the number of muscles analysed to gain a more comprehensive understanding of the synergistic dynamics involved in walking. Specifically, including minor stabilizer muscles could provide further details on the control strategies adopted by the CNS [11].

However, the results of this study, even if focused on only five muscles, highlight the importance of muscle synergies in gait control and their variability among subjects. The use of pooled scalogram allowed for a detailed view of muscle interactions, providing

new insights into the motor control strategies adopted by the CNS. These findings could have significant clinical applications, particularly for the rehabilitation of individuals with motor deficits. Identifying key synergies and understanding their physiological role is a crucial step towards developing personalized therapeutic interventions aimed at improving muscle coordination and movement functionality.

## 7.1 Conclusions

The strong alignment between the time-based results from the pooled scalogram and Non-Negative Matrix Factorization supports the reliability the pooled scalogram for synergy analysis. Both techniques showed consistent temporal activation patterns, validating the pooled scalogram as a robust method for evaluating muscle coordination during gait. The added value introduced by the pooled scalogram is its ability to provide additional insights by analyzing muscle synergies in the frequency domain, which NMF cannot achieve. This frequency information could have significant clinical relevance, particularly in rehabilitation, where understanding both the timing and frequency of muscle synergies may inform more targeted interventions. Further studies could also explore the use of pooled scalogram under different pathological conditions to assess how muscle synergies change in response to specific pathologies or therapeutic interventions. Understanding these variations could enhance the effectiveness of rehabilitation interventions, further personalizing them to the specific needs of patients. Additionally, integrating advanced signal analysis techniques, such as predictive models based on artificial intelligence, could provide further insights into the strategies adopted by the CNS to coordinate complex movements.

# Bibliography

[1] Purves, D., Augustine, G.J., Fitzpatrick, D., Hall, W.C., LaMantia, A.S., & White, L.E. (2018). Neuroscience (6th ed.). *Sinauer Associates*.

[2] Borzelli, D., Morano, M., Fioretti, S., & Di Nardo, F. (2025). The pooled scalogram: A wavelet-based approach to detect the co-activation of several muscles in the time-frequency domain. *Biomedical Signal Processing and Control*, 99, 106802.

[3] Ting, L.H., & McKay, J.L. (2007). Neuromechanical approaches for understanding muscle synergies: From circuits to behavior. *Current Opinion in Neurobiology*, 17(6), 622-628.

[4] d'Avella, A., Saltiel, P., & Bizzi, E. (2003). Combinations of muscle synergies in the construction of a natural motor behavior. *Nature Neuroscience*, 6(3), 300-308.

[5] Latash, M.L. (2012). The bliss (not the problem) of motor abundance. *Experimental Brain Research*, 217(1), 1-5.

[6] Lee, D.D., & Seung, H.S. (1999). Learning the parts of objects by non-negative matrix factorization. *Nature*, 401, 788-791.

[7] von Tscharner, V. (2000). Intensity analysis in time-frequency space of surface myoelectric signals by wavelets of specified resolution. *Journal of Electromyography and Kinesiology*, 10(6), 433-445.

[8] Addison, P.S. (2002). The Illustrated Wavelet Transform Handbook. *CRC Press*.

[9] Kandel, E.R., Schwartz, J.H., & Jessell, T.M. (2013). Principles of Neural Science (5th ed.). *McGraw-Hill*.

[10] Shadmehr, R., & Smith, M.A. (2014). Neuroscience of Motor Control: From Movements to Behavior. *MIT Press*.

[11] Ivanenko, Y.P., Cappellini, G., & Lacquaniti, F. (2004). Five basic muscle activation patterns account for muscle activity during human locomotion. *Journal of Physiology*, 556(1), 267-282.

[12] Perry, J., & Burnfield, J.M. (2010). Gait Analysis: Normal and Pathological Function (2nd ed.). *SLACK Incorporated*.

[13] Whittle, M.W. (2014). Gait Analysis: An Introduction (5th ed.). *Butterworth-Heinemann*.

[14] Neumann, D.A. (2010). Kinesiology of the Musculoskeletal System: Foundations for Rehabilitation (2nd ed.). *Elsevier*.

[15] Winter, D. A. (2009). Biomechanics and Motor Control of Human Movement (4th ed.). *Wiley*.

[16] Ting, L. H., & Chvatal, S. A. (2021). Decomposing muscle activity in motor tasks: methods and interpretation. *Current Opinion in Neurobiology,* 68, 54-61.

[17] Ding, L., Yang, Y., Huang, D., & Geng, Z. (2010). A muscle-reflex model that encodes principles of legged mechanics produces human walking dynamics and muscle activities. *IEEE Transactions on Neural Systems and Rehabilitation Engineering*, 18(3), 263-273.

[18] Tresch, M.C., & Jarc, A. (2009). The case for and against muscle synergies. Current Opinion in *Neurobiology*, 19(6), 601-607.

[19] Clark, D.J., Ting, L.H., Zajac, F.E., Neptune, R.R., & Kautz, S.A. (2010). Merging of healthy motor modules predicts reduced locomotor performance and muscle coordination complexity post-stroke. *Journal of Neurophysiology*, 103(2), 844-857.

[20] Safavynia, S.A., Torres-Oviedo, G., & Ting, L.H. (2011). Muscle synergies: Implications for clinical evaluation and rehabilitation of movement. *Topics in Spinal Cord Injury Rehabilitation*, 17(1), 16-24.

[21] Fox, M.D., & De Sa, E. (2021). Motor Control Strategies in Human Gait: Neural Mechanisms of Locomotion and Muscle Coordination. *Frontiers in Human Neuroscience*, 15, 645834.

[22] De Luca, C.J. (2006). Electromyography. In *Encyclopedia of Medical Devices and Instrumentation*, 98-109.

*[23]* Konrad, P. (2005). The ABC of EMG: A Practical Introduction to Kinesiological Electromyography. *Noraxon U.S.A. Inc.*

[24] Hermens, H.J., Freriks, B., Merletti, R., et al. (1999). European Recommendations for Surface Electromyography. *SENIAM Project*.

[25] Merletti, R., & Farina, D. (2016). Surface Electromyography: Physiology, Engineering, and Applications. *John Wiley & Sons*.

[26] De Luca, C.J. (2002). Surface electromyography: Detection and recording. *DelSys Incorporated*.

[27] Phinyomark, A., et al. (2009). A Review of Time-Domain Feature Extraction in Surface Electromyography. *Journal of Medical and Biological Engineering,* 30(6), 419-428.

[28] Farina, D., & Merletti, R. (2008). A Novel Approach for Feature Extraction from Surface EMG Signals Using Time-Frequency Analysis. *IEEE Transactions on Biomedical Engineering,* 55(2), 671-680.

[29] Phinyomark, A., et al. (2011). Feature Extraction and Selection for Myoelectric Control Based on Wavelet Transform and Phase Space Reconstruction. *Expert Systems with Applications,* 38(7), 8621-8628.

[30] Phinyomark, A., et al. (2011). Wavelet Approach for Feature Extraction from EMG Signals. *The Annual International Conference of the IEEE Engineering in Medicine and Biology Society,* 2011, 1697-1700.

[31] Wang, Y. X., & Zhang, Y. J. (2012). Nonnegative matrix factorization: A comprehensive review. *IEEE Transactions on Knowledge and data engineering*, 25(6), 1336-1353.

[32] Kim, J., & Park, H. (2008). Sparse Non-negative Matrix Factorization for Clustering. In Pacific-Asia Conference on Knowledge Discovery and Data Mining (pp. 332-343). *Springer*.

[33] Tresch, M.C., Cheung, V.C., & d'Avella, A. (2006). Matrix Factorization Algorithms for the Identification of Muscle Synergies: Evaluation on Simulated and Experimental Data Sets. *Journal of Neurophysiology*, 95(4), 2199-2212.

[34] Bizzi, E., & Cheung, V.C.K. (2013). The Neural Origin of Muscle Synergies. Frontiers in Computational Neuroscience, 7, 51.

[35] Di Nardo, F., Morbidoni, C., & Fioretti, S. (2024). Surface electromyographic signals collected during long-lasting ground walking of young able-bodied subjects (version 1.0.1). *PhysioNet*.

[36] Di Nardo, F., & Fioretti, S. (2013). Statistical analysis of surface electromyographic signal for the assessment of rectus femoris modalities of activation during gait. *Journal of Electromyography and Kinesiology*, 23(3), 556-562.

[37] Bizzi, E., Cheung, V. C. K., d'Avella, A., Saltiel, P., & Tresch, M. (2008). Combining modules for movement. *Brain Research Reviews, 57*(1), 125-133.

[38] Santello, M., Baud-Bovy, G., & Jörntell, H. (2016). Neural bases of hand synergies. *Frontiers in Computational Neuroscience, 10*, 82.

[39] Cheung, V.C.K., Turolla, A., Agostini, M., Silvoni, S., Bennis, C., Kasi, P., & Bizzi, E. (2009). Muscle synergy patterns as physiological markers of motor cortical damage. *Proceedings of the National Academy of Sciences,* 106(49), 21264-21269.

[40] Ting, L. H., & McKay, J. L. (2007). Neuromechanics of muscle synergies for posture and movement. *Current Opinion in Neurobiology, 17*(6), 622-628.

[41] Dominici, N., Ivanenko, Y.P., Cappellini, G., d'Avella, A., Mondi, V., Cicchese, M., Sylos-Labini, F., & Lacquaniti, F. (2011). Locomotor primitives in newborn babies and their development. *Science,* 334(6058), 997-999.

[42] Zajac, F. E. (1989). Muscle and tendon: properties, models, scaling, and application to biomechanics and motor control. *Critical Reviews in Biomedical Engineering, 17*(4), 359-411.

[43] Hof, A. L. (2007). The equations of motion for a standing human reveal three mechanisms for balance. *Journal of Biomechanics, 40*(2), 451-457.

[44] Kautz, S. A., & Patten, C. (2005). Interlimb influences on paretic leg function in poststroke hemiparesis. *Journal of Neurophysiology, 93*(5), 2460-2473.